TECHNISCHE UNIVERSITÄT DRESDEN

HEINRICH HEINE UNIVERSITÄT DÜSSELDORF

9th German Ferrofluid Workshop

Benediktbeuern
September 22nd - 25th
2009

Book of Abstracts

Program of the

9th German Ferrofluid Workshop

Benediktbeuern, 22.9.-25.9.2009

Tuesday, September 22nd

14:00 – 14:30	***Opening***		
14:30 - 14:55	Th. John, R. Stannarius	*Brownian ratchet effect in ferrofluids*	33
14:55 - 15:20	D. Lerche, U. Mertens, Ch. Pietsch, Ch. Eichholz, H. Nirschl, K.Trommler	*Charakterisierung von dispergierten Nano- und Mikromagnetpartikeln in Gravitationsfeldern unter Einwirkung überlagerter Magnetfelder*	45
15:20 - 15:45	H. Rahn, D. Eberbeck, L. Trahms, S. Odenbach	*Calibration of a polychromatic X-ray tomography equipment for biological tissue samples enriched with magnetic nanoparticles*	62
15:45 - 16:15	***Coffee break***		
16:15 - 16:40	C. Gürler, A. Bian, A.M. Schmidt	*Polymerization from Magnetically Induced Hot Spots: A Kinetik Investigation*	26
16:40 - 17:05	J. Jordanovic, S.H.L. Klapp	*Field-induced structure formation and dynamics of ferrofluid multilayer films*	35
17:05 - 17:30	I.Yu.Chuenkova, V.M. Kozhevnikov, M.I. Danilov, S.S. Yastrebov, L.Yu. Iskakova, A.Yu. Zubarev	*Phase transitions in ferrofluids induced by electrical field*	14
17:30 - 19:00	***Postersession 1***		

Wednesday, September 23rd

9:00	***Departure for excursions***	
	R. Richter "Title to be announced "	
15:00	***Return from excursions***	
15:30 - 17:00	*Round table discussion*	*Young researchers interactive session*
17:00 - 20:00	***Postersession 2***	

Thursday, September 24th

9:00 - 10:15	P. Ilg	*Molecular dynamics for ferrofluids*	
10:15 - 10:40	R. Müller, S. Dutz, M. Zeisberger	*Investigations on Magnetic Particles Prepared by Cyclic Growth*	56
10:40 - 11:05	N. Buske, S. Dutz	*Colloidal Stability of Water Based Dispersions Containing Large Single Domain Particles of Magnetite*	12
11:05 - 11:30	***Coffee break***		
11:30 - 11:55	A. Wiedenmann, R. Gähler, C. Dewhurst, U. Keiderling, S. Prévost, J. Kohlbrecher	*Ordering and Relaxation Dynamics of Magnetic Nanoparticles studied by Stroboscopic Small Angle Neutron Scattering*	79
11:55 - 12:20	S. Altmeyer, Ch. Hoffmann, A. Leschhorn, M. Lücke	*Influence of homogeneous Magnetic Fields on the Flow of a Ferrofluid in the Taylor-Couette System*	1
12:20 - 12:45	F. Ludwig, A. Guillaume, E. Heim, M. Schilling	*Characterization of magnetic core-shell nanoparticle suspensions using ac susceptibility for frequencies up to 1 MHz*	47
12:45 - 14:00	***Lunch***		
14:15 - 14:40	R. Baumann, G. Glöckl, S. Nagel, W. Weitschies	*Ferrofluids for inhalative Chemotherapy*	3
14:40 - 15:05	S. Lyer, R. Tietze, R. Jurgons, H. Richter, F. Wiekhorst, K. Schwarz, L. Trahms, Ch. Alexiou	*Distribution of Magnetic Nanoparticles after Magnetic Drug Targeting in an Ex Vivo Bovine Artery Model*	49
15:05 - 15:30	U. Paiphansiri, M. Dass, I. Brüstle, S. Sharma, V. Rasche, V. Mailänder, K. Landfester	*Potential Use of Nanocapsules Containing Magnetic Nanoparticles Prepared by Inverse Miniemulsion for MRI*	60
15:30 - 15:55	O. Mykhaylyk, Y. Sanchez-Antequera, N. Tresilwised, S. Thalhammer, D. Adigüzel, M. Döblinger, Th. Bein, P. Sonne Holm, Ch. Plank	*Magnetic Nanoparticles for Gene Delivery: Some Determinants of Efficient Delivery Vectors*	58
15:55 - 16:20	***Coffee break***		
16:20 - 16:45	J. Belardi, N. Schorr, O. Prucker, J. Rühe, S. Wells. V. Pattel	*Artificial Cilia: Nature Inspired Microactuators for use in Microfluidic Systems*	5
16:45 - 17:10	V. Böhm, J. Popp, I. Zeidis, K. Zimmermann	*An Approach to the Mechanics of Ferrofluid-/Ferroelastomer based Locomotion Systems*	8
17:10 - 19:00	***Postersession 3***		

19:30 - ??? ***Conference Dinner***

Friday, September 25th

9:00 - 10:15	S. Behrens	*Magnetic Nanoparticles and Multicomponent Nanostructures: Syntheses, Functionalization, and Potential Applications*	
10:15 - 10:40	Z. Wu, A. Müller, R. Zierold, K. Nielsch, C. Wege, C. E. Krill	*Synthesis and Magnetoviscosity of Novel Ferrofluids Prepared by Templating Virus Particles or Nanopores*	80
10:40 - 11:05	J.J. Cerdà, P.A. Sánchez, R. Webber, S. Kantorovich, E. Krutikova, V. Ballenegger, T. Sintes, A. Ivanov, C. Holm	*Theory and simulations applied to the understanding of magnetic systems: bulky ferrofluids, shifted ferrofluids and magnetic filaments*	66
11:05 - 11:30	***Coffee break***		
11:30 - 11:55	P. Bender, A. Günther, A. Tschöpe, R. Birringer	*Synthesis and characterisation of uniaxial ferrogels with Ni nanorods as the magnetic phase*	7
11:55 - 12:20	M. Krekhova, G. Lattermann, H. Schmalz	*Soft Thermo-Reversible Organoferrogels*	39
12:20 - 12:45	T. Friedrich, I. Rehberg, R. Richter	*Magnetic Traveling-Stripe-Forcing: Transport and Pattern Formation*	20

12:45 – 13:00 ***Closing***

Posters

Nr.			Seite
1	Borin, D.; Müller, R.; Odenbach, S.	*Magnetorheological characterization of a ferrofluid based on the clustered iron oxide nanoparticles*	10
2	Eberbeck, D.; Zirpel, P.; Trahms, L.	*Experimental investigation of dipolar interaction in suspension of magnetic nanoparticles*	16
3	Engler, H.; Odenbach, S.	*Parametric induced oscillation of thermomagnetic convection in ferrofluids*	18
4	Gitter, K.; Odenbach, S.	*Quantitative targeting-maps as result of experimental investiga-tions on a branched tube model in magnetic drug targeting*	21
5	Gollwitzer, Ch.; Rehberg, I.; Lange, A.; Richter, R.	*"Frozensweig": A Cool Instability in the Limit of* $\eta \rightarrow \infty$	22
6	Gorschinski, A.; Habicht, W.; Walter, O.; Dinjus, E.; Behrens, S.	*A simple aminoalkyl siloxane-mediated route to functional mag-netic metal nanoparticles and microspheres*	23
7	Günther, A.; Bender, P.; Tschöpe, A.; Birringer, R.	*Diffusion of magnetic nickel nanorods in colloidal dispersions*	25
8	Heim, E.; Schwoerer, A.; Harling, S.; Ludwig, F.; Menzel, H.; Schilling, M.	*Release behavior characterization of hydrogels by fluxgate magnetorelaxometry*	27
9	Heinrich, D.; Goni, A. R.; Cerioni, L.; Osán, T. M.; Pusiol, D. J.; Thomsen, C.	*Time dependent NMR spectroscopy on ionic and citrate ferrofluids*	29
10	Ilg, P.; del Gado, E.	*Chain-formation vs.gelation in dipolar colloids*	31
11	Kaiser, A.; Schmidt, A. M.	*Magnetic Capsules and Pickering Emulsions Stabilized by Core-Shell Particles*	36
12	Krause, H.-J.; Pretzell, A.; Zhang, Y.; Offenhäusser, A.	*Magnetic Nanoparticle Detection and Characterization using a High Temperature radio-frequency Superconducting Quantum Interference Device*	37
13	Krichler, M.; Odenbach, S.	*Magnetic Field Induced Change of Thermal Conductivity of Ferrofluids*	41
14	Lange, A.; Odenbach, S.	*Thermomagnetic convection in magnetic fluids influenced by spatially modulated fields*	43
15	Leschhorn, A.; Reindl, M.; Altmeyer, S.; Hoffmann, C.; Lücke, M.; Odenbach, S.	*Stability of the circular Couette flow of a ferrofluid*	46
16	Marten, G.U.; Gelbrich, T.; Schmidt, A. M.	*Magnetic Polymer Brushes for Controlled Drug Delivery*	51
17	Matoussevitch, N.; Boennemann, H.	*Recent development at the STREM Nanolab*	53

18	Matura, P.; Lücke, M.	*Thermomagnetic convection in a ferrofluid layer exposed to a time-periodic magnetic field*	54
19	Messing, R.; Frickel, N.; Schmidt, A. M.	*Magnetosensitive $CoFe_2O_4$ PAAm Hydrogels*	55
20	Müller, B.; Wotschadlo, J.; Pachmann, K.; Buske, N.; Heinze, Th.; Clement, J. H.	*Distribution of leukocyte subpopulations after short-term applica-tion of magnetic core-shell nanoparticles*	56
21	Reindl, M.; Leschhorn, A.; Lücke, M.; Odenbach, S.	*Flow control of ferrofluids exposed to magnetic fields*	65
22	Sanchez, P.A.; Cerdá, J. J.; Sintes, T.; Ballenegger, V.; Piro, O.; Holm, C.	*Adsorption and self-organization properties of semi-flexible magnetic filaments*	67
23	Schmitz, R.	*Hydrodynamic Interaction*	68
24	Schorr, N.; Belardi, J.; Prucker, O.; Rühe, J.; Patel, V.; Wells, S.	*A Ferrogel Microactor - Towards Artificial Cilia*	69
25	Thom, K.; Aurich, K.; Kühn, J.-P.; Weitschies, W.	*Magnetic labeling of the vaccine adjuvant $Al(OH)_3$ for magnetic resonance tracking*	70
26	Tietze, R.; Müller, R.; Lyer, S.; Schreiber, E.; Alexiou, Ch.; Steinmetz, H.; Zeisberger, M.	*Adsorption of the Chemotherapeutic Agent Mitoxantron on Iron Oxide Nanoparticles*	72
27	Urban, M.; Musyanovych, A.; Schmidtke-Schrezenmeier, G.; Schrezenmeier, H.; Mailänder, V.; Landfester, K.	*Fluorescent Superparamagnetic Biodegradable Poly(L-lactide) Nanoparticles by Combination of Miniemulsion and Emulsion/Solvent Evaporation Techniques*	74
28	Wagner, K.; Seemann, T.; Wyrwa, R.; Müller, R.; Clement, J. H.; Schnabelrauch, M.	*Novel Catechol Containing Shell Materials for Magnetic Nanoparticles*	76
29	Weeber, R.; Cerda, J.; Kantorovich, S.; Holm, C.	*Peculiarities of shifted magnetic dipoles*	78

Ordering and Relaxation Dynamics of Magnetic Nanoparticles studied by Stroboscopic Small Angle Neutron Scattering.

A. Wiedenmann [1 *], R. Gähler [1], C. Dewhurst [1], U. Keiderling [2], S. Prévost [3], J. Kohlbrecher [4]

[1] Institut Laue-Langevin, F-38042 Grenoble Cedex, France
[2] Helmholtz-Zentrum Berlin, D-14109 Berlin, Germany
[3]Technical University Berlin D-10623 Berlin, Germany
[4] Laboratory for Neutron Scattering, ETH Zurich & PSI, CH-5232 Villigen PSI, Switzerland

Recently, stroboscopic Small Angle Neutron Scattering (SANS) techniques have been developed which allow ordering and relaxation processes of magnetic moments in nano-particles to be monitored [1,2]. By applying a periodic external magnetic field the time-resolved SANS response to a forced oscillation could be analyzed. For conventional SANS with a continuous neutron flux the shortest accessible time range is limited to few milliseconds resulting due to the wavelength spread. With the pulsed frame overlap TISANE technique [3] a dynamical range of micro-seconds can be exploited which is similar to that of X-ray photon-correlation spectroscopy.

Here we present a combination of stroboscopic neutron techniques applied to magnetic colloids. SANS scattering response in an oscillating magnetic field was measured as a function of temperature, frequency and amplitude of the applied field. The fraction of particle moments that can follow the oscillating field produces scattering patterns alternating between fully isotropic and strongly anisotropic.

We extended the stroboscopic technique by using polarized neutrons with polarisation analysis (POLARIS) for which spin non-flip (--) and (++) and spin-flip (-+) scattering cross-sections are different and depend on time. Since the neutron spin follows adiabatically the applied oscillating field we observed oscillating POLARIS cross sections for the whole time period as long as there was no delay of the magnetic moment reorientation. When the magnetisation reversal is delayed for a certain time range neutron spin and particle moment are no longer in phase and the time-dependent scattering intensity will jump from (--) to (++) or vice versa. This discontinuity in the POLARIS contrasts makes the technique very sensitive to the determination of such delayed responses i.e. to the analysis of relaxation times.

[1] Wiedenmann, A., Keiderling, U., Habicht, K., Russina, M., Gähler, R. Phys. Rev. Lett. **97**, 057202 (2006).
[2] Wiedenmann, A., Keiderling, U., Meissner, M., Wallacher, D., Gähler, R., May, R. P., Prévost, S., Klokkenburg, M., Erné, B., Kohlbrecher, J. Phys.Rev.**B77**,184417(2008)
[3] R. Gähler and R. Golub, Z. Phys. B **56**, 5 (1984).

An Approach to the Mechanics of Ferrofluid-/Ferroelastomer based Locomotion Systems

V. Böhm, J. Popp, I. Zeidis, K. Zimmermann

Faculty of Mechanical Engineering, Technische Universität Ilmenau, PF 10 05 65, 98684, Germany

The design of mobile robots, working really autonomously is an actual problem. The application of ferrfluids/ferroelastomers is one possibility for a wireless transfer of energy and control informations to a mobile system, based on undulatory locomotion. For this kind of locomotion the interaction between the ferrofluid and the magnetic field has to be known.

Flow of magnetic fluid layer

In [1–3] the motion of an incompressible magnetic fluid (MF) layer on an undeformable substrate, produced by a nonuniform magnetic field, is analyzed. The perturbation of the free surface is given, the corresponding average flow rate and the necessary magnetic field for it are defined.
Now we consider a direct problem of the flow of a viscous MF. In this case a traveling magnetic field is given, and the equation of the free surface and the corresponding average flow rate has to be found. We assume that the travelling magnetic field has the form:

$$H^2 = {H_0}^2 + A^2 \sin(kx - \omega t).$$

Here, H_0, A, k and ω are constants. The magnetic permeability of the fluid μ is assumed to be constant. The environment is unmagnetizable and the pressure on the free fluid surface is constant. In this case the body magnetic force is absent and the magnetic field manifests itself in a surface force acting on the free surface [4]. The gravity is taken into account.

The system of equations consists of the continuity and Navier-Stokes equations:

$$\operatorname{div} \vec{V} = \vec{0},$$

$$\frac{\partial \vec{V}}{\partial t} + (\vec{V} \cdot \nabla)\vec{V} = -\frac{1}{\rho} \operatorname{grad} p + \nu \cdot \triangle \vec{V} + \vec{g}.$$

Here, $\vec{V} = (u, w)$ and p are the velocity vector and the fluid pressure, ν is the kinematic fluid viscosity coefficients, ρ is the fluid density, $\vec{g}$ is the acceleration gravity vector, and t is time.
On the rigid substrate $z = 0$, the conditions of adhesion and non-flowing are satisfied:

$$\vec{V}(z = 0) = \vec{0}.$$

On the unknown free surface $z = h(x, t)$ (Fig. 1) conditions of two types, kinematic and dynamic ones, should satisfied.
The kinematic condition has the form:

$$\frac{dh}{dt} = \frac{\partial h}{\partial t} + u\frac{\partial h}{\partial x} = w.$$

The dynamic conditions of continuity of the normal and tangential stresses on the free surface $z = h(x, t)$ take the form:

$$\left[-p + \frac{\gamma}{R} - \frac{H^2}{8\pi}(\mu - 1)\right] \vec{n} + \tau_{ij} n^j \vec{e}^i = \vec{0}.$$

Here τ_{ij} are the viscous stress tensor components, R is the radius of curvature of the surface, $z = h(x, t)$, $\vec{n}$ is the vector of outward normal to the surface, $\vec{e}^i$ are the basis vectors, γ is the film surface tension coefficient. The magnetic field H is assumed to be fixed, since the non-inductive approximation $\mu - 1 \ll 1$.

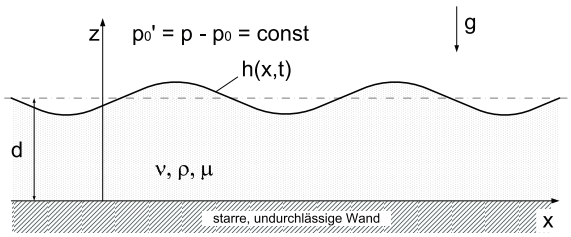

Figure 1: Magnetic fluid layer

The continuity equation is fulfilled with a flow function $\Psi(x, z, t)$, with

$$u = -\frac{\partial \Psi}{\partial z}, \;\; w = \frac{\partial \Psi}{\partial x}.$$

This fact makes it possible to reduce the problem to the search of one function $\Psi(x, z, t)$.

Dynamics of the magnetic fluid surface

In [5] the analytical solutions of the problem of the determination of the surface shape of the MF containing different magnetizable bodies (spherical and cylindrical) in uniform magnetic field are found.

In this paper the numerical solution described the dynamics of the surface shape of the MF containing a cylindrical body in the applied magnetic field is obtained. The applied vertical magnetic field H_∞ increases from zero to 1000 Oe, then it decreases from 1000 Oe to zero. So the magnetic field H_∞ depends on time by formula: $H_\infty = \alpha t$, $t < 1000$, $H_\infty = 1000 - \alpha(t - 1000)$, $t > 1000$. On Fig. 2 the surface shapes of the MF for different value of the increasing field (Fig. 2 a,b,c,d) and the decreasing field (Fig. 2 e,f,g,h) are given ($\alpha = 1$ Oe/sec). It is shown that for some critical values of the increasing field the MF volume breaks and the tow or free MF volumes appear (Fig. 2 b,d), and for some another critical values of the decreasing field the MF volumes join (Fig. 2 f,h). So hysteresis of the surface shape of the magnetic fluid is found. A comparison of the results of analytical and numerical researches with the experiments shows an acceptable agreement.

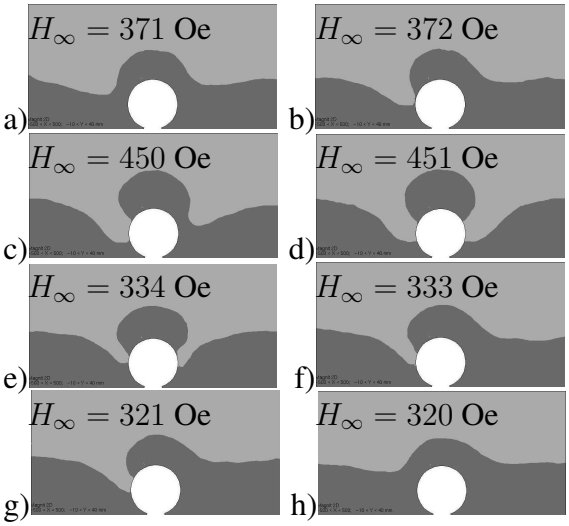

Figure 2: Magnetic fluid surface

Acknowledgments

This work is supported by Deutsche Forschungsgemeinschaft (DFG) (projects Zi 540-11/1 and Zi 540-14/1).

References

[1] Zimmermann K, Zeidis I, Behn C.: Mechanics of terrestrial locomotion. Springer, 2009.

[2] Zimmermann K, Zeidis I, Naletova V.A., Turkov V.A.: Waves on the Surface of a magnetic Fluid Layer in a traveling magnetic Field. JMMM, 268, 2004, pp. 227 - 231.

[3] Zimmermann K., Zeidis I., Naletova V.A., Turkov V.A., Bachurin V.E.: Locmotion based on a Two-Layers Flow of magnetizable Nanosuspensions. JMMM, 290 - 291, 2005, pp. 808 - 810.

[4] Rosenzweig R.E. Ferrohydrodynamics. Cambridge University Press, 1985.

[5] Zimmermann K., Naletova V.A., Zeidis I., Turkov V.A., Pelevina D.A., Böhm V., Popp J.: Surface of a magnetic fluid containing magnetizable bodies in an applied uniform magnetic field. Magnetohydrodynamics, Vol. 44, No. 2, 2008, pp. 175 - 182.

Phase transitions in ferrofluids induced by electrical field

I.Yu.Chuenkova[1], V. M. Kozhevnikov[1], M. I. Danilov[1], and S. S. Yastrebov[1]

L.Yu. Iskakova[2], A.Yu. Zubarev[2]

[1] *North-Caucasus Thechnical State University, Kulakova Ave 2, 355029, Stavropol, Russia*

[2] *Ural State University, Lenina Ave 51, 620083, Ekaterinburg, Russia*

It is well known that magnetic field induces various internal structural transfomations in ferrofluids. These transformations lead to significant change of macroscopical physical properties of these systems (see, for example [1]). Effect of electrical field on the phase behavior and properties of ferrofluids is studied significantly less. We present results of experiments which demonstrate rich set of equilibrium and dissipative phase transformations in ferrofluids subjected into external electrical field. It may open new promising perspectives of ferrofluid practical applications.

The ferrofluid under study consisted of the particles of Fe_3O_4 suspended in kerosene, stabilized by the olein acid. The mean diameter of the ferroparticle was 15 nm, the particle volume concentration φ_0=0.04. The ferrofluid was placed between two glass plates covered with thin electroconductive layer of $In_2O_5 \cdot SnO_2$. The thickness of the ferrofluid layer was 20 μm.In our experiments electrical current J through the cell has been controlled and kept constant, the electrode potential difference U has been detected. To control the current we used the series connection with voltage source and resistors of the resistances R=1.5; 4; 5 and 10 MOhm. The optical observations of the ferrofluid structures have been carried out both in the reflected and transmitted light.

The experiments with the resistance R=1.5MOhm have demonstrated that in the region of the current density j=0 – 0.017A/m^2 the ferrofluid was macroscopically homogeneous. In the region j=0.017 – 0.021 A/m^2 dense cylindrical-like cells (domains), shown in Fig.1a, have been occurred in ferrofluid. The cell diameter increased from 25 to 80 μm with the electrical current.

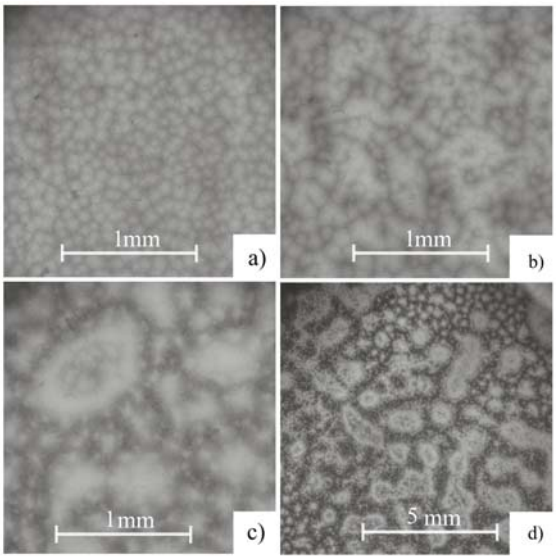

Fig.1. Structures in the ferrofluid layer under the permanent current density j and permanent voltage U_p. a $-j$ = 0.025 A/m^2, U_p = 9 V; b – j = 0.037 A/m^2, U_p = 12 V; c $-j$ = 0.056 A/m^2, U_p = 17 V, d – j= 0.073 A/m^2, U_p = 22 V. Light regions correspond to the relatively low concentration of ferroparticles, the dark ones – to the high concentration.

When the current density j exceeded 0.021A/m^2, auto-oscillations of the voltage, illustrated in Fig.2, appeared. Appearance of these auto-oscillations under the action of the electrical current is qualitatively new phenomenon which has not been detected in ferrofluids subjected into magnetic fields.

Appearance of the voltage auto-oscillations was accompanied by the qualitative change of the concentration structures – instead of cylindrical-like they became irregular and labyrinth-like (Fig. 1, b-d). The irregular structures existed up to the current density j=0.1A/m^2. When j increased from 0.021 to 0.1 A/m^2, the characteristic size of these structures increased from 500 to 2000 μm.

The transition from the cylindrical to the irregular structures was smooth and in the region j=0.013-0.015 A/m^2 both types of these structures existed simultaneously.

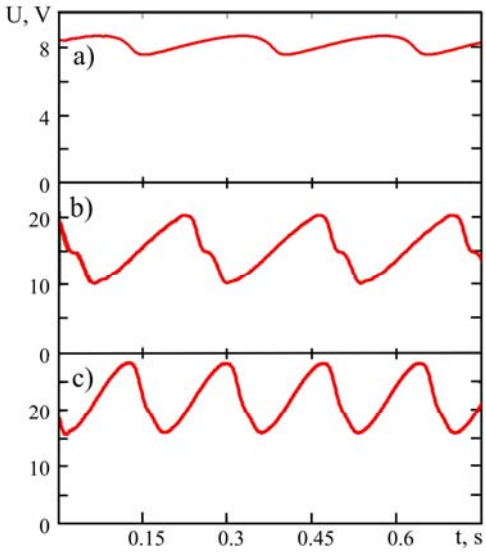

Fig.2. The voltage U auto-oscillations on the cell electrodes when the current density is: a – j=0.025 A/m^2, b – j = 0.048 A/m^2, c – j=0.085 A/m^2

When current density j exceeded 0.1 A/m^2 the self-oscillation disappeared. At the same time labyrinth-like structures became unstable and transformed into "moving" structures which moved in a horizontal plane parallel to the electrodes. Simultaneously spiral waves near the electrode surface appeared (Fig.3.)

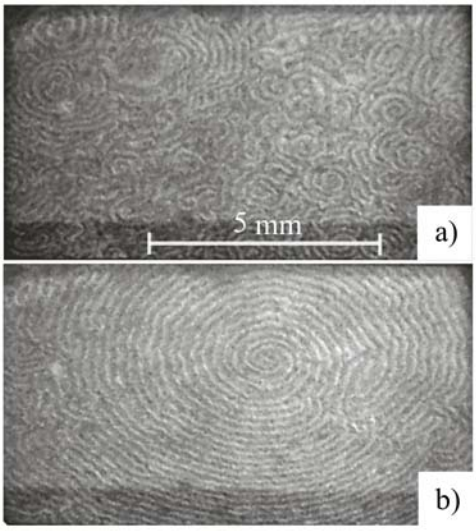

Fig.3. The spiral waves: a) – j = 0.102 A/m^2, ; b) – j = 0.072 A/m^2, .

The transition from the irregular labyrinths to the moving spiral waves was sharp and was accompanied by appearance of the convective flow in the ferrofluid. While decreasing of the electrical current the moving waves existed up to j=0.048 A/m^2. Then the motionless labyrinths and the voltage auto-oscillations restored. Thus the transition from the labyrinths to the moving structures had the hysteresis character.

Theoretical description of the structural transformations included: a) equation of diffusion of the ferroparticles, polarized by the electrical field. This equation took into account the polar interaction between particles and the ponderomotive forces, acting on the particles, as well. b) Equation for the fluid electrical charge density. c) The Poissonian equation for the electrical potential. d) Electrochemical boundary conditions on the electrodes.

These equations present nonlinear problem for the particle concentration, local electrical charge density and electrical potential as well. Linear analysis of this system shows that the homogeneous state of the ferrofluid is unstable when electrical current j exceeds some critical magnitude; evolution of the instability takes place in the auto-oscillation regime and leads to appearance of the labyrinth-like structures.

In conclusion, our new types of equilibrium and dissipative phase transitions in ferrofluids subjected into electrical field have been detected. Theoretical model which describes these transformations is suggested.

This work has been supported by the Russian Fund of Fundamental Investigations, grants 07-02-00079, 07-01-960769 Ural, Fund CRDF, PG07-005-02, grants of the Russian Federal Education Agency, projects 2.1.1/2571 and 2.1.1/1535 .

References

[1]. S.Odenbach, *Magnetoviscous Effects in Ferrofluids*, Springer, 2002; *Ferrofluids, Magnetically Controllable Fluids and their Applications*. Ed. S.Odenbach, Springer, 2002

Influence of homogeneous magnetic fields on the flow of a ferrofluid in the Taylor–Couette system

S. Altmeyer, Ch. Hoffmann, A. Leschhorn, M. Lücke

Institut für Theoretische Physik
Universität des Saarlandes
D-66123 Saarbrücken, Germany

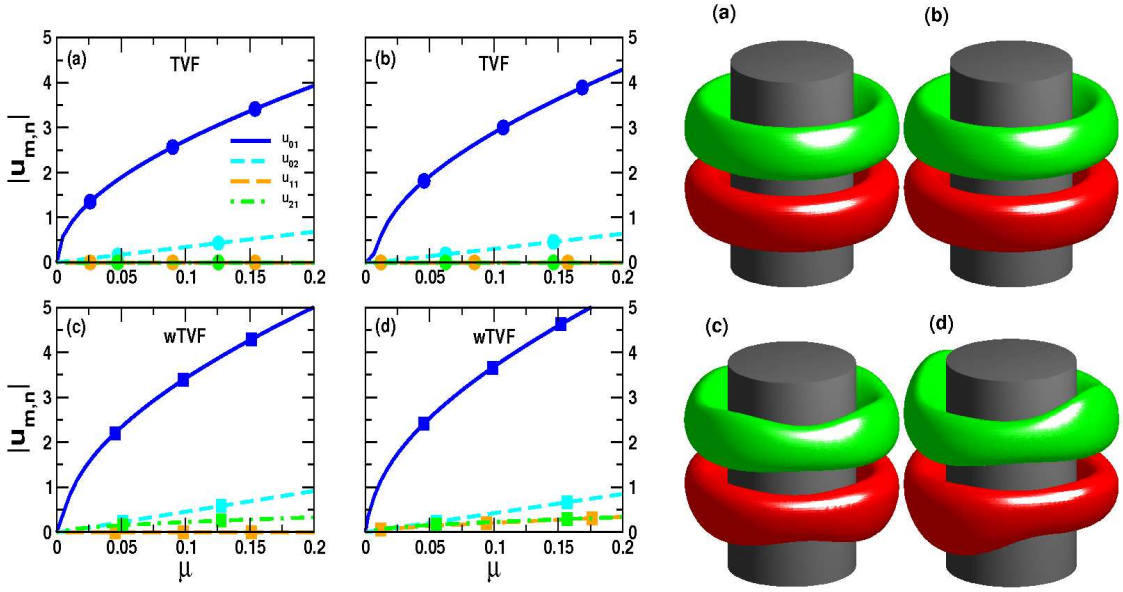

The influence of a homogeneous magnetic field on a ferrofluid is investigated numerically in the Taylor–Couette system consisting of a viscid fluid in the gap between two concentric, independently rotating cylinders. This is done by solving the full Navier-Stokes equations (NSE) with a combination of a finite difference and a Galerkin method for a fixed axial periodicity length.

In the literature one finds many models which describe the magnetization dynamics in ferrofluids. For our numerical calculations, we use an approximation analogous to the model of Niklas et al. [1, 2], i.e. magnetization is stationary and lies near the equilibrium magnetization for sufficently small relaxation times.

Structure, dynamics, symmetry properties, bifurcation and stability behaviour of Taylor vortex flow (TVF) and spiral vortex flow (SPI) that all appear via primary bifurcations out of the unstructured basic flow are investigated for pure axial (H_z) as well as pure transversal (H_x) magnetic fields and a combination of them. The left figure depicts the bifurcation behaviour of TVF using azimuthal (m) and axial (n) Fourier components $u_{m,n}$ of the radial velocity u depending on the inner cylinder rotation speed R_1 given by the reduced control parameter

$$\mu := R_1(H_x, H_z)/R_{1,c}(H_x, H_z) - 1.$$

The right figure presents isosurfaces of the azimuthal vorticity $\partial_z u - \partial_r w$ (u: radial, w: axial velocity component) of the primary bifurcating structure. The upper (lower) iso-surface tubes represents negative (positive) values of vorticity. We present results for outer cylinder at rest

and different combinations of H_x and H_z (a)-(d).

(a) $H_x = 0, H_z = 0$: stable, toroidally closed, and rotationally symmetric TVF bifurcate out of the basic state.

(b) $H_x = 0, H_z > 0$: onset of TVF is shifted towards larger R_1.

(c) $H_x > 0, H_z = 0$: see (d)

(d) $H_x > 0, H_z > 0$: onset is shifted towards larger R_1; additionally, higher azimuthal modes are stimulated and the primary bifurcating structure now becomes 'modulated', namely wavy Taylor vortices (wTVF).

Remarks:
(1) The wTVF, generated via $H_x > 0$, is a *non-rotating* structure with a pinned phase in contrast to 'classic' wavy vortices which occur via secondary bifurcations out of TVF and *rotate* azimuthally.
(2) The influence of magnetic forces on SPI and wSPI is analogous to the above discussed Taylor vortex case and is also presented.

References

[1] M. Niklas, Influence of Magnetic Fields on Taylor Vortex Formation in Magnetic Fluids, Z. Phys. B, **68**, 493 (1987)

[2] M. Niklas and H. Müller-Krumbhaar and M. Lücke, Taylor–Vortex flow of ferrofluids in the presence of general magnetic fields, J. Magn. Magn. Mater., **81**, 29 (1989)

Ferrofluids for inhalative Chemotherapy

R. Baumann, G. Glöckl, S. Nagel, W. Weitschies

Institute of Pharmacy, Ernst-Moritz-Arndt-University, D-17487 Greifswald, Germany

Introduction

Lung cancer, especially non-small cell lung cancer, is difficult to treat with poor prognosis for patient survival. Although there are established drugs, these do not show any effect in more than 50% of the patient population. It may be possible to accumulate effective drug doses in diseased lung regions by an inhalative magnetic drug targeting.

Aerosols offer the possibility of locoregional drug delivery allowing for far smaller doses of chemotherapeutic agents and reduction of systemic exposure. One of the major drawbacks of inhalation is the loss of chemotherapeutic drugs due to exhalation of droplets smaller than 1 µm which are not deposited in the airways. In this case, the magnetic retention forces acting on the aerosol droplets may increase the deposition probability in the diseased lung. In order to avoid therapy-limiting adverse reactions caused by the deposition of large droplets in the upper airways the reduction of droplet size is also a major concern.

Materials and Methods

The basis of the magnetic aerosol is a waterbased magnetite citrate ferrofluid. Modified according to a method by Buske ferrous chloride hydrate ($FeCl_2$-$4H_2O$) and ferric chloride hydrate ($FeCl_3$-$6H_2O$) are solved in water. A solution of ammonium hydroxide is added to precipitate magnetic nanoparticles. The resulting gel is stirred, heated and washed. Citric acid is added to coat the magnetic nanoparticles in order to prevent aggregation and sedimentation. Then, the ferrofluid is stirred, heated and washed again. The core size of the magnetite nanoparticles determined by vibrating sample magnetometry using Chantrell´s method [1] is about 10 nm.

Droplets of varying size were generated by using different nebulizers with differing atomizing principles. The atomizer eFlow (Pari GmbH, Germany), which generates aerosols using a vibrating membrane, creates a median mass diameter (MMD) of 8 µm and the pneumatic nebulizer Pari Boy SX (Pari GmbH, Germany) 3 µm. Furthermore, we used glycerol, ethanol, polyvinylpyrrolidone (PVP) and sodium chloride as additives in order to vary the droplet size of aerolized ferrofluid.

The droplet size was measured by laser diffraction.

The aerosol was sprayed centrally into the magnetic field of two opposing circular disc magnets in varying distances. The magnetic field gradients around the magnetic poles were calculated using Mathematica. Magnetic particles deposited onto flappers were decomposed and analyzed using atomic absorption spectrometry.

Results and Discussion

The strongest magnetic field gradients were generated at the magnets edges of the opposing circular disc magnets. The gradients near the pole surface were up to 120 T/m. At a distance of 2 cm between the two opposing magnets a nearly homogeneous gradient of 15 to 20 T/m was achieved. The gradients decrease with increasing distance.

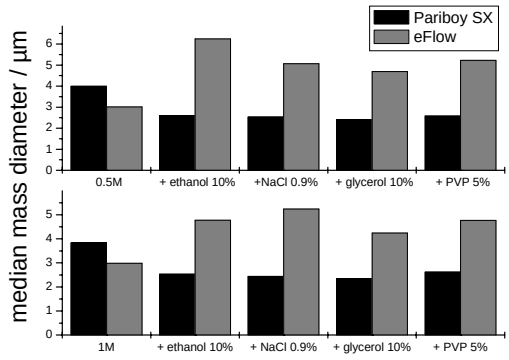

Fig. 1: MMD of aerosol droplets generated by Pariboy SX and eFlow measured by laser diffractometry.

Ethanol, glycerol, sodium chloride and PVP reduce the MMD of the droplets generated by Pariboy. The droplet size of eFlow is increased by addition of adjuvants. High fluctuations in aerosol droplet size created by eFlow were observed which do not relate to surface tension or density.

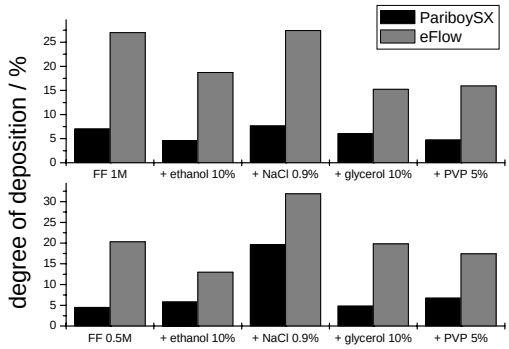

Fig. 2: Degree of aerosol deposition of 1M (top) and 0.5M (bottom) ferrofluid and influence of ethanol, sodium chloride, glycerol and PVP at 20 mm distance between magnetic poles.

Atomic absorption spectrometry showed that up to 27% of iron were intercepted onto the paper. The deposited amount was reduced with dilution of the ferrofluid. The best deposition was achieved by eFlow. This was most likely caused by the lower flow velocity compared to the pneumatic nebulizer and the large droplet size of up to 6.5 µm that is generated by the vibrating membrane. Large droplets contain more iron nanoparticles and are deflected easier. But this high deposition is not applicable for the magnetic drug targeting. Aerosol droplets of this size only reach the upper airways and lead to adverse reactions due to high deposition in mouth and trachea.
The addition of sodium chloride increased the deposition of ferrofluid. On the contrary ethanol, glycerol and PVP decreased the ferrofluid deposition.

Conclusion

The highest degree of deposition was reached by eFlow generating large aerosol droplets which are not applicable for MDT. Future effort will be directed towards the generation of smaller droplets with diameters between 0.5 µm and 1 µm.

References

[1] Chantrell, R. W.; Popplewell, J.; Charles, S. W. *IEEE Trans. Magn.* **1978,** 14, (5), 975-977.

A simple aminoalkyl siloxane-mediated route to functional magnetic metal nanoparticles and microspheres

A. Gorschinski[1], W. Habicht,[1] O. Walter,[1] E. Dinjus,[1] S. Behrens[1]

[1] *Forschungszentrum Karlsruhe, Postfach 3640, 76021 Karlsruhe*

The synthesis of superparamagnetic metal nanoparticles has been previously described, *e.g.*, by applying $Co_2(CO)_8$ with organometallic precursors (aluminium trialkyls),[1] or polysiloxane micelles.[2] Besides the control of size, structure, and composition, surface properties and functionalities of nanoparticles are an important issue of research, *e.g.*, for further preparing functional multicomponent nanostructures or nanocomposites.

We use amino-functionalized siloxanes not only to directly control particle nucleation and growth by coordinating to the metal surface but also to provide reactive siloxane groups on the particle surface as a functional interface for further deposition of oxides, such as SiO_2 and TiO_2. This procedure permits the synthesis of Co and Fe nanoparticles of various sizes by thermolysis of $Co_2(CO)_8$ or $Fe(CO)_5$ in solution, respectively, and the preparation of magnetic microspheres.

As show by UV-visible and FTIR spectrometry the reaction proceeds via a homomolecular disproportionation in which the uncharged $Co_2(CO)_8$ initially disproportionates into cobalt(II) cation and cobalt carbonylate anion. There are several key parameters that control the growth aspects including type and concentration of metal precursor and siloxane, metal to siloxane ratio, reaction temperature, heating rate, etc. The delicate choice of these key parameters allows to tune, *e.g.*, the size of the particles. After surface passivation with low doses of oxygen (*smooth oxidation*), the nanoparticles show a good resistance to oxidation. The presented procedure can be also applied for the synthesis of iron nanoparticles by decomposing $Fe(CO)_5$ in the presence of APTES. The size, structure, and magnetic properties of the particles were characterized by TEM, EDX, XPS, Mössbauer spectroscopy, XRD, AES-ICP, and magnetic measurements.

The applied bifunctional siloxane compound not only controls particle formation by complexation of cobalt but also serves as a coupling agent for SiO_2 and TiO_2 deposition, resulting in functional magnetic microspheres. Such magnetic microspheres are typically based on magnetic iron oxide nanoparticles. Microspheres equipped with magnetic metal nanoparticles are interesting since they exhibit a much higher M_s and magnetophoretic mobility. However, Co is easily oxidized which is probably among the reasons why much less examples of $Co@SiO_2$ microspheres exist in the literature. Magnetic $Co@SiO_2$ microspheres are obtained by adding and heating TEOS in water/ethanol in the presence of the APTES-functionalized Co nanoparticles. The $Co@SiO_2$ microspheres can be further functionalized with a molecular Rh precursor via formation of a phosphine complex and used as a magnetically recyclable catalyst in hydroformylation reactions (hydroformylation of 1-octene). Magnetic $Co@TiO_2$ microspheres are obtained by hydrolysis of titanium (IV) n-butoxid in the presence of the Co nanoparticles. TiO_2 is typically applied as photocatalytic system for the treatment of various biological, organic, or inorganic pollutants in water.[3]

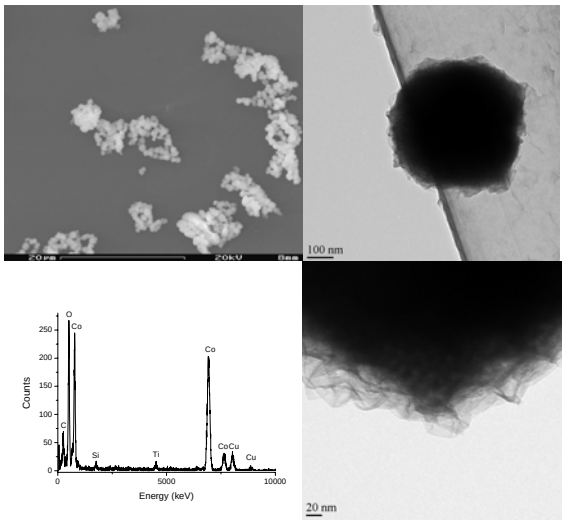

Fig. 1. SEM and TEM images and EDX spectrum of magnetic TiO_2 microspheres.

References

[1] H. Bönnemann, W. Brijoux, R. Brinkmann, N. Matoussevitch, N. Waldöfner, N. Palina, and H. Modrow, *Inorganica Chimica Acta*, **2003**, 350, 617.

[2] J. Stevenson, M. Rutnakornpituk, M. Vadala, A. Esker, S. Charles, S. Wells, J. Dailey, and J. Riffle, *J. Magn. Magn. Mater.*, **2001**, 225, 47.

[3] X.M. Song, J.M. Wu, and M. Yan, *Thin Solid Films*, **2009**, 517, 4341.

Artificial Cilia:
Nature Inspired Microactuators for use in Microfluidic Systems

J. Belardi, N. Schorr, O. Prucker, J. Rühe[1]
S. Wells. V. Pattel[2]

[1] *Departement of Microsystems Engineering (IMTEK), Georg Köhler Allee 103, 79110 Freiburg, Germany*
[2] *Liquids Research Limited, Bangor, Gwynedd, United Kingdom, LL57 2UP*

Handling of liquids in sub millimeter sized channels is essential for microfluidic systems. We developed microactuators inspired by small oscillating hairs called Cilia found in nature. Our microactuators are based on polymers filled with magnetic nanoparticles. These particle filled polymers can be structured into artificial Cilia by photolithography.

Micro fluidic systems

In micro fluidic systems small amounts of liquids are handled in sub millimeter sized channels. Microfluidic systems can be used to miniaturize complete laboratories into credit card sized lab-on-a-chip platforms. Lab-on-a-chip platforms allow fast and automatic analysis of liquids even with small amounts of material.
Manipulation of liquids, especially mixing, is challenging as inertia is negligible and no turbulence occur. Active micromixers are difficult to integrate while passive mixers cannot be turned off if no mixing is desired.

Cilia: natural microactuators

Nature developed small oscillating hairs called Cilia for local manipulation of liquids. Cilia can be found on microorganisms like Paramecium as well as in larger organisms.
Each Cilium performs an asymmetric motion and moves a small amount of liquid. Surfaces covered with thousands of Cilia working together are very effective to generate flow. Paramecium for example uses Cilia covered surfaces for propulsion. Darnton et al attached bacteria to a surface and proved that this "bacterial carpet" can move liquids[1].

Nature inspired microactuators

Inspired by nature, artificial Cilia have recently been published. Toonder et al described artificial Cilia actuated by an electrostatic force[2]. Evans et al fabricated nanorods by curing PDMS filled with superparamagnetic particles inside templates[3]. They showed that these "biomimetic Cilia" react to magnetic fields.
We developed a photosensitve polymer based on n-Butylacrylate (nBA) and Methacryloyloxybenzophenone (MABP) [4]. nBA was chosen because of its elasic modulus at room temperature. The Polymer was mixed with surfactant stabilized superparamagnetic nanoparticles (LRL, Bangor, UK). This composite material could be processed into artificial Cilia by photolithography.

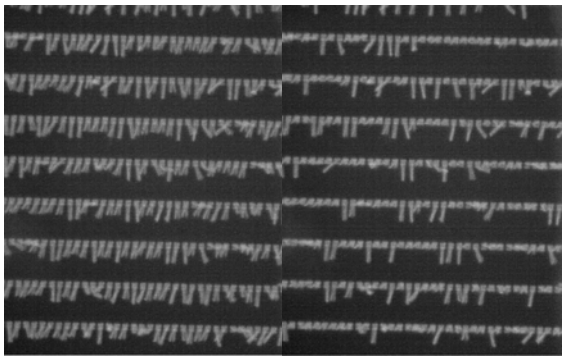

Figure 1: Artificial Cilia in liquid enviroment, actuated by magnetic force. The spacing between two cilia rows is 90µm.

The artificial Cilia were attached to silicon substrates with one end using a patterned sacrifcial layer[6,7]. These substrates were integrated into microfluidic channels and actuation by an external magnetic field in liquid environment was proven.

Acknowledgments

We gratefully acknowledge financial support from the EU 6th Framework program (NMP4-CT-2006-033274).
Thanks to Simon Bodendorfer, Marco Beaumont and Mathias Lauterbach for technical assistance.

References

[1] N. Darnton, L. Turner, K. Breuer, H. C. Berg, *Biophysical Journal* **2004**, *86*, 1863.
[2] J. d. Toonder, F. Bos, D. Broer, L. Filippini, M. Gillies, J. d. Goede, T. Mol, M. Reijme, W. Talen, H. Wilderbeek, V. Khatavakar, P. Anderson, *Lab on a Chip* **2008**, *8*, 533.
[3] B. A. Evans, A. R. Shields, R. L. Carroli, S. Washburn, M. R. Falvo, R. Superfine, *Nano Letters* **2007**, *7*, 1428.
[4] R. Toomey, D. Freidank, J. Rühe, *Macromolecules* **2004**, *37*, 882.
[6] O. Prucker, C. A. Naumann, J. Ruhe, W. Knoll, C. W. Frank, *Journal of the American Chemical Society* 121, 8766-8770 (1999).
[7] K. Schuh, O. Prucker, J. Ruhe, *Macromolecules* 41, 9284-9289 (2008).

Synthesis and characterisation of uniaxial ferrogels with Ni nanorods as the magnetic phase

P. Bender[1], A. Günther[1], A. Tschöpe[1], R. Birringer[1]

[1]*Technische Physik, Universität des Saarlandes, Postfach 151150, Geb. D2 2, D-66041 Saarbrcken*

Nanorods with a diameter of approximately 15 nm and high aspect ratios (n $>$ 3) were synthesised via current-pulsed electrodeposition of Nickel into porous alumina templates. The nanorods were released from the template by dissolution of the alumina layer in aqueous NaOH to which PVP (polyvinylpyrrolidone) was added as surfactant. A thorough washing procedure resulted in stable colloidal dispersions of the magnetic particles. These magnetic fluids were used to prepare gelatine-based ferrogels. In particular, uniaxial ferrogels were obtained by aligning the uniaxial magnetic nanoparticles with an external homogeneous magnetic field prior to gel formation. The development of the magnetic anisotropy during the sol-gel transition as well as the influence of the elastic properties of the hydrogel matrix were analysed using magnetization measurements.

Magnetorheological characterization of a ferrofluid based on the clustered iron oxide nanoparticles

D. Borin[1], R. Müller[2], S. Odenbach[1]

[1] *Technische Universität Dresden, Chair of Magnetofluiddynamics, 01062, Dresden, Germany*
[2] *Institute of Photonic Technology, Albert-Einstein-Strasse 9, 07745, Jena, Germany*

Recently [1], magnetic iron oxide nanoparticles coated with carboxymethyldextran shell were prepared and magnetically characterized. It was found that grains with diameter of 10-30 nm form clusters with size of 50-70 nm covered with a dextran shell. The mean hydrodynamical diameter of clusters measured by PCS was about 100 nm. The goal of the current study was the investigation of the magnetorheological properties of a ferrofluid based on these clusters.

The cluster particles for the ferrofluid sample used in this work were prepared following the procedure described in [1], although particles were suspended in vacuum oil P3 Pfeiffer with a concentration of about 2 vol. %. The stabilization of the magnetic particles with oleic acid has been performed according to [2]. The sample was diluted to 0.1 vol.% for the rheological experiments.

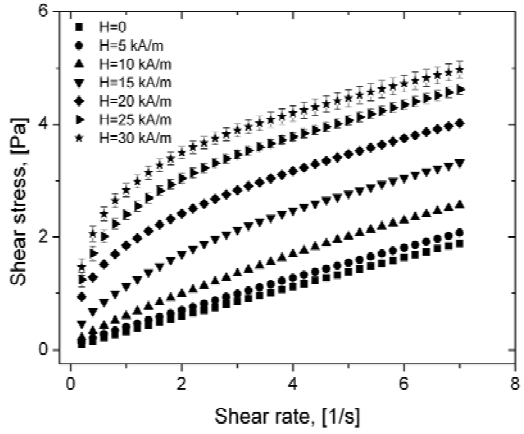

Figure 1. Flow curves for different magnetic field strength.

The flow curves (figure 1) were measured using a shear rate controlled rheometer [3]. In the absence of a magnetic field the behavior of the sample is Newtonian, but as the applied field rises, the apparent viscosity of the fluid increases considerably. For small shear rates the flow curves are strongly non-linear and the sample shows the typical shear-thinning behavior.

Moreover the dependence of the static yield stress on magnetic field strength has been measured with the shear stress controlled rheometer [4]. The results of the experiments are shown in figure 2.

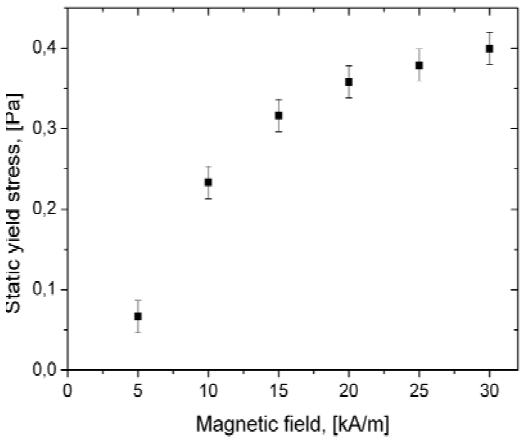

Figure 2. Static yield stress plotted as a function of magnetic field strength.

The increase of yield stress with magnetic field strength is sharp for low fields and it tends to saturate afterwards. On the one hand this behavior can be explained with the magnetic saturation of particles and on the other hand with the fact that only a small number of structures can be formed due to the low amount of magnetic particles in the fluid (0.1 vol.%). A comparable

behaviour has earlier also been found in experiments performed with low concentrated ferrofluids based on nanodisk cobalt particles [5].

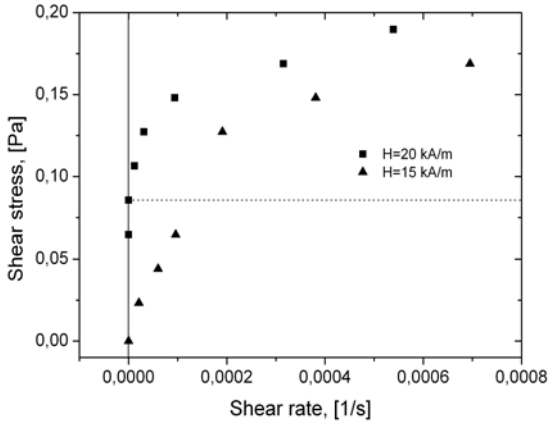

Figure 3. Flow curves measured with a shear stress controlled rheometer for H=15 kA/m and H=20 kA/m. The dashed line indicates the the yield stress value of 0,086 Pa for H=20 kA/m.

In contrast to [5] the flow curves shown in figure 3 for two different magnetic field strength show a dynamic yield stress. For H=20 kA/m a yield stress of 0,086 Pa has been measured, whereas for H=15 kA/m no yield stress was observed. The particle clusters are obviously able to form stable structures despite of the presence of a shear flow due to their large size and total magnetization for the stronger magnetic field. That means that the magnetic cluster-cluster interaction exceeds the stress needed to continuously break the aggregates for this field strength. This behavior is similar to magnetorheological fluids, which normally contain multidomain magnetic particles of micron size.

The performed investigation shows that a ferrofluid based on clusters of iron oxide nanoparticles coated with an oleic acid shell can be accounted to a kind of intermediate magnetically controllable fluids between classical ferrofluids and MR fluids. This ferrofluid is a very promising candidate for further research on the complex processes, occurring due to the joint action of magnetic field and shear flow. Beside this, the synthesis and characterization of such fluids may be the next step on the way to the development of stable magnetic colloids with significant magnetorheological effects.

Acknowledgments

Technical assistance of Thomas Gundermann and Benjamin Fischer in the preparation of the measurements is greatly acknowledged.

References

[1] S Dutz, W Andrä, R Hergt, R Müller, Ch Oestreich,Ch Schmidt, J Töpfer, M Zeisberger and M Bellemann, J. Magn. Magn. Mater. 311 (2007) 51

[2] R Müller, R Hiergeist, H Steinmetz, N Ayoub, M Fujisaki and W Schüppel J. Magn. Magn. Mater. 201 (1999) 34

[3] S Odenbach, T Rylewicz, M Heyen, J. Magn. Magn. Mater 201 (1999) 155

[4] H Shahnazian and S Odenbach, Appl. Rheol. 18(5) (2008) 54974

[5] H Shahnazian, D Gräf, D Borin and S Odenbach, J. Physics D: Appl. Phys. (submitted)

Colloidal Stability of Water Based Dispersions Containing Large Single Domain Particles of Magnetite

N. Buske [1], S. Dutz [2]

[1] *Magnetic Fluids, Köpenicker Landstr. 203, 12437 Berlin, Germany*
[2] *Institute of Photonic Technology, Albert-Einstein-Str. 9, 07745 Jena, Germany*

Definition and motivation

The crystal size of Large Single Domain Particles (LSDP) of magnetite is assumed to range between 20 und 100 nm. In this region the particles show increasing coercivity and relative remanence with increasing particle diameter [1].

The extraordinary magnetic properties of these particles and the corresponding dispersions can be used in magnetorelaxometry (MRX), magnetic resonance imaging (MRI), magnetic particle imaging (MPI), hyperthermia, drug targeting, and magnetofection.

The preparation problem is to establish a sufficient colloidal stability. This problem will be discussed here from the point of the DLVO-theory as well as with some experimental test results.

Preparation of LSDP-dispersions

Adopting an idea by NISHIO et al. [2], the LSDP were prepared by slow oxidation of ferrous chloride solutions with sodium nitrate at alkaline conditions (pH = 12) under inert N_2 atmosphere.

The preparation process was modified to obtain relatively small 20-25 nm magnetite LSDP in order to increase the probability for colloidal stabilization. After accomplishing LSDP-synthesis, the particles were dispersed by addition of hydrochloric acid. In the second step, the particles were covered with citric acid, carboxylated polysaccharides or bilayers of oleoylsarcosine to obtain water based dispersions, cf. Fig.1.

Results

Generally, the obtained LSDP-dispersions consisted of two parts:

a) A concentrated sediment of agglomerated particles,
b) The supernatant of a diluted sedimentation stable dispersion.

The particles of b) could be concentrated by evaporation of water or by sedimentation in a strong magnetic field gradient.

From selected samples TEM magnitudes, hydrodynamic size, Zeta-potential, magnetic properties and XRD indicated 20-25 nm core sizes of colloidal stable dispersion, in accordance with estimations according to DLVO-theory.

According to our hypothesis, the LSDP syntheses should proceed via a green rust intermediate as suggested by studies with similar reaction conditions [3].

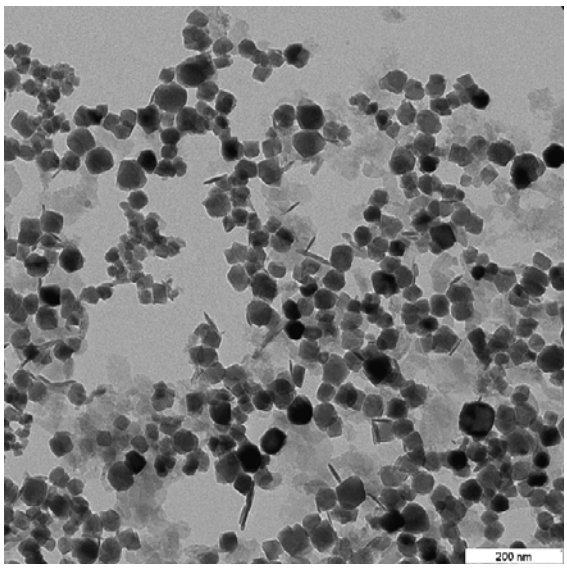

Fig. 1: TEM image of 20-25 nm LSDP, bilayer stabilized

References:

[1] S. Dutz. Nanopartikel in der Medizin. *Verlag Dr. Kovač*, Hamburg, (2008).
[2] K. Nishio, M. Ikeda, N. Gokon, S. Tsubouchi, H. Narimatsu, Y. Mochizuki, S. Sakamoto, A. Sandhuc, M. Abe, H. Handa. *J. Magn. Magn. Mater.* 310: 2408–2410, (2007).
[3] C.K. Vogt. *Dissertation* TH Karlsruhe (2006).

Adsorption and self-organization properties of semi-flexible magnetic filaments

Pedro A. Sánchez [1], Joan J. Cerdà [2] Tomás Sintes [1], V. Ballenegger[3], Oreste Piro[1] and Christian Holm[2]

[1]*Instituto de Física Interdisciplinar y Sistemas Complejos, IFISC (CSIC-UIB), Universitat de les Illes Balears, 07122 Palma de Mallorca, Spain*
[2]*Institute for Computational Physics. Universität Stuttgart. 70569 Stuttgart, Germany* [2]*Institut UTINAM, Université de Franche-Comté, CNRS, 16, route de Gray, 25030 Besançon cedex France.*

Despite magnetic filaments have been used by nature since long time ago in magnetostatic bacterias [1], Humankind has just begun to caress its potential for novel applications [2]. The continuous improvements on the synthesis of artificial magnetic filaments, reducing the size of the magnetic particles and improving the grafting between particles, has set the onset in the creation of particles which resemble magnetic polymers but in the scale of tenths of nanometers. In difference to the magnetic polymers [3], the magnetic filaments can exhibit nonzero magnetization at room temperature. The study of the physical properties of such systems via numerical simulations can help to elucidate the potential of the magnetic filaments for practical applications.
In the present work we focus on the study of the adsorption process and phase transitions of such magnetic filaments near attractive surfaces. Extensive Molecular Dynamics simulations in 2+1 dimensions using a coarse bead-spring chain model have been performed. The effects of the temperature, dipolar coupling parameter of the magnetic particles, stiffness, chain length, fraction of magnetic particles, and concentration of chains on the adsorption and phase transitions near magnetic and non-magnetic surfaces are reviewed.

Acknowledgments
J.J. Cerdà and C. Holm want to thank the project DFG grant HO 1108/12-1 and the TR6. All authors are grateful to the DAAD organization and the French *Ministère des affaires étrangères et européennes* for providing financial support.

References

[1] A. Komeili *et al*, *Science* **311**, 242 (2006)

[2] S. J. Blundell *et al*, *J. Phys. Condens. Matter* **16**, R771 (2004)

[3] M. Kamachi, *J. Macromol. Sci.* **C42**, S41 (2002)

Distribution of leukocyte subpopulations after short-term application of magnetic core-shell nanoparticles

B. Müller[a], J. Wotschadlo[a,b], K. Pachmann[a], N. Buske[c], Th. Heinze[b], J.H. Clement[a]

a) Clinic for Internal Medicine II, Dept. Hematology and Oncology, University Clinic Jena, Erlanger Allee 101, D-07747 Jena, Germany ;e-mail: joachim.clement@med.uni-jena.de;
b)Center of Excellence for Polysaccharide Research, Friedrich Schiller University of Jena, Humboldtstrasse 10, D-07743 Jena, Germany
c) MagneticFluids, Köpenicker Landstrasse 203, D-12437 Berlin, Germany

Cancer is one of the main causes of death. Most of the cancer patients do not die from the primary tumor but from distant metastases which develop during the progression of cancer. Key events are the establishment of tumor vasculature and the invasion of tumor cells into the surrounding tissue and the circulation. These cells are suspected to be an origin of distant metastases. Therefore there is a need to eliminate these cells from the circulation especially from the peripheral blood.

We could show previously, that the time-course of the labeling of tumor cells and leukocytes from peripheral blood differs dramatically within the first 20 minutes with a maximum discrepancy between 8 and 12 minutes.

In this work, we analysed the effect of magnetic core shell nanoparticles on the survival of leukocytes in general and the distribution of leukocyte subpopulations during incubation and subsequent separation.

Leukocytes were prepared by erythrocyte lysis from whole blood samples. Cells were inoculated with magnetic core/carboxymethyl-dextran nanoparticles with an average magnetite/maghemite core TEM-size varying between 3 and 15 nm for 4 min to 30 minutes. The incubation medium (PBS/EDTA) contained 2.5% human plasma. Magnetically labeled cells were separated by MACS using a SuperMACS and MS columns. The separated cells were counted and analyzed by FACS according to size and granularity. T-Lymphocytes were identified by CD3 and B-Lymphocytes by CD19.

At first we analysed the labelling of leukocytes over a period of 30 minutes. The leukocytes accumulated in the positive fraction continuously from 10% after 4 minutes to 42% after 30 minutes. With regard to the subpopulations, granulocytes represented the majority of cells in both, the positive and negative fraction. Most of the lymphocytes as central components of the immune system remained in the negative fraction. The distribution of T-lymphocytes differs dramatically from B-Lymphocytes. Whereas the amount of B-Lymphocytes differed only slightly over an incubation time of 16 min, the number T-Lymphocytes in the positive fraction increased 2.5-fold from 4 minutes to 16 minutes. At 4 minutes 20% of total lymphocytes in the positive fraction were T-Lymphocytes. This portion rose to 70% after 16 minutes. A critical parameter is the integrity of the leukocytes especially in the negative fraction. During the incubation the loss of cells increased from 27% (4 min) up to 50% (30 min).

In conclusion, the enrichment of tumor cells from peripheral blood with regard to the preservation of leukocytes in the negative fraction should be limited to 4 to 12 minutes incubation time.

This work was supported by DFG priority program 1104, grant CL 202/1-2.

Magnetic traveling-stripe-forcing: transport and pattern transformation

Th. Friedrich[1], I. Rehberg[1], R. Richter[1]

[1]*Experimentalphysik V, Universität Bayreuth, Germany*

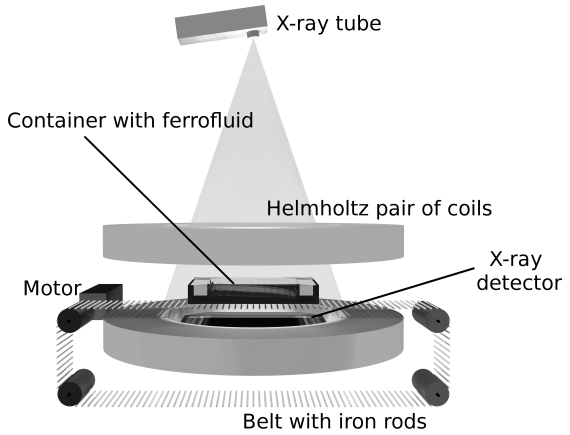

Figure 1: Sketch of the experimental setup

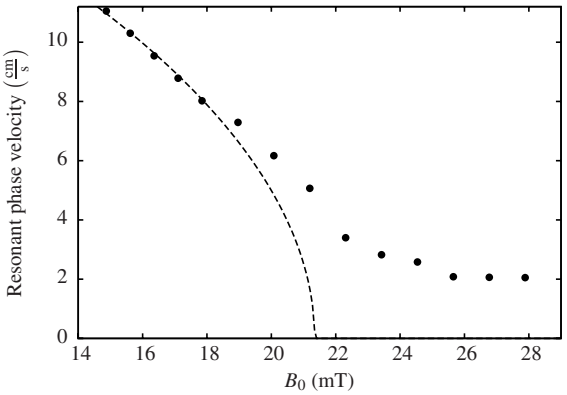

Figure 2: Comparison between theory (dashed line) and experimental data (points)

We measure the response of a layer of ferrofluid to a spatio-temporally modulated magnetic field[1] of the shape

$$B(x,t) = B_0 + \Delta B \sin(\omega t - k_c x) \quad (1)$$

by means of X-rays[2, 3], as sketched in Fig. 1. We unveil the formation of a liquid ramp as a consequence of the lateral transport of ferrofluid [4, 5]. The inclination of the liquid ramp as a function of the traveling velocity of the magnetic modulation exhibits a maximum. This resonant phase velocity is compared to the phase velocity of plane surface waves of a magnetic liquid, where the nonlinear magnetization of the liquid is taken into account. Figure 2 shows, that for undercritical fieldstrength, the data points nicely agree with the calculated curve.

As B_0 reaches the critical value B_c, the phase velocity for plane waves drops to zero. For overcritical magnetic induction the model of plane waves fails. Here an interesting competition between the static hexagonal pattern[6, 3] and the travelling lamellar modulation[7] takes place. We observe square patterns, where under homogeneous magnetic fields only hexagonal patterns occur.

References

[1] A. Beetz, C. Gollwitzer, R. Richter, and I. Rehberg. *J. Phys.: Condens. Matter*, 20(20):204109, 2008.

[2] R. Richter and J. Bläsing. *Rev. Sci. Instrum.*, 72:1729–1733, 2001.

[3] C.Gollwitzer, G. Matthies, R. Richter, I. Rehberg, and L. Tobiska. *J. Fluid Mech.*, 571:455–474, 2007.

[4] R. Krauss, M. Liu, B. Reimann, R. Richter, and I. Rehberg. Pumping fluid by magnetic surface stress. *New J. Phys.*, 8:18, 2006.

[5] L. D. Mao and H. Koser. *J. Magn. Magn. Mater.*, 289:199–202, 2005.

[6] R. Friedrichs and A. Engel. *Phys. Rev. E*, 64:021406–1–10, 2001.

[7] S. Rüdiger, E. M. Nicola, J. Casademunt, and L. Kramer. *Phys. Rep.*, 447:73–111, 2007.

Quantitative targeting-maps as result of experimental investigations on a branched tube model in magnetic drug targeting

K. Gitter, S. Odenbach

Technische Universität Dresden, Chair of Magnetofluiddynamics, 01062, Dresden, Germany

Among proposed techniques for delivering drugs to specific locations magnetic drug targeting (MDT) is a promising approach due to its high targeting efficiency. Furthermore, unwanted side-effects are considerably reduced. MDT involves binding medicinical agents, respectively chemotherapeutics, to biocompatible magnetic nanoparticles (MNP), injecting these into the blood stream supplying a tumor and using a high gradient magnetic field in order to concentrate these particles – and therefore the attached agents – within the chosen region. While in-vivo investigations, respectively animal-experiments, are promising [1], the understanding of hydrodynamics and transport-phenomena [2-5] is still challenging, both with regard to targeting the particles towards the chosen region and secondly to capture them in the target-area.

In the present work experiments on a half-Y-branched glass tube model as a model-system for a blood vessel supplying a tumor are performed in order to contribute to the understanding of basic phenomena. Quantitative measurements of the targeted net amount of magnetic nanoparticles that is diverted into the branch due to the field of an axially magnetized cylindrical permanent magnet are provided. As a quantitative result, novel drug-targeting-maps (DTMs) are presented, combining e.g. the magnetic volume-force in characteristic locations of the branched tube model together with the magnet position versus the net amount of targeted magnetic nanoparticles.

Quantitative data result of inductivity-measurements of calibrated coil-like containers capturing the outflow of each branch. The generated quantitative result is promising for MDT as a whole, but also indicates that various phenomena and the influence of parameters have to be investigated further, following the approach and technique of this work.

Acknowledgments

Funding of DFG-project DFG-OD18-13 is thankfully acknowledged.

References

[1] A. S. Lubbe, C. Alexiou, C. Bergemann, “Clinical applications of magnetic drug targeting”, J. Surg. Res. 95, 200, (2001)

[2] R. Ganguly, I. K. Puri, “Field-induced self-assembled ferrofluid aggregation in pulsatile flow”, Physics of Fluids, 17, 097104 (2005)

[3] E. J Furlani, E. P Furlani, “A model for predicting magn. targeting of multifunct. particles in microvasculature“, J. Mag. Mag. Mat. 312, 187 (2007)

[4] R. M. Erb, D. S. Sebba, “Magnetic field induced concentration gradients in magnetic nanoparticle suspensions: Theory and experiment“, J. Appl. Phys, 103, 063916 (2008)

[5] A. D. Grief, G Richardson, “Mathematical modelling of magnetically targeted drug delivery“, J. Mag. Mat. Mat. 293 (2005)

"Frozensweig": A Cool Instability in the Limit of $\eta \to \infty$

Christian Gollwitzer[1], Ingo Rehberg[1],Adrian Lange[2], Reinhard Richter[1]

[1] *Experimentalphysik V, Universität Bayreuth*
[2] *Lehrstuhl für Magnetofluiddynamik, TU Dresden*

The Rosensweig Instability

When a layer of magnetic fluid is exposed to a sufficiently large magnetic field, the surface of the liquid becomes unstable in favour of a periodic pattern of spikes [1]. A linear stability analysis can provide not only the critical magnetic induction B_c of this instability, but also the wavelength of the developing pattern and its growthrate for small amplitudes [2, 3]. It is, however, rather difficult to measure the full topography during the evolution of the pattern due to the fast timescale of the process. The established methods are either fast [4] or able to determine the full surface topography [5]. This difficulty can be overcome by performing the experiment at a lower temperature, where the viscosity is high. In this way the growth of the pattern can be slowed down from tenths of a second [4] to minutes and the dynamics can be followed easily.

Experiment

We use a highly viscous commercial ferrofluid and cool it down to a temperature of 10 °C, where the viscosity amounts to 4.48 Pa s. A homogeneous magnetic field is applied, which is oriented normal to the layer of fluid. The surface topography of the ferrofluid is measured using an X-ray technique [5], capable of recording a frame every 134 ms. The evolution of the pattern is observed when the magnetic induction is suddenly switched to an overcritical value. Figure 1 displays $\mathrm{d}A/\mathrm{d}t$ as a function of A, i.e. it is a representation of the amplitude equation. The linear growthrate corresponds to the slope at $A = 0$ in this plot. We find an excellent agreement between our experiments (dashed line) and ab initio calculations (solid line).

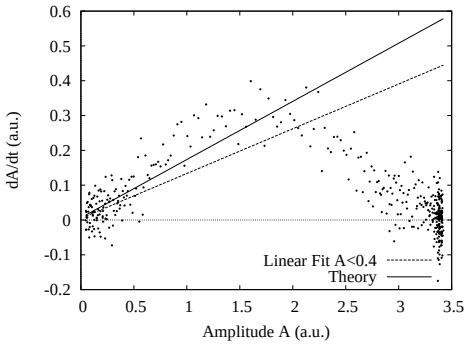

Figure 1: Measured amplitude equation, linear fit (dashed) and theory (solid)

Acknowledgments

We thank Carola Lepski for measuring the surface tension of the ferrofluid.

References

[1] M. D. Cowley and R. E. Rosensweig, J. Fluid Mech. **30**, 671 (1967).

[2] A. Lange, B. Reimann, and R. Richter, Magnetohydrodynamics **37**, 261 (2001).

[3] H. Knieling, A. Lange, G. Matthies, I. Rehberg, and R. Richter, Proc. Appl. Math. Mech. **7**, 4140025 (2007).

[4] H. Knieling, R. Richter, I. Rehberg, G. Matthies, and A. Lange, Phys. Rev. E **76**, 06630 (2007).

[5] R. Richter and J. Bläsing, Rev. Sci. Instrum. **72**, 1729 (2001).

[6] M. C. Cross and P. C. Hohenberg, Rev. Mod. Phys. **65**, 851 (1993).

Diffusion of magnetic nickel nanorods in colloidal dispersions

A. Günther, P. Bender, A. Tschöpe, R. Birringer

Technische Physik, Universität des Saarlandes, Postfach 151150, Geb. D2 2, D-66041 Saarbrücken

Ni nanorods with a diameter of ~ 15 nm and varying lengths were synthesized by pulsed electrodeposition of Ni into porous alumina templates. The nanorods were extracted from the matrix by dissolution of the alumina and were dispersed in water or water-glycerine mixtures. These colloidal dispersions were investigated with respect to the diffusion of the rods. The rotational diffusion was characterized by AC susceptibility measurements whereas the translational diffusion was studied by single particle tracking (SPT) and analysis of the observed trajectories. Additionally, rotational diffusion coefficients as well as translational diffusion coefficients were determined from dynamical light scattering measurements. Both diffusion coefficients were analyzed with regard to the influence of the size of the nanorods and the viscosity of the liquid matrix.

Polymerization from Magnetically Induced *Hot Spots*: A Kinetik Investigation

C. Gürler[1], A. Bian[2], A. M. Schmidt[1]

[1] *Institut für Organische Chemie und Makromolekulare Chemie, Heinrich-Heine-Universität, Universitätsstr. 1, D-40225 Düsseldorf, Germany, email: schmidt.annette@uni-duesseldorf.de*
[2] *Department of Chemistry, University of Calgary, Alberta, Canada*

An interesting aspect of nanotechnology research is the ability of dipolar nanoparticles to transform electromagnetic energy into heat. This provides the possibility of activating a thermal physical or chemical process in a specifically confined environment by selective heating.

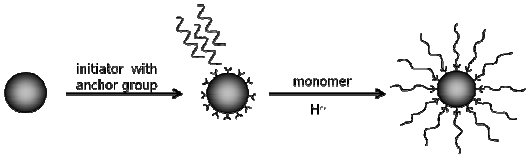

Fig. 1: Surface-initiated polymerization from cobalt nanoparticles activated by magntic heating

The particles of our interest are magnetically blocked cobalt nanoparticles that undergo fast heat dissipation by Brownian rotation upon irradiation in an alternating magnetic field of kHz frequency.
The local heat (*hot spot*) allows the activation of a polymerization process predominantly on the particle-medium interface. By using surface-attached initiator groups, a brush like core-shell structure is obtained.[1]
This novel approach for the facile synthesis of polymer-coated single core nano-objects is now verified by a detailed kinetic investigation that confirms the proposed mechanism of polymerization activation. We investigated the kinetic behavior of the magnetically activated surface-initiated polymerization of ε-caprolactone in cobalt nanoparticle dispersions. The efficiency of the reaction in a magnetic field was compared to a standard method, where the particles are conventionally heated.

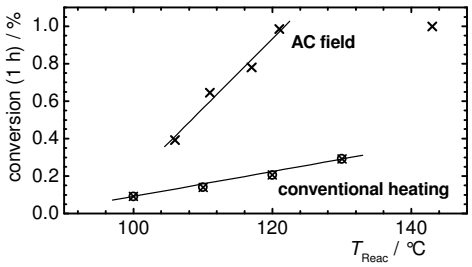

Fig. 2: Comparison between the efficiency of ε–caprolactone polymerization via magnetic heat ing and conventional heating

In conventionally heated polymerizations, a pseudo first order kinetics is clearly indicated by the logarithmic course of the monomer conversion with time. In contrast, field heated experiments show an enhanced polymerization rate in the beginning of the reaction that equalizes to that of the conventional heated reaction in the further course.
We extract kinetic constants for both processes in a temperature regime from 60 °C to 90 °C bulk temperature. The results support the presence of an effective temperature profile on the particle surface that supports the locoregional polymerization process.

Acknowledgement

We gratefully acknowledge DFG (Emmy-Noether Program) for financial support.

References

[1] C. Gürler, M. Feyen, S. Behrens, N. Matoussevitch, A. M. Schmidt, *Polymer* **49**, 2211, (2008)

Release behavior characterization of hydrogels by fluxgate magnetorelaxometry

E. Heim[1], A. Schwoerer[2], S. Harling[3], F.Ludwig[1], H. Menzel[3], M. Schilling[1]

[1] *Institut für Elektrische Messtechnik und Grundlagen der Elektrotechnik, TU Braunschweig, Hans-Sommer-Str. 66, D-38106 Braunschweig*
[2] *Institut für Biochemie und Biotechnologie, TU Braunschweig, Spielmannstr. 7, D-38106 Braunschweig*
[3] *Institut für Technische Chemie, TU Braunschweig, Hans-Sommer-Str. 10, D-38106 Braunschweig*

Introduction

In [1] we have introduced a new nondestructive characterization method for hydrogels based on the magnetic relaxation behavior of superparamagnetic nanoparticles and have investigated the formation process of hydrogels. Hydrogels are under investigation as new drug delivery systems for bioactive molecules. They have the ability to incorporate a huge amount of water or buffer. Therefore, they offer optimal conditions for long in-vivo lifetimes of, e.g., proteins. For hydrogels there exist different preparation methods and release mechanisms [2].

Materials

Here, we investigate the release process of hydrogels formed by photocross-linking of hydroxyethyl methacrylate hydroxyethylstarch (HESHEMA) in deionized water with 0.1 wt.% Irgacure 2959 as photoinitiator and a ferrofluid content of 1.3 vol.% (Fig 1).

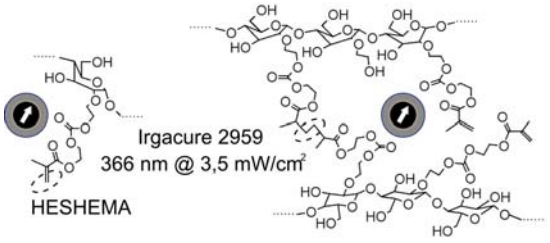

Fig. 1: Embedding of MNPs in starch hydrogels by photocross-linking.

As ferrofluid we use superparamagnetic nanoparticles (MNP) with a magnetite core and a gum arabicum shell (50 mg/mL) suspended in water. The photoinitiator and the UV light do not interact with the ferrofluid alone [1]. Hydrogel samples with three different network densities were prepared in triplicate. Each hydrogel sample of 150 µL volume was irradiated with UV light (λ = 366 nm, I ~ 3.5 mW/cm²) for 30 min. and subsequently measured with our fluxgate MRX system in unshielded environment [3].

Experiment results

The hydrogel samples were covered with 100 µL α-amylase solution and incubated at 37 °C in a thermal shaker at 300 rpm shaking speed (eppendorf comfort, Germany). The stability of the MNPs under the degradative conditions was monitored by analyzing MNPs in α-amylase solution incubated parallel to the hydrogel samples. In Fig. 2 the relaxation curves of two stability test samples are shown at the starting day and after 25 days of incubation.

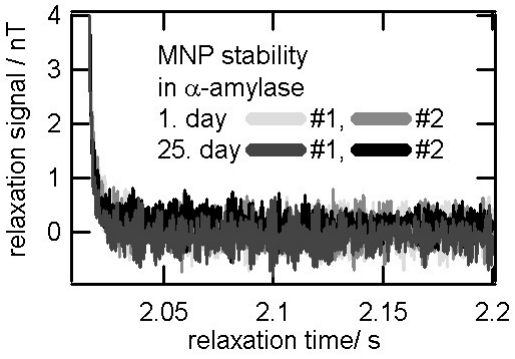

Fig. 2: Test of stability of two MNP samples in α-amylase.

As can be seen the relaxation curves did not change. It is evident that the gum arabicum shell is not degenerated by the α-amylase.

To analyze the release behavior two reference samples were prepared. For completely immobilized MNPs, a HESHEMA sample containing MNPs was freeze-dried. For completely mobile MNPs an unpolymerized HESHEMA solution with MNPs and 100 µL α-amylase solution was prepared. In Fig 3 the relaxation curve measured for the two reference samples are

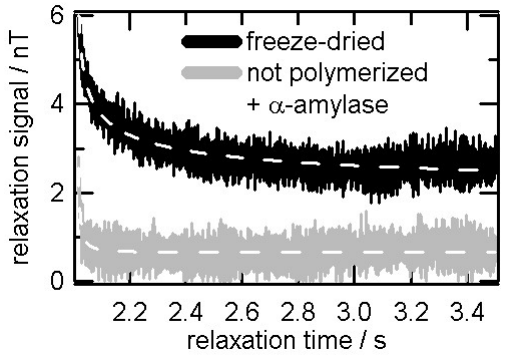

Fig. 3: Comparison of relaxation curves of completely immobilized MNPs in freeze-dried hydrogel and mobile MNPs in unpolymerized hydrogel.

To demonstrate the degradation of the hydrogel, the fraction of mobile MNPs – determined from the differential signal between two selected points of the relaxation curve – is plotted versus time in Fig. 4.

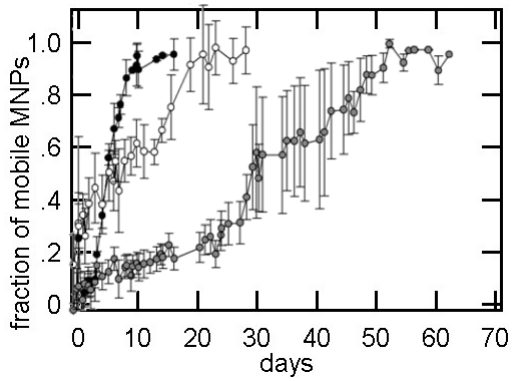

Fig 4: Release behavior of hydrogels with three different network densities.

The smaller the differential signal, the higher the amount of MNPs relaxing via the Brownian mechanism. To obtain the fraction of mobile MNPs, the differential signal is normalized to that of the mobile reference sample.

MNPs embedded in the hydrogel matrix are limited in their mobility. The relaxation of embedded MNPs takes place via the Néel relaxation mechanism. Hydrogels with a lower network density have pores of larger size than networks with higher network densities. These large pores can release the MNPs by diffusion faster than smaller pores. In addition, the mobility in larger swollen pores is relieved. The pore structure enables the penetration of α-amylase in the hydrogel matrix. α-amylase cleaves the HES-backbone. These effects can occur faster and with a more pronounced effect in a low density network than in hydrogels with higher network density. The experiments show that the MNPs with gum arabicum shell are stable in α-amylase solution and can be used to characterize the release behavior of hydrogels.

Acknowledgments

This work was financially supported by the DFG via SFB 578.

References

[1] E. Heim, S. Harling, F. Ludwig, H. Menzel, M. Schilling, J. Phys.: Condens. Matter **20**, 204106-1 – 5 (2008)

[2] C. S. Satish, K. P. Satish, H. G. Shivakumar, Indian J. Pharm. Sci. **68** 133 (2006)

[3] F. Ludwig, S. Mäuselein, E. Heim, M. Schilling, Rev. Sci. Instrum. **76,** 106102 (2005)

Time dependent NMR spectroscopy on ionic and citrate ferrofluids

D. Heinrich[1], A.R. Goñi[2], L. Cerioni[3], T. M. Osán[3], D.J. Pusiol[3], C. Thomsen[1]

[1] *Institut für Festkörperphysik, Technische Universität Berlin, Hardenbergstraße 36, 10623Berlin, Germany*
[2] *ICREA, Institut de Ciència de Materials de Barcelona, Esfera UAB, 08193 Bellaterra, Spain*
[3] *Spinlock SRL, Av. Sabattini 5337, Córdoba, Argentina – CONICET Argentina*

Magnetic nanoparticles colloidally suspended in a ferrofluid exhibit a tendency to form clusters and chain-like structures under the influence of an external magnetic field; an effect which in the past years has been extensively studied theoretically [1-3] as well as experimentally [4-7]. Recently, we used Raman spectroscopy to monitor the metastable cluster formation and its dynamics in surfacted and ionic ferrofluids [5-7]. Here we present results of a complementary study of the magnetic-field induced behavior of a water-based ionic (IFF) and citrate (CFF) ferrofluid with a concentration of 1 vol.% using nuclear magnetic resonance (NMR) spectroscopy. For the measurements we used a low-resolution NMR spectrometer working at room temperature with a homogeneous magnetic field of 225 mT.

In the experiments, ionic and citrate electrostatically stabilized ferrofluids which had not been exposed previously to any magnetic field are placed at 300 K in the bore of the NMR spectrometer. Figure 1 shows the NMR spectra of the two samples, in comparison to that of pure water. The main peak of the IFF and the CFF is blue-shifted with respect to the resonance frequency of "pure and free" water molecules [8] by approximately 17 kHz and 75 kHz, respectively. Both peaks are attributed to the dynamic environments of water molecules from the solvation layers close around the magnetic grains in the corresponding ferrofluid [8].

Figure 2 shows the time evolution of the amplitude and frequency of the NMR peak of the IFF on a time scale of more than one hour. The amplitude of the NMR signal exhibits a slight increase in the first 300 s

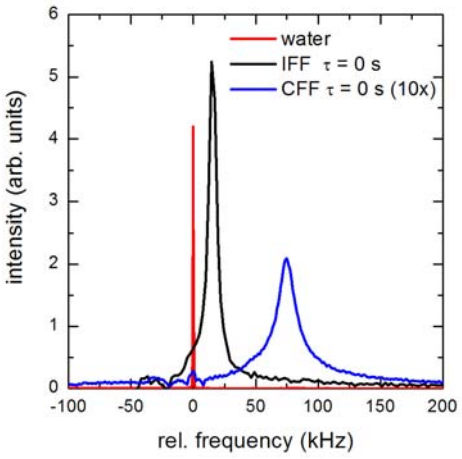

Fig.1 NMR spectra of an ionic (black) and citrate (blue) ferrofluid in comparison with water (red) in a magnetic field of 225 mT.

followed by a strong reduction in intensity, reaching its minimum after approximately 15 minutes. In contrast, the frequency shift changes abruptly from 17 kHz to 3 kHz at the point when minimum amplitude is reached. We attribute the peak at 3 kHz to the NMR signal stemming from water molecules far from the magnetic particles (low field regions). Its amplitude increases monotonically, saturating at times longer than one hour. This contrasting behavior of NMR signal is readily understood by considering the dynamical processes within the ferrofluid triggered by an external magnetic field, as revealed by Raman spectroscopy [7].

The decay of the amplitude of the peak at 17 kHz is, thus, attributed to the field-induced clustering of the magnetic nanograins to form chain-like structures. As a result, the amount of water molecules in the high-field regions around the magnetic particles continuously decreases due to the building up of the chains, leading to the

observed reduction in peak intensity. In fact, a characteristic time constant of (130 ± 15) s is obtained for this decay, which is in very good agreement with the clustering times measured with Raman on the same IFF sample [7]. On the other hand, the much slower increase in amplitude of the NMR signal, now at 3 kHz, corresponding to water molecules far from the grains, gives evidence of a sluggish long-ranged ordering of the chains in a sort of "layered crystal structure" [9], forming in the homogeneous magnetic field of the NMR spectrometer. The characteristic time for this ordering obtained from a fit to the data points is (420 ± 50) s. Hence, the sudden change in frequency of the NMR signal is taken as evidence of a *first-order phase transition* from a ferrofluid containing chains of magnetic grains to a phase where the chains are closely packed into layers forming ordered stacks in the magnetic field direction.

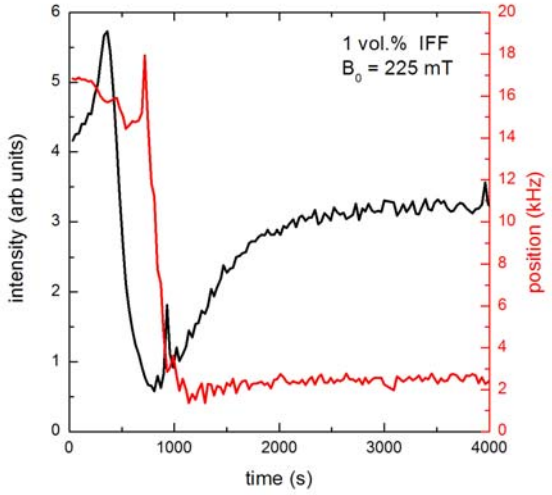

Fig.2 Time evolution of the amplitude (black) and the frequency (red) of the NMR signal for the IFF.

This transition, in contrast, occurs in the citrate FF only in the presence of magnetophoresis induced by an inhomogeneous magnetic field. Figure 3 displays the first and the last spectrum of a time-dependent NMR series for the CFF in two different situations. The fluid in Fig. 3a was not placed in any external field, whereas the sample of Fig. 3b was subjected to the strongly inhomogeneous field of a permanent magnet for 120 s. Without magnetophoresis (Fig. 3a) the amplitude of the NMR signal changes slightly but the frequency remains nearly constant at a high value of 75 kHz. For the fluid which was placed in the field gradient (Fig. 3b) the NMR peak behaves similarly but having a much lower frequency from the start. This clearly indicates that the CFF needs the net force of the gradient field for the building of the chain-like structures and the formation of the layered phase. We believe that this is a consequence of the much smaller size (10 nm compared to about 100 nm) of the nanograins of the citrate compared to the ionic ferrofluid, respectively.

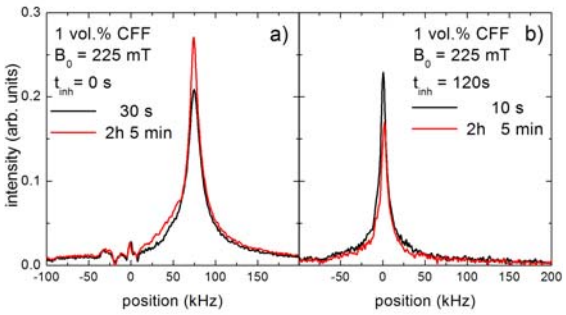

Fig.3 NMR Spectra of a CFF. The Sample was placed for 0s (a) and 120s (b) on the external magnet. The black line is the initial and the red line the final state.

References

[1] A.O. Ivanov, Z. Wang, and C. Holm, Phys. Rev. E **69**, 031206 (2004).

[2] H. Morimoto, T. Maekawa, and Y. Matsumoto, Phys. Rev. E **68**, 061505 (2003).

[3] Z. Wang, C. Holm, and H.W. Müller, Phys. Rev. E **66**, 021405 (2002).

[4] A. Wiedenmann, J. Magn. Magn. Mat. **272-276**, 1487 (2004).

[5] J.E. Weber, A.R. Goñi, D.J. Pusiol, and C. Thomsen, Phys. Rev. E **66**, 021407 (2002).

[6] J.E. Weber, A.R. Goñi, and C. Thomsen, J. Magn. Magn. Mat. **277**, 96 (2004).

[7] D. Heinrich, A.R. Goñi, and C. Thomsen, J. Chem. Phys. **126**, 124701 (2007).

[8] C.E. González, D.J. Pusiol, A.M.F. Neto, M. Ramia, and A. Bee, J. Chem. Phys. **106**, 4670 (1998).

[9] J. Jordanovic, S.H.L. Klapp, Phys. Rev. Lett. **101**, 038302 (2008).

Chain-formation versus gelation in dipolar colloids

Patrick Ilg[1], Emanuela Del Gado[1]

[1] *Polymer Physics, ETH Zürich, Wolfgang-Pauli Str. 10, CH-8093 Zürich*

Introduction

The formation of chain-like structures in dipolar colloids in general and ferrofluids in particular is well-known (see e.g. [1] and references therein). These structures severly influence the dynamical and rheological properties of the fluid (for a recent review see e.g. [2]). More recently, it has been found that in the presence of an external field, chains of dipolar particles can also self-assemble into columnar structures with a local hexagonal ordering [3]. Under certain conditions, and preferrably in the absence of an external field, different particle chains can also build physical bonds and thus form a reversible network [4]. Our aim here is to study the conditions for network formation as well as the corresponding magnetic and dynamical properties, which are expected to be rather different compared to those in the chain-formation regime.

Model system

We study a system of interacting, dipolar particles, where each particle is composed of two interpenetrating spheres ("dumbbell"), rigidly kept at a fixed distance d [4]. The spheres carry point charges q, such that each particle is equipped with a finite dipole of strength $\mu = qd$. In addition to Coulomb interaction between charges, the spheres interact with each other by a soft repulsive potential in order to prevent permanent agglomeration.
We have carried out constrained molecular dynamics simulation of this model system at several values of particle concentrations and reduced interaction strengths. Following earlier work [4], a small distance d of around 20% of the particle diameter is chosen such that the dumbbells can be thought of as slightly elongated spheres.

Results

We study in detail the structural and dynamical properties of model dipolar colloids described above. For weak and moderate dipolar interaction strengths compared to thermal energy, we find very similar behavior to previous ferrofluid models (see e.g. [2,5]). However, for increasing dipolar interaction strength relative to thermal motion, we observe characteristic changes between network and chain regimes [6]. The cluster size distribution, for example, changes from an exponential to a power law shape and dynamics is found to be slowed down significantly, both being typical fingerprints of a network structure [7]. By applying an external field, we find that the network can reversibly be transformed into a chain-structure, which is accompanied by a highly non-linear initial susceptibility [6]. Figure 1 illustrates the changes between a network and a chain-structure found in the simulations. Such structural transformations which occur upon applying external fields might have interesting applications as "smart materials".

References

[1] P. G. de Gennes and P. A. Pincus, Phys. Kondens. Mater. **11**, 189, (1970), M. Klokkenburg et

al, Phys. Rev. Lett. **96**, 037203, (2006), C. Holm and J.J. Weis, Curr. Opin. Colloid Interface Sci. **10**, 133, (2005), A.-P. Hynninen and M. Dijkstra, Phys. Rev. Lett. **94**, 138303, (2005).

[2] P. Ilg and S. Odenbach *Ferrofluid Structure and Rheology*, in S. Odenbach (Ed.) *Colloidal Magnetic Fluids*, Lecture Notes in Physics **763**, Springer (2009).

[3] A. Wiedenmann, A. Hoell, M. Kammel, and P. Boesecke, Phys. Rev. E **68**, 031203, (2003), M. Klokkenburg et al, Phys. Rev. Lett. **97**, 185702, (2006), P. Ilg, Eur. Phys. J. E **26**, 169, (2008).

[4] R. Blaak, M. A. Miller, and J.-P. Hansen, EPL **78**, 26002, (2007). M. A. Miller, R. Blaak, C. N. Lumb, and J.-P. Hansen. J. Chem. Phys. **130**, 114507, (2009).

[5] Z. Wang, C. Holm, and H. W. Müller, Phys. Rev. E **66**, 021405, (2002). J. P. Huang, Z. W. Wang, and C. Holm, Phys. Rev. E **71**, 061203, (2005).

[6] E. Del Gado and P. Ilg, preprint 2009.

[7] E. Del Gado, A. Fierro, L. de Arcangelis, and A. Coniglio, Phys. Rev. E **69**, 051103, (2004).

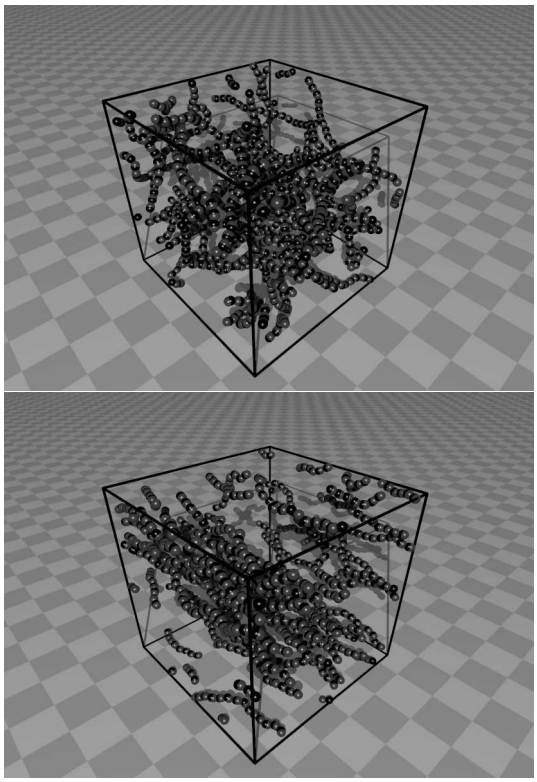

Figure 1: Snapshot of network configuration in the absence of field (top) and chain-structure in the presence of an external field (bottom).

Brownian ratchet effect in ferrofluids

Thomas John and Ralf Stannarius

Institut für Experimentelle Physik, Fakultät für Naturwissenschaften, Universität Magdeburg, Universitätsplatz 2, D-39106 Magdeburg, Germany

We investigate experimentally a Brownian ratchet system suggested by Engel et al. [1] and compare the measurements with two different models. The ratchet system is based on a magnetite ferrofluid (Ferrotec APG935) with magnetic particles in a thermal bath of carrier fluid. An external static magnetic field and perpendicular to it an oscillatory magnetic field act on the ferrofluid particles, the total magnetic field contains no rotating component. The directed effective rotation of the particles due to the ratchet effect induce a macroscopic torque density of the fluid. The torque on a spherical ferrofluid sample is measured in dependence on the field parameters. A quantitative comparison with predictions from a microscopic [2] and a phenomenological model [3] are given. Both models describe certain aspects of the measurements correctly only in limited parameter ranges. Qualitative discrepancies between these models and experiment are found.

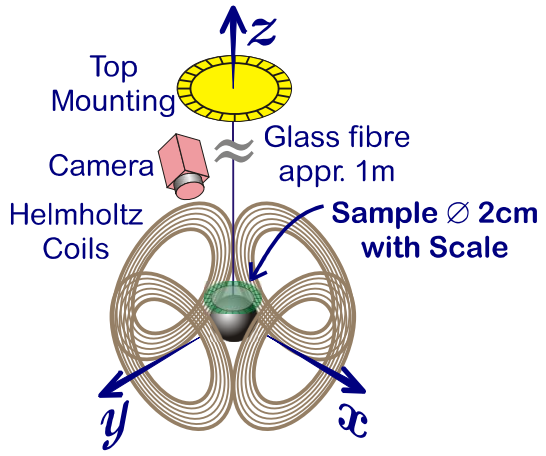

Figure 1: Experimental setup

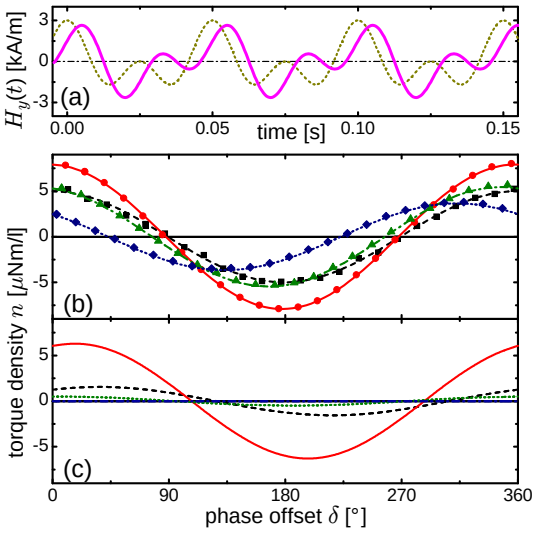

Figure 2: (a) Exemplary excitation field $H_y(t)$ at phase shift $\delta = 0°$(solid line) and $\delta = 90°$ (dotted line). (b) Measured torque densities at frequencies $f = 5$ Hz (dashed line), 20 Hz (solid line), 100 Hz (dash-dotted line) and 500 Hz (dotted line).(c) Calculated torque densities $n(\delta)$ from microscopic model at same frequencies and depicted in same line styles as (b). The phenomenological model predicts the same sinusoidal dependencies but different amplitudes and phases.

The applied magnetic field is a superposition of an static field H_x in x-direction and a suitable time-periodic field in y direction. As suitable waveform we use the superposition of two harmonic functions [1], exemplarily

$$H_y(t) = H_y^1 \cos(2\pi f t) + H_y^2 \sin(4\pi f t + \delta).$$

The phase difference δ represents a contin-

uous measure for the asymmetry in time. In dependence on the shape of the excitation we measure a torque from the spherical sample, using a sensitive torsional pendulum. Both models predicts an effective torque density (torque per ferrofluid volume) averaged over one period of excitation. Both models predict a sinoidal dependence respect to δ in agreement with our experiments. We extract the amplitudes of the sin dependencies for further comparisons.

An obvious important parameter is the frequency f of the excitation. The microscopic model (Brownian motion of particles) predicts an resonance like behaviour with am maximum at the inverse Brownian relaxation time $\tau_{\mathrm{B}} = \pi\eta d_{\mathrm{h}}^3/(2k_{\mathrm{B}}T)$, with the hydrodynamic diameter d_{h} of the particles. A maximum of $n_{max}(f)$ has been found in experiments too. Taken an assumed polydispersity of the ferrofluid particles into account in the microscopic model, the resonance frequency is in the same order of magnitude. This model also predicts a fast decay at high frequency, witch is not be observed in our experiments. The phenomenological model (solid magnet with Debye-Relaxation) predicts no resonance behaviour but a saturation in the high frequency limit. In experiments, we found a resonance like behaviour *and* a saturation at high frequencies too (in the accessible frequency range).

In conclusion, if a suitable external *nonrotating* magnetic field applied to a ferrofluid, we has been measured an induced torque on the fluid. The microscopic models describes this effect with an effective particle rotation because of a Brownian ratchet effect. The phenomenological model describes it with a Debye relaxation. Both models can not explain the measured values in coherence. In particular, the predictions of the resonance behaviour and the high frequency limit are totally different and different. An expansion of the simple microscopic model (fixed magnetic moment with particle orientation) may be helpfully to understood this phenomenon in ferrofluids in particular and for Brownian ratchet systems in general.

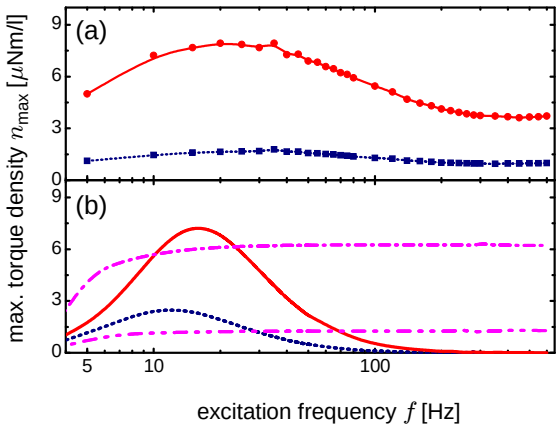

Figure 3: Measured (a) and calculated (b) maximal amplitudes of the torque densities n_{max} as function of the exiting frequency f in $H_y(t)$ at magnetic field amplitudes at $H_x = H_y^1 = H_y^2 = 1.5\,\mathrm{kA/m}$ (solid line, circles), $1\,\mathrm{kA/m}$ (dotted line,squares), microscopic model (solid line, dashed line), phenomenological model (dash dotted line, dash dot dot line) respectively.

We thanks Volker Becker and Andreas Leschhorn for stimulating discussions.

References

[1] A. Engel, H. W. Müller, P. Reimann and A. Jung, Ferrofluids as thermal ratchets, *Phys. Rev. Lett.* **91** 060602 (2003)

[2] A. Engel and P. Reimann, Thermal ratchet effects in ferrofluids, *Phys. Rev. E* **70** 051107 (2004)

[3] M. I. Shliomis, Comment on Ferrofluids as thermal ratchets, *Phys. Rev. Lett.* **92** 188901 (2004)

Field-induced structure formation and dynamics of ferrofluid multilayer films

J. Jordanovic[1] and S. H. L. Klapp[1]

[1]*Institute of Theoretical Physics, Secr. EW 7-1, Technical University Berlin, Hardenbergstr. 36, 10623 Berlin*

We present Molecular Dynamics (MD) computer simulation results for the structure formation and dynamics of ferrofluids under the combined influence of external magnetic fields and spatial confinement. The ferrofluids are modeled via the Stockmayer potential involving dipole-dipole and van der Waals-like interactions. The surfaces alone already create an inhomogeneous structure, that is, layer formation of the particles. Our MD simulations predict that the number and internal structure of these layers can be controlled by homogeneous magnetic fields, in qualitative agreement with experiments [1]. For suitable surface separations, strong fields directed perpendicular to the film plane do not only align the particles but create additional layers in the system (see Fig. 1). The opposite effect occurs with an in-plane (parallel field) which can induce a collapse of layers. Both effects are accompanied by pronounced particle rearrangements in lateral directions [2]. A perpendicular field yields an increase of the nearest-neighbour distance within a layer, whereas particles in adjacent layers tend to arrange in energetically favourable head-to-tail configurations. Under certain circumstances (strong coupling, low density) one even observes a field-induced crystallization of these layered systems [3]. In a parallel field, on the other hand, the particles form long in-plane chains which tend to be shifted by half a particle diameter relative to one another, yielding a local hexagonal ordering. Finally, we discuss the interplay between the structural changes generated by external fields and the translational and rotational mobility of the particles [4].

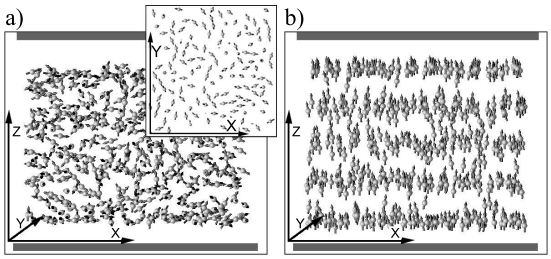

Figure 1: MD configurations at a surface separation of five particle diameters (a) in zero field (inset: top-view of the contact-layer), (b) in a strong perpendicular field [1].

Acknowledgments
We gratefully acknowledge financial support by the DFG within the Collaborative Research Center (Sfb) 448 ,,Mesoscopically structured composites" (project B6).

References

[1] J. Jordanovic and S. H. L. Klapp, Phys. Rev. Lett. **101**, 038302 (2008).

[2] J. Jordanovic and S. H. L. Klapp, Phys. Rev. E **79**, 021405 (2009).

[3] J. Jordanovic and S. H. L. Klapp, Mol. Phys. **107**, 599 (2009).

[4] J. Jordanovic and S. H. L. Klapp, in preparation.

Magnetic Nanoparticle Detection and Characterization using a High Temperature radio-frequency Superconducting Quantum Interference Device

H.-J. Krause[1], A. Pretzell[1], Y. Zhang[1], A. Offenhäusser[1]

[1] *Forschungszentrum Jülich, Institute of Bio- and Nanosystems (IBN-2), 52425 Jülich, Germany*

Introduction

For detection and characterization of coated and functionalized magnetic nanoparticles (MNP), three magnetic detection techniques are established: Magnetorelaxometry (MRX) [1], linear AC susceptometry (ACS) [2] and the so-called frequency mixing technique, a nonlinear susceptometry (NLS) [3]. We have set up a magnetic readout system based on a liquid-nitrogen cooled radio-frequency (rf) superconducting quantum interference device (SQUID) which allows to measure MNP in liquid state utilizing all three techniques [4-6].

Experimental

We use a planar rf-SQUID gradiometer as sensor because of its high magnetic gradient field sensitivity and its large dynamic range. The small sensor area and the short baseline of 3.7 *mm* allows to realize short sample-sensor distances and a good suppression of homogeneous environmental disturbance fields. The gradiometer sensor is fabricated by pulsed laser deposition of Yttrium-Barium-Copper-Oxide (YBCO) on a single crystal $LaAlO_3$ substrate, with one step-edge Josephson junction forming across a ion-beam-etched ditch in the substrate [6]. The gradiometer is read out via inductive coupling to a lumped-element LC resonance circuit (tank circuit) at its resonance frequency of approx. 800 *MHz*. The sensitivity of the gradiometer was measured to be $(47.8 \pm 0.5)\ nT/(cm \cdot \Phi_0)$. For frequencies above 50 *Hz*, the noise-equivalent magnetic gradient resolution was found to be $(8.6 \pm 1.6)\ pT/(cm \cdot Hz^{0.5})$. The setup is schematically depicted in Fig. 1. The instrument consists of a copper tank placed inside an stainless steel vacuum chamber. Liquid nitrogen from a large reservoir is supplied to the tank by a double-walled transfer line. The SQUID is mounted on top of a sapphire finger affixed to the tank. When the system is filled with liquid nitrogen, a temperature of 78 *K* is reached at the sapphire finger. In order to lower the operating temperature to 75 *K*, the pressure above the reservoir is reduced by means of a rotary pump.

A glass capillary for sample supply with an inner diameter of 800 μm and 100 μm wall thickness is guided across the gradiometer SQUID sensor. The dewar chamber is equipped with fine-threaded plexiglass wheel which allows to adjust the height of the capillary with µm-precision. The vacuum distance between the warm capillary and the cold SQUID can thus be minimized down to 100 μm.

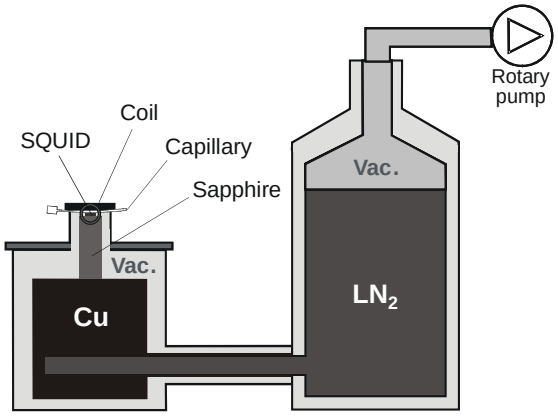

Fig. 1. Schematic of the setup.

The magnetic field lines of the magnetized particles in the capillary thread the two pickup loops of the gradiometer underneath in the configuration depicted in Fig. 2. In order to optimally couple the signal into the gradiometer, one loop of the gradiometer is displaced from the capillary normal by half the distance between capillary and SQUID plane. At the sides of the capillary, copper coils are mounted (cf. Fig. 1) for generating an excitation field in transverse direction with a strength of up to 0.5 *mT*.

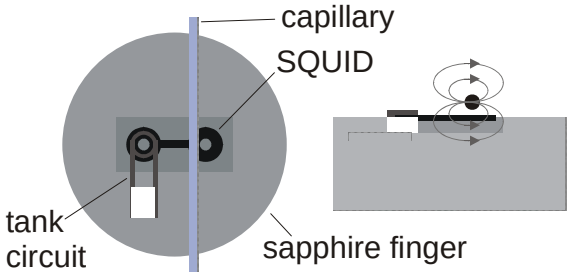

Fig. 2. Top view (left) and cross-section (right) of the SQUID measuring head.

Sensitivity

The sensitivity of the system to iron content was measured using ACS. Liquid samples of Resovist nanoparticles at different concentrations (sample volume 1 μl) were supplied via the glass capillary. The measured data yielded a calibration of 0.39 $nT{\cdot}ml/(cm{\cdot}\mu mol)$ at a frequency of 530 *Hz* and an excitation field amplitude of 20 μT. In conjunction with measured gradiometer noise, the resultant noise-equivalent iron resolution is 1.2 $ng{\cdot}Hz^{-1/2}$. In 1 *Hz* bandwidth, this corresponds to a minimally detectable iron mass of 3.4 *ng*. It should be noted, however, that long-term drift of the balance practically restricts the resolution to approx. 50 *ng* of iron.

Determination of MNP properties

Under the assumption of a lognormal size distribution model, the MRX technique allows to determine the average size of the magnetic cores, the anisotropy constant and the saturation magnetization [7]. In addition, magnetic dipole-dipole interactions and chain formation of the particles can be characterized. Furthermore, the MRX technique allows to determine the binding state and to temporally resolve the binding kinetics [8].

With ACS [3,9], the mean hydrodynamic size and its standard deviation can be determined. The increase in size due to biocompatible coating and functionalization can be controlled and agglomeration of particles can be monitored [9].

The NLS technique [3] allows a quantification of MNP with a very large dynamic range. The method is based on the generation of intermodulation products at the nonlinear magnetization curve of MNP when using AC excitation at two different frequencies.

Magnetic immunoassay

A simple assay based on streptavidin coated MNP and varying concentrations of biotinylated agarose beads has been successfully performed with the system in MRX and in ACS mode. Using NLS and induction coil detection, magnetic immunoassays for CRP, *Y. pestis* and other analytes have been realized [10].

References

[1] R. Kötitz *et al.*, JMMM 194 (1999) 62
[2] B. Payet *et al.*, JMMM 186 (1998) 168
[3] H.-J. Krause *et al.*, JMMM 311 (2007) 436; P.I. Nikitin *et al.*, JMMM 311 (2007) 445
[4] M. Schmidt *et al.*, SUST 19 (06) S261
[5] A. Pretzell *et al.*, in: Proc Eurosensors XXII, Dresden, pp. 1362-5 (2008)
[6] A. Pretzell *et al.*, HTS rf SQUID system for MNP detection, Sensor Lett 7 (2009, in press)
[7] D. Eberbeck *et al.*, J Phys Cond Mat 18 (2006) S2829 ; F. Ludwig *et al.*, J Appl Phys 101 (2007) 113909
[8] Eberbeck *et al.*, JMMM 321 (09) 1617
[9] A. Prieto Astalan *et al.*, JMMM 311 (2007) 166 ; F. Ludwig *et al.*, JMMM 321 (2009) 1644
[10] M.H.F. Meyer *et al.*, Biosens Bioelectron 22 (2007) 973; Meyer *et al.*, J Microbiol Meth 68 (2007) 218

Soft Thermo-Reversible Organoferrogels

M. Krekhova[1], G. Lattermann[2], H. Schmalz[1]

[1] *Makromolekulare Chemie II, Universität Bayreuth, D-95440 Bayreuth*

[2] *Grüner Baum 32, D-95448 Bayreuth*

Recently, the morphology and magnetic properties of thermo-reversible organo-ferrogels (FGs), obtained by physical gelation of ferrofluids (FF) with two different gelators based on polystyrene-*block*-poly-(ethylene-*co*-butylene)-*block*-polystyrene triblock copolymers (SEBS: Kraton G1650 $S_{15}EB_{70}S_{15}^{100}$ and Kraton G1652 $S_{15}EB_{70}S_{15}^{77}$, both 30 wt% PS) have been studied [1,2]. In our nomenclature the subscript numbers give the weight percentage of the corresponding blocks, and the superscript number denotes the overall molecular weight in Kg/mol. These ferrogels have been successfully used for the investigation of the magneto-deformation of a viscoelastic magnetic sphere in a homogeneous magnetic field [3]. The thermoreversibility of the ferrogels, i.e. the possibility to repeat the gelation procedure many times, made these systems suitable for the analysis of the elastic contribution in Rosensweig instabilities. For such experiments usually very soft ferrogels with a storage modulus $G' \approx 100$ Pa are required. However, ferrogels based on Kraton G1650 and G1652 have a plateau modulus G'_0 of about 1000 Pa at room temperature, and a storage modulus G' of about 100 Pa above the softening temperature T_{soft}, where the system is in the visco-elastic fluid state (Fig. 1). Thus, up to now it was only possible to study Rosensweig instabilities near to the softening temperature [4].

The motivation of our present investigation was to construct softer thermo-reversible organoferrogels, i.e. exhibiting a lower plateau modulus G'_0, which would enable us to study Rosensweig instabilities in the elastic gel state at room temperature.

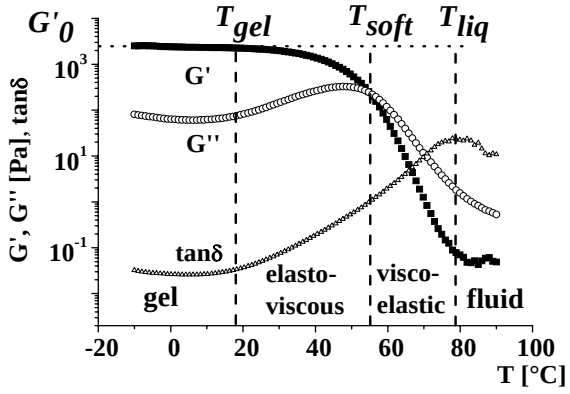

Fig. 1. Temperature sweep for FG: 5 wt% G 1650 per paraffin oil, FF: 21 wt% magnetite in A 50B, f = 1 Hz, γ = 10 %.

To that aim three different strategies have been explored:

1) Mixtures of tri- and diblock copolymers. In this case the diblock copolymer could act as a plasticizer;

2) Triblock copolymers with longer middle blocks, i.e. lower PS content. Here, the concentration and size of the PS – micellar cores, acting as physical cross linking sites, should be smaller;

3) Asymmetric triblock copolymers having PS end blocks of different length. Due to the asymmetry bridging between different PS cores should be favored. Consequently, gelation is expected to occur at lower gelator concentrations, resulting in softer gels.

The FGs based on FF with magnetite in paraffin oil Finavestan A 50B (Total Deutschland GmbH) have been prepared using the following gelators:

1) Kraton G1726 (Kraton Polymers, Belgium), a mixture of triblock and diblock copolymers: 30 wt% $S_{15}EB_{70}S_{15}^{77}$ + 70 wt% $S_{15}EB_{35}^{38}$ (½ $S_{15}EB_{70}S_{15}^{77}$);

2) Kraton MD6932 (Kraton Polymers, Belgium): $S_{10}EB_{80}S_{10}^{130}$;

3) Asymmetric triblock terpolymers: $S_{13}EP_{77}S_{10}^{119}$ and $S_8EP_{71}S_{21}^{121}$, synthesized via anionic polymerization and subsequent catalytic hydrogenation (EP = ethylene-*alt*-propylene).

Ferrogels based on gelators 1) and 2) show a lower softening temperature T_{soft} with respect to the earlier used gelators G1650 and G1652, with T_{soft}(G1726) > T_{soft} (MD 6932), as determined by the falling ball method. However, the plateau modulus G'_0 in the gel state, which is independent on frequency over the whole measurement range (0.01 - 100 Hz), was about 1000 Pa or even higher. The results are shown in Table 1 for the lowest possible gelator concentration resulting in the formation of stable homogeneous FGs.

	NGs		**FGs**	
Gelator (wt%)	***G'₀* [Pa]**	**T_{soft} [°C]**	***G'₀* [Pa]**	**T_{soft} [°C]**
G1650 (3.5)	900	35	1000	50
G1652 (4.0)	500	27	1000	40
G1726 (5.0)	550	26	1200	30
6932 (6.0)	2000	22	1600	24
$S_{13}EP_{77}S_{10}^{119}$ (3.5)	250	56	300	45
$S_8EP_{71}S_{21}^{121}$ (3.5)	100	34	130	45

Table 1. Plateau modulus G'_0 and softening temperatures T_{soft} for NGs and FGs based on different gelators from rheology (f = 1 Hz, γ = 5%), FF: 22 wt% magnetite in A 50B.

In contrast, ferrogels based on asymmetric triblock copolymers (approach 3) exhibit a significantly reduced plateau modulus G'_0 (Table 1). This is attributed to the differences in morphology with respect to ferrogels based on G1650 and G1652.

For both asymmetric gelators we cannot see a domain (or cluster) structure of the network (Fig. 2), as observed for the symmetric gelators G1650 and G1652 [2]. The network is very homogeneous, indicating an increased fraction of elastic bridges in between the insoluble PS domains (dark appearing spherical domains in Fig. 2a) due to the different length of the PS end blocks. Consequently, the magnetite particles (black dots in Fig. 2b) are uniformly distributed in the network in between the PS domains (bright areas in Fig. 2b). In addition, a more regular network structure was detected by SAXS, too, as indicated by the presence of higher order reflections.

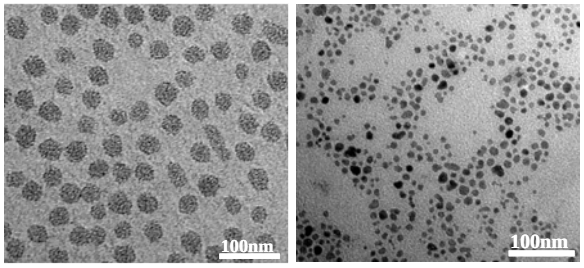

(a) stained with RuO_4 **(b)** not stained

Fig. 2. TEM image of NG (a) and FG (b); gelator: 3.5 wt% $S_8EP_{71}S_{21}^{121}$, FF: 22 wt% magnetite in A 50B.

In conclusion, ferrogels with plateau moduli G'_0 significantly below 1000 Pa are accessible with asymmetric triblock copolymers, only, which might be attributed to the observed change in the network structure.

Acknowledgments

Financial support by the German Science Foundation (Research Group FOR 608, project 8) is gratefully acknowledged. We thank Dr. Birgit Fischer (HASYLAB, Hamburg) for the SAXS measurements.

References

[1] G. Lattermann, M. Krekhova, *Macromol. Rapid Commun.* **2006**, *27*, 1373; ibid. **2006**, *27*, 1968.

[2] M. Krekhova, G. Lattermann, *J. Mater. Chem.* **2008**, *18*, 2842.

[3] C. Gollwitzer, A. Turanov, M. Krekhova, G. Lattermann, I. Rehberg, R. Richter, *J. Chem. Phys.* **2008**, *128*, 164709.

[4] C. Gollwitzer, M. Krekhova, G. Lattermann, I. Rehberg, R. Richter, *Soft Matter* **2009**, *5*, 2093.

Synthesis and Magnetoviscosity of Novel Ferrofluids Prepared by Templating Virus Particles or Nanopores

Z. Wu[1], A. Müller[2], R. Zierold[3], K. Nielsch[3], C. Wege[2], C. E. Krill III[1]

[1] *Institute of Micro and Nanomaterials, Universität Ulm, 89081 Ulm, Germany*
[2] *Institute of Molecular Biology and Virology of Plants, Universität Stuttgart, 70569 Stuttgart, Germany*
[3] *Institute of Applied Physics, Universität Hamburg, 20355 Hamburg, Germany*

Experimental investigations of the internal structure of ferrofluids—carried out e.g. by cryogenic TEM [1] or small-angle neutron scattering (SANS) [2]—suggest that the magnetoviscosity observed in ferrofluid samples [3] can be attributed to the field-induced formation of chain-like aggregates of the component nanoparticles. Because these particles are weakly bound to their neighbors, even moderate shear forces suffice to break apart the chains, resulting in shear thinning—a significant obstacle to the technological exploitation of switchable magnetic-field-induced viscosity enhancement in applications.

Recently, Birringer *et al.* [4] proposed a strategy to suppress this shear thinning effect by replacing the spherical-shaped nanoparticles of conventional ferrofluids with rod-shaped counterparts. Inspired by this idea, we have begun synthesizing novel ferrofluids consisting of suspensions of anisotropic particles prepared by templating virus particles or the holes in a nanoporous membrane.

In the biotemplate-based approach, we first attempted to metallize the exterior surface of *Tobacco mosaic virus* (TMV)—a nanotube-shaped particle with a length of 300 nm, an outer diameter of 18 nm and an interior channel 4 nm in width—with Ni. Most likely as a result of rapid oxidation, such samples rarely manifested a measurable magnetization. However, to our great surprise, we discovered that the simple addition of non-metallized TMV to a conventional ferrofluid induces a significant enhancement in magnetoviscosity. Various amounts of freeze-dried, bare TMV were mixed into the commercial ferrofluid SusTech LCE-25, which consists of ~15 nm cobalt ferrite nanoparticles suspended in diethylene glycol. The complex viscosity of the resulting suspensions was measured in squeeze-flow geometry by a piezo-membrane axial vibrator (IdM Ulm) [5] operated at driving frequencies between 10 and 200 Hz on liquid volumes less than 100 µl. By means of an electromagnetic coil, the samples were subjected to axial magnetic fields as strong as 150 mT.

Figure 1 illustrates the dependence of the real part of the complex viscosity, η', on the concentration of TMV in the sample. Even at the highest TMV concentration, the viscosity is virtually unchanged from that of the conventional ferrofluid when no magnetic field is applied; however, at B = 110 mT and f = 10 Hz, the viscosity is enhanced by more than one order of magnitude. Moreover, the samples containing TMV were observed to retain their field-induced viscosity to higher excitation frequencies than did the conventional ferro-

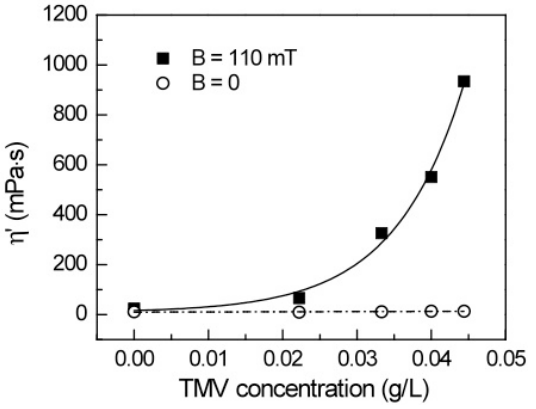

Fig. 1: Real part of the complex viscosity plotted as a function of the concentration of TMV in SusTech LCE-25 ferrofluid, both with and without a magnetic field applied perpendicular to the flow direction. Measurements made at 10 Hz.

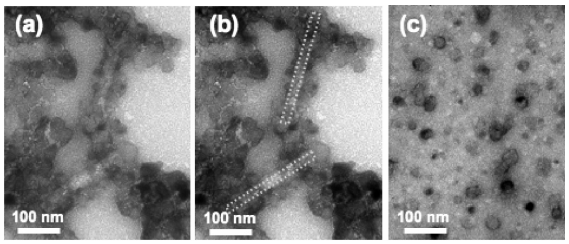

Fig. 2: (a) TEM micrograph of a ferrofluid containing bare TMV: magnetic nanoparticles are seen to be clustered around individual virus particles (outlined in (b)). (c) TEM micrograph of the same ferrofluid as in (a), but containing no virus—note the homogenous spatial distribution of nanoparticles.

fluid, indicating a greater stability against shear thinning.

Transmission electron micrographs provide a tantalizing explanation for the physical origin of this unexpected effect: in samples containing TMV, the ferromagnetic nanoparticles were observed to have aggregated around the virus particles, effectively creating rod-like magnetic structures [Fig. 2(a,b)]. On the other hand, in samples without TMV, the nanoparticles showed no sign of such clustering [Fig. 2(c)]. Apparently, the TMV "scaffolds" the cobalt ferrite particles into forming chain-like arrangements, which, in turn, may be responsible for the remarkable enhancement in magnetoviscosity.

As an alternative approach to the large-scale synthesis of anisotropic ferromagnetic particles, we are investigating the use of atomic layer deposition (ALD) to coat the surface of nanoporous aluminum oxide membranes with iron oxide [6], thus yielding mass quantities of ferromagnetic nanotubes, as illustrated in Fig. 3. Following dissolution of the membrane, the nanotubes can be suspended in a carrier liquid to form a "nanotube ferrofluid." Since the dimensions of the nanotubes can be controlled precisely by this approach, it ought to be possible to quantify the influence of particle shape and magnetic moment on the magnetoviscosity of a ferrofluid and compare the experimental results to the predictions of various theoretical models.

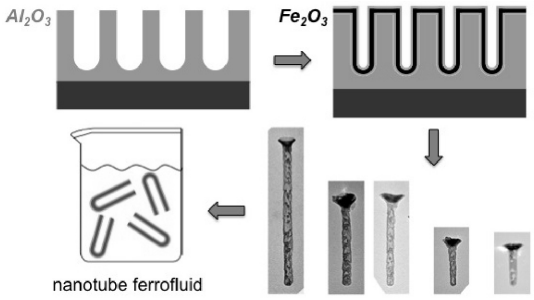

Fig. 3: Atomic layer deposition of magnetic nanotubes in nanoporous Al_2O_3 membranes. Individual nanotubes shown at the lower right range in length from 200 to 800 nm, with diameters of ~40 nm.

Acknowledgments

The authors wish to thank Dr. Hans-Martin Sauer of SusTech for kindly providing the ferrofluid LCE-25, and they gratefully acknowledge numerous valuable discussions with P. Martinoty. Financial support was provided by the Deutsche Forschungsgemeinschaft through SPP 1165.

References

[1] K. Butter, P. H. H. Bomans, P. M. Frederik, G. J. Vroege and A. P. Philipse, *Nature Mater.* **2** (2003) 88; *J. Phys.: Condens. Matter* **15** (2003) S1451.

[2] A. Wiedenmann, U. Keiderling, R. P. May and C. Dewhurst, *Physica B* **385–386** (2006) 453; L. M. Pop and S. Odenbach, *J. Phys.: Cond. Matter* **18** (2006) S2785.

[3] S. Odenbach, *Magnetoviscous Effects in Ferrofluids* (Springer, Berlin, 2002).

[4] R. Birringer, H. Wolf, C. Lang, A. Tschöpe and A. Michels, *Z. Phys. Chem.* **222** (2008) 229.

[5] L. Kirschenmann, Doctoral thesis, Ulm University (2003); J. J. Crassous, R. Régisser, M. Ballauff and N. Willenbacher, *J. Rheol.* **49** (2005) 851.

[6] J. Bachmann, J. Jing, M. Knez, S. Barth, S. Mathur, U. Gösele and K. Nielsch, *J. Am. Chem. Soc.* **129** (2007) 9554.

Thermomagnetic convection in magnetic fluids influenced by spatially modulated fields

A. Lange and S. Odenbach

TU Dresden, Institute of Fluid Mechanics, Chair of Magnetofluiddynamics, 01062 Dresden, Germany

Introduction

Thermomagnetic convection appears if a horizontal layer of magnetic fluid in a constant external magnetic field is subjected to a vertical temperature gradient ∇T. Due to this gradient, the magnetization of the fluid shows a gradient, ∇M too, which points antiparallel to the direction of ∇T. ∇M by itself is associated with the gradient of the internal field H_i inside the fluid, $\nabla H_i = -D\nabla M$, where D is the demagnetization factor for the used geometry of the setup. If a fluid volume is adiabatically moved from the bottom to the top across the fluid layer with thickness d, a difference in the magnetization exist between the fluid volume and the surrounding fluid. That difference together with the gradient of the internal field gives a resulting force which points in the same direction as the adiabatic movement. As a consequence initial disturbances can be enhanced and a convective flow can be triggered. Contrary, the friction between adjacent fluid volumes and the effect of heat conduction act against the onset of flow. All three effects are summed up in the magnetic Rayleigh number

$$Ra_{\mathrm{m}} = \frac{\mu_0 K^2 \Delta T^2 d^2}{\kappa \eta} \qquad (1)$$

which has to surpass a critical value before thermomagnetic convection sets in. The difference in the temperature between the bottom and the top plate is given by ΔT, K denotes the pyromagnetic coefficient $K = -(\partial M/\partial T)_H$, κ the thermal conductivity, and η the dynamic viscosity.

Whereas the thermomagnetic convection in static magnetic fields is well studied theoretically [1] as well as experimentally [2–4], analyses for modulated magnetic fields are just starting to appear. A first work on parametric modulation of the thermomagnetic convection was done by Engler and Odenbach [5] in 2008. The case of a spatially modulated magnetic field has not been studied yet and it is therefore the aim of this work.

System and analysis

A spatially modulated magnetic field can be easily realized by placing spatially modulated iron bars inside a spatially constant external field as seen Fig. 1. In such a way, many combinations of modulations can be realized: a modification by one or two bars, by bares with the same or with different wavelengths or by bars which are placed with a certain phase shift to each other. These options emphasise the advantages of spatial modulations over temporal modulations, where the setup is restricted to small frequencies [5].

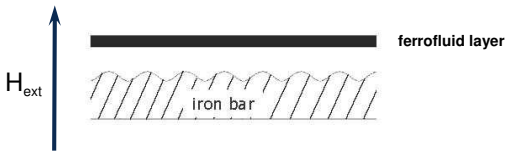

Figure 1: Sketch of a possible setup for a spatially modulated magnetic field.

In order to conduct a linear stability analy-

sis for the ground state of thermomagnetic convection, one has to know the particular form of the magnetic field. The corresponding numerical calculations were done for the symmetric case of two iron bares with the same wavelength of $\lambda \simeq 0.03$m placed below and above a layer of $d = 2$ mm. Figure 2 shows the color-coded spatial variation of the strength of the vertical component B_y of the magnetic induction in the (x,y)-plane. The sinusoidal dependence of B_y on x can be well fitted by an ansatz of the form $B_\mathrm{y} \sim f(y) \cdot \cos(kx)$, where the wave number is defined as $k = (2\pi)/\lambda$ (see Fig. 3).

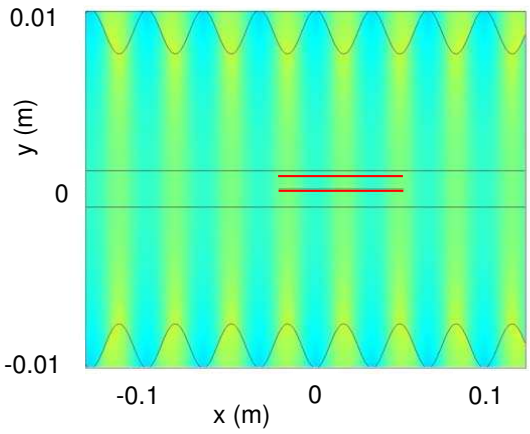

Figure 2: Color-coded strength of B_y with high (low) values indicated by yellow (blue). The black solid lines indicate the ferrofluid layer (center) and the iron bars (top, bottom), respectively. Along the two red lines the numerical data are compared with the approximation (see Fig. 3).

With the knowledge of the magnetic field for the chosen setup, the ground state of the system can be determined as solution of the Navier-Stokes and heat conduction equation. In contrast to the classical Rayleigh-Bénard system, i.e., $\mathbf{B} = 0$, the ground state is not the quiescent one. In fact the solution yields a double vortex structure for the flow field combined with a vertical temperature gradient as known from the classical setup. Details of this flow field will be presented and

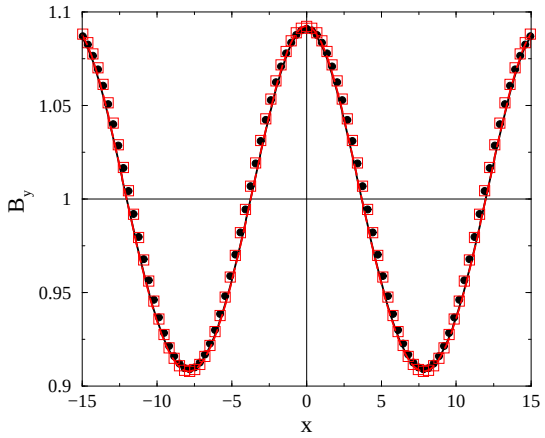

Figure 3: B_y versus x for $y = 0$ (black) and $y = 0.8$ mm (red). The solid lines indicate the numerical results, the black symbols the values of the approximation. Both agree very well.

a linear analysis of its stability against small fluctuations conducted. The result of such an analysis will relate the critical magnetic Rayleigh number with the thermal one, illuminating the interplay of both the thermally as well as the magnetically driven convection.

References

[1] B. A. Finlayson, J. Fluid Mech. **40**, 753 (1970)

[2] L. Schwab and U. Hildebrandt and K. Stierstadt, J. Magn. Magn. Mat. **39**, 113 (1983)

[3] L. Schwab and K. Stierstadt, J. Magn. Magn. Mat. **65**, 315 (1987)

[4] L. Schwab, J. Magn. Magn. Mat. **85**, 199 (1990)

[5] H. Engler and S. Odenbach, J. Phys.: Condens. Matter **20**, 204135 (2008)

D. Lerche (Vortragender), U. Mertens, Ch. Pietsch
LUM GmbH, Rudower Chaussee 29 (OWZ) 12489 Berlin
Ch. Eichholz, H. Nirschl
Universität Karlsruhe, Karlsruhe
K.Trommler
Bilacon GmbH, Jahnsdorf
info@lum-gmbh.de, www.lum-gmbh.com

Charakterisierung von dispergierten Nano- und Mikromagnetpartikeln in Gravitationsfeldern unter Einwirkung überlagerter Magnetfelder

Die Charakterisierung von Teilchen im Bereich der Nano- oder Biotechnologie erlangt mit der stetig komplexeren Teilchenstruktur eine immer größere Bedeutung. Dies betrifft einmal die Produktanforderungen (z.B. Magnetbeads) und zum anderen die Realisierung und Optimierung von verfahrenstechnischen Trennverfahren (z.B. Magnetseparation). Um diesen neuen Anforderungen gerecht zu werden, müssen neben der Größe und der Form der Teilchen zunehmend elektrische und magnetische Teilcheneigenschaften analysiert werden.
Die messtechnische Erfassung der Teilchengröße bis hin zu wenigen Nanometern ist prinzipiell gelöst und auch die Formbeschreibung und Formmessung der Teilchen sind weitgehend erarbeitet (vgl. ISO-Normen des TC24). Die Charakterisierung der magnetischen Eigenschaften von Teilchen und der Einfluss von Magnetfeldern auf das Verhalten von Dispersionen stehen dagegen erst am Anfang.
Im Vortrag werden erste Ergebnisse beschrieben, wie ein statisches Magnetfeld die Sedimentation im Gravitations- bzw. Zentrifugalfeld beeinflusst. Mittels spezieller Anpassungen von Stabilitätsmessgeräten (LUMiReader, LUMiFuge), welche die Applikation eines zusätzlichen Magnetfeldes ermöglicht, können Magnetteilchen charakterisiert werden. Die Magnetfelder können sowohl bezüglich der Stärke als auch der Richtung (senkrecht oder parallel zur Sedimentationsrichtung) variiert werden. Erste Ergebnisse mit magnetisierbaren Modellpartikeln und magnetisierbaren Zellen werden vorgestellt und analysiert. Es wird gezeigt, dass das magnetfeldüberlagerte Seperationsverhalten in Gravitations- bzw. Zentrifugalfeldern eine einfache Methode ist, um grundlegende Auslegungsdaten für eine spätere Separation (z.B. Magnetic Fishing) zu erlangen. Des Weiteren bieten diese Verfahren eine Möglichkeit zur Charakterisierung bzw. Qualitätskontrolle bei der Herstellung von funktionalisierten Magnetbeads.

Supported by BMWi (Grant Kz. 0327414A

Stability of the circular Couette flow of a ferrofluid

A. Leschhorn[1], M. Reindl[2], S. Altmeyer[1], C. Hoffmann[1],
M. Lücke[1], S. Odenbach[2]

[1] *Institut für Theoretische Physik, Universität des Saarlandes, 66041 Saarbrücken*
[2] *Institut für Strömungsmechanik, Technische Universität Dresden, 01062 Dresden*

The gap between two concentric rotating cylinders is filled with a ferrofluid. We analyze the influence of an homogeneous magnetic field parallel to the cylinder axis on the the stability of the circular Couette flow (CCF). The predictions of different theoretical models are compared with experimental data. In particular we investigate in what way the stability boundary depends on the particle size distribution of the ferrofluid.

Characterization of magnetic core-shell nanoparticle suspensions using ac susceptibility for frequencies up to 1 MHz

F. Ludwig, A. Guillaume, E. Heim, and M. Schilling

Institut für Elektrische Messtechnik und Grundlagen der Elektrotechnik, TU Braunschweig, Hans-Sommer-Str. 66, D-38106 Braunschweig

Magnetic nanoparticles (MNPs) find wide application in medicine and bioanalytics. As has been demonstrated in [1-3], the measurement of the magnetorelaxometry (MRX) and the analysis of the experimental curves with the moment superposition model (MSM) is a quick and powerful tool for the estimation of structure parameters like core and hydrodynamic size distributions. The accessible range of relaxation time constants of the MNPs is limited by the switch-off time of the magnetizing field, which amounts typically to a few 10s up to a few 100s of a μs, by the bandwidth of the magnetic field sensors – 3 kHz for our fluxgate MRX system - , and by the deadtime between switching off the magnetizing field and data acquisition for SQUID MRX systems. Consequently, relaxation processes with time constants below about 100 μs can not be detected.

An alternative magnetic technique is the measurement of the complex magnetic susceptibility. Whereas the signal is recorded in the time domain for MRX, in ac susceptibility it is measured in the frequency domain. Measurements of the ac susceptibility have successfully been used for the study of magnetic nanoparticles properties as well as for the realization of homogeneous bioassays. Here we report on measurements of the real and imaginary part of the ac susceptibility on aqueous suspensions of magnetic core-shell nanoparticles in the frequency range up to 1 MHz. This frequency range corresponds to relaxation time constants down to about 1 μs. Taking into account that the Brownian time constant of spherical particles is given by

$$\tau_B = \frac{\pi \eta d_h^3}{2 k_B T} \qquad (1)$$

one obtains for a viscosity of water of η = 1 mPa·s and a temperature T = 295 K a minimum detectable hydrodynamic diameter of about d_h = 14 nm.

The ac susceptibility setup consists of a 1 MHz LockIn amplifier eLockIn203 from Anfatec AG and a twin set of excitation and detection coils. The MNP sample is placed in one of the detection coils and the differential voltage is measured. From out-of-phase and in-phase parts of the differential voltage signal real and imaginary part of the complex susceptibility can be calculated. To provide a constant amplitude of the excitation field, a special transinductance amplifier circuit was developed providing field amplitudes up to about 90 μT. To eliminate the influence of parasitic phase errors, the differential voltage signal of a blank measurement is taken into account in the signal analysis.

To investigate the ac susceptibility of MNP suspensions when a static magnetic field is superimposed, an additional cylindrical coil with its axis parallel to the ac excitation field coils was used.

As sample containers for all studied MNP solutions standard microtiter vials with a sample volume of 150 μL were used.

The ac susceptibility of various MNP suspensions was measured in the frequency range between typically 100 Hz and 1 MHz. From the position of the maximum in the imaginary part χ'' the hydrodynamic size is determined. For monodisperse MNPs, the maximum lies at $\omega \cdot \tau = 1$ and the hydrodynamic diameter can be deter-

mined with (1). For multidisperse MNPs, the distributions of core and hydrodynamic diameters have to be taken into account. Fig. 1 depicts the measured imaginary part $\chi''(f)$ of the ac susceptibility for a Fe_3O_4 NP suspension. The high-frequency part of the spectrum is caused by the Néel relaxation of MNPs with small cores.

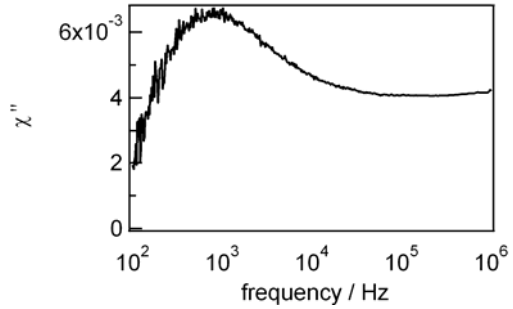

Fig. 1: Imaginary part χ'' of ac susceptibility of Fe_3O_4 NP suspension.

If a static magnetic field is superimposed, the position of the Brownian relaxation peak shifts toward higher frequencies. Fig. 2 depicts the imaginary part of the ac susceptibility of a $CoFe_2O_4$ NP suspension for values of the superimposed static magnetic field between 39 μT and 3.15 mT. As can clearly be seen, the maximum in χ'' shifts with increasing static field to higher frequencies whereas the amplitude decreases.

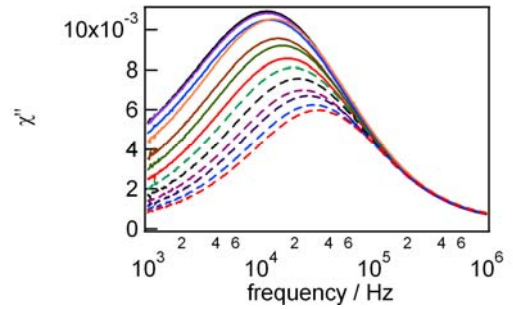

Fig. 2: Imaginary part of ac susceptibility of $CoFe_2O_4$ NP suspension for different static magnetic field values.

From the position of the maximum in the imaginary part at zero static field, a hydrodynamic diameter of $d_h = 33$ nm is found using (1), in good agreement with the value from dynamic light scattering measurements. The positions of the maxima in χ'' are plotted in Fig. 3 as a function of static magnetic field. The dependence of the Brownian time constant on magnetic field was theoretically dealt with by Shliomis and Raikher [4] and can be described by

$$\tau_B = \tau_B(0)\frac{\xi}{L(\xi)}\left[1-\coth^2(\xi)+\xi^{-2}\right] \quad (2)$$

where $\xi = \mu_0 mH/(k_B T)$. The dashed line in Fig. 3 shows the dependence calculated for $\xi = 1200 \cdot B$. Taking $M_s = 4 \cdot 10^5$ A/m for cobalt ferrite, this corresponds to a core diameter of about 28 nm which is slightly larger than the value estimated from the initial susceptibility of static *M(H)* curve measured with a VSM.

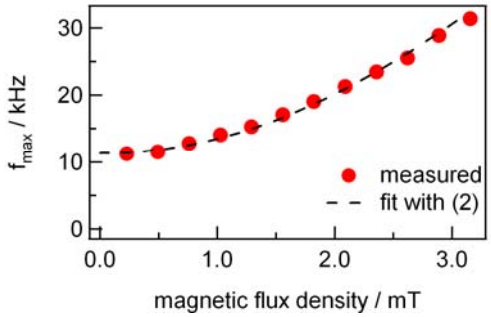

Fig. 3: Dependence of the peak frequency of χ'' on static magnetic flux density.

The experimental results demonstrate that measurements of the complex susceptibility on MNP suspension in a static magnetic field allow one to estimate both hydrodynamic and core size distributions. The extension of the frequency range to 1 MHz provides additional information on the Néel relaxation contribution.

Acknowledgments

This work was financially supported by the DFG via SFB 578 and by the BMBF under contract number 13N9174.

References

[1] D. Eberbeck, F. Wiekhorst, U. Steinhoff, and L. Trahms, J. Phys.: Condens. Matter **18,** S2829 (2006).

[2] F. Ludwig, E. Heim, M. Schilling, and K. Enpuku, J. Appl. Phys. **103**, 07A314 (2008).

[3] F. Ludwig, E. Heim, and M. Schilling, J. Appl. Phys. **101**, 113909 (2007).

[4] M. I. Shliomis and Y. L. Raikher, IEEE Trans. Magn. **16**, 237 (1980).

Distribution of Magnetic Nanoparticles after Magnetic Drug Targeting in an *Ex Vivo* Bovine Artery Model

S. Lyer[1], R. Tietze[1], R. Jurgons[1], H. Richter[2], F. Wiekhorst[2], K. Schwarz[2], L. Trahms[2] and Ch. Alexiou[1]

1 Division of experimental Oncology and Nanomedicine (Head: Prof. Dr. med. Ch. Alexiou) in the Department of Oto-Rhino-Laryngology, Head and Neck Surgery, University Erlangen-Nürnberg, Germany

2 Physikalisch-Technische Bundesanstalt, Berlin, Germany

Introduction

The major dilemma of cancer therapy is, that often the dose of systemically applied chemotherapeutics needed to annihilate all tumor cells would also end the life of the patient. Therefore a tremendous number of patients with inoperative solid tumors are diagnosed with not curable cancer.

Magnetic Drug Targeting (MDT) is a new promising attempt for treating malignancies. This method uses super paramagnetic nanoparticles bound to chemotherapeutics, focused by a strong external magnetic field to the tumor region. This leads to higher doses of the chemotherapeutic agent in the region of the malignancy, even if the overall dose is reduced [1]. Currently this approach has been investigated for the treatment of solid tumors near the body surface by applying a chemotherapeutic agent bound to a ferrofluid intra-arterially near the tumor [1, 2, 3].

In this study we are focusing on the latter approach. The intra-arterial application of super paramagnetic nanoparticles has the advantage of avoiding the clearance of the major part of the particles by liver and spleen before they reach the tumor. By using a strong external magnetic field gradient, significantly more nanoparticles can be accumulated in the tumor in comparison to the intravenous application [1].

One crucial point for this method is a detailed understanding of the mechanisms of particle deposition along vessels, when MDT is applied. Therefore we use an *ex vivo* bovine artery model to investigate the various parameters influencing the distribution and deposition of the particles along the arteries [4].

To measure the distribution of the nanoparticles in the arteries Magnetorelaxometry (MRX) is a very sensitive and fast method. [3]. Here, we investigated the feasibility of MRX to measure non-invasively the accumulation profile along the artery in our *ex vivo* bovine artery model.

Material and Methods

Freshly isolated bovine arteries were mounted in a tempered glass container attached to a buffer circuit. A flow rate of 6ml/min was conducted by a peristaltic pump. The two arteries used for this study had a diameter of about 0.6cm ± 0.1cm and were rinsed thoroughly with BSA buffer (0.114M NaCl, 3mM KCl, 2.5mM CaCl2, 1mM KH2PO4, 0.8mM MgSO4, 24mM NaHCO3, 1.0g/l Glucose, 6.25g/l Serum Albumin, Sigma, Germany. The electromagnet (Siemens Healthcare, Germany) was positioned over the middle part of the artery and the magnetic field gradient at the artery was adjusted to 16T/m (magnetic field strength: 0.32 Tesla). 1 ml of magnetic nanoparticles were applied into the circuit to pass the bovine artery under the influence of the external magnetic field. After 25 minutes the magnetic field was switched off. The only difference was the flow direction. RA001: The buffer was pumped through the artery. RA002: The buffer was drawn through the artery.

To evaluate the biodistribution of MNP after MDT the arteries were cut into 11

equal sections of approximately 1cm length.
The MRX setup has already been described in detail previously [5]. For the quantification of the iron oxide content in the tissue samples, a calibration curve of a dilution series of the iron oxide particles originally used in the experiment was measured first. The reference particles were immobilized in plaster. For background correction and examining the detection limit an empty paraffin column was measured. The resulting detection limit was 320ng ± 50ng.

Results

Both arteries showed a raising accumulation of nanoparticles the closer their position was to the tip of the pole shoe (Fig. 1). Both arteries show a ramp with raising signals in flow direction in front of the pole shoe from the most distal section to the central sections of the arteries. And both arteries show a sudden drop of iron content directly after the section with the maximal signal and a plateau of only slowly falling (RA001) or even slightly rising signals (RA002). Besides these common findings the profiles of both arteries differ apparently from each other. Artery RA001, where the particles where pumped through the artery, shows slower raising signals beginning 5 sections ahead of the section with the highest signal (Fig. 1A).
In contrast to that the profile of artery RA002 shows a very short and steep ramp (Fig. 1B). The drop in signal intensity is more pronounced when the particles were pumped compared to when they are drawn.
Over all the profile of artery RA001 shows a more Gauss-like distribution of magnetite along the artery in flow direction. Very interesting is the finding that both the maximum of particle deposition and the absolute accumulation of magnetite was higher in artery RA002 with the particles being drawn through the system.

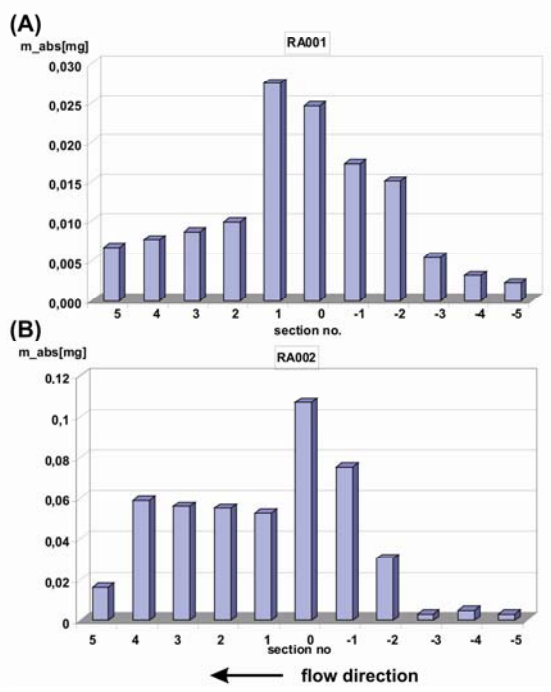

Fig. 1: Magnetite content [mg] of each section of artery RA001 and RA002 along the flow direction. Section "0" was intended to be positioned directly under the pole shoe of the electron magnet.

Conclusion

In this study we could show, that MRX is a feasible method to measure particle deposition after MDT in our *ex vivo* artery model. The differences in the profiles of the two arteries show, that there might be hydrodynamic influences caused by the flow direction during the experiments. This has to be taken into account for further studies for a better understanding of the mechanisms of particle deposition in an artery during MDT.

Acknowledgments

This work was supported by the DFG research programs "AL552/3-1 and TR408/4-1"

References

[1.]Alexiou C, Jurgons R, Schmid RJ et al. (2003) *J Drug Target* 11:139-149.
[2.]Alexiou C. et al.(2006) *J Nanosci Nanotechnol* 6:2762-2768.
[3.]Wiekhorst F et al. (2006) *J Nanosci Nanotech* 6:3222-3225
[4.]Seliger C et al. (2007). *JMMM* 311:358-362
[5.]Eberbeck D, et al. (2006) *J Phys Cond Matter* 18:2829-2846

Magnetic Polymer Brushes for Controlled Drug Delivery

G.U. Marten[1], T. Gelbrich[2], A. M. Schmidt[1]

[1] *Institut für Organische Chemie und Makromolekulare Chemie, Heinrich-Heine-Universität, Universitätsstr. 1, D-40225 Düsseldorf, Germany, email: schmidt.annette@uni-duesseldorf.de*
[2] *current adress: Quigen GmbH, Hilden, Germany*

Magnetic polymer brushes[1] represent a growing field in biomedical applications. Some examples include hyperthermia, bioseparation or drug targeting. The surface grafted polymer shell allows the steric stabilization of single magnetic cores with excellent dilution stability. In addition, it also permits a great diversity of chemical and physical properties by varying the chemical structure of the polymers. By using functional comonomers, a high degree of functional groups can be achieved in the polymer shell.

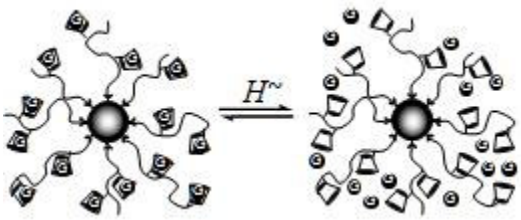

Fig.1: Drug release from functional nanoparticles via intrinsic heating

The combination of highly functionalized particles, magnetic heating, and thermoresponsive behavior can be used to create a system for magnetically controlled drug delivery. Therefore, magnetic FeO_x-nanoparticles (d_{core} = 12 nm) are functionalized and stabilized with a copolymer shell via surface initiated Atom Transfer Radical Polymerization (ATRP). The copolymers show a lower critical solution temperature (LCST) in water, hence the particles show a thermoresponsive dispersion behavior. Additionally, the copolymers contain functional groups which are able to bind drugs or dyes. The obtained particles are characterized with respect to their functionalization, composition, thermal and magnetic properties and their dispersibility in water or physiological buffer. β-Cyclodextrine (β-CD) is able to form host/guest complexes with a large number of weakly water-soluble substances, including potential agents or dyes. To achieve magneto-responsive drug delivery systems (Fig.1), we copolymerize an oligo(ethyleneglycol) methylether methacrylate (OEGMA) derivative with (3-β-cyclo-dextrine-1,2,3-triazol-4-yl)methyl methacrylate (CDMA) (Fig.2) that contains a β-CD-functional side chain to form complexes with a potential agent showing a thermosensitive complexation-release behavior. The decomplexation can be forced by conventional heating or via intrinsic heating in an alternating magnetic field.

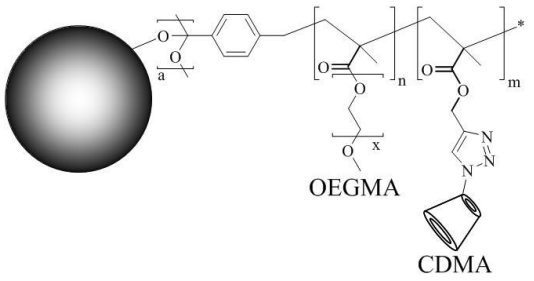

Fig.2: Chemical composition of the magnetic polymer brushes

We describe the synthesis and properties of the particles, along with the thermosensitive dispersion behavior and complexation of guests with differing qualities and functions.

Acknowledgement
We gratefully acknowledge DFG (Emmy Noether Program) and the FCI for financial support.

References

[1] A. M. Schmidt, *Macromol. Rapid Commun.* **26**, 93–97, 2005; A. Kaiser, T. Gelbrich, A. M. Schmidt, *J. Phys.: Condens. Matter* **18,** 2563–2580, 2006; T. Gelbrich, M. Feyen, A. M. Schmidt, "Magnetic Thermoresponsive Core-Shell Nanoparticles", *Macromolecules* **39** , 3469-3472 (2006)

Recent development at the STREM Nanolab

N. Matoussevitch[1], H. Boennemann[1]

[1] *Strem Chemicals GmbH, Berliner Str. 56, D-77694 Kehl, Germany*
E-mails: nina-stremgmbh@web.de ; h.boennemann@web.de

During the last few years our focus was to develop novel Co-, Fe-, and Fe/Co-particles. Metallic and bimetallic Co, Fe and Fe/Co nanoparticles were prepared via the thermolysis of metal carbonyls in the presence of aluminium alkyls and subsequent sealing the surface via smooth oxidation. Obtained particles are monodisperse (ca. 10 nm), air-stable, and dispersible in a plethora of carrier-liquids including water to give stable magnetic fluids for technical and medical applications. We continue to produce these products.

There are a few advantages to use the metallic Co-, Fe-, or Fe/Co-nanoparticles particles and magnetic fluids (MFs). As compared to iron oxide the metallic particles exhibit a higher saturation magnetization at the same volume concentration; they X-ray contrast is higher; to reach the same magnetic effect we can use much smaller amount of particles. But in some cases and for some applications to use the magnetic fluids with magnetite is more reasonable.

Now in STREM Nanolab we start to produce the high concentrated magnetite magnetic fluids on base of kerosene, hydrocarbons, mineral and vacuum oils and water according [1,2] (see Fig.1).

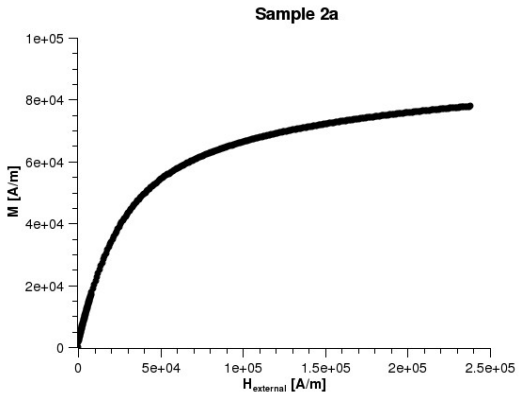

Fig.1. Magnetisation of magnetite MF in kerosene

Via dilution of concentrated MF it is possible to reach any tailored concentration.

Water-based magnetite magnetic fluids stabilized by different type of surfactant or biocompatible substances can be use in bio-medicine.

Recently, in STREM Nanolab we establish all things for Synthesis of Au_{55}-cluster ($Au_{55}[P(C_6H_5)_3]_{12}Cl_6$) according G. Schmid's method [3], using diborane, which is obtained during the synthesis. We can produce Au_{55}-clusters soluble in dichlormetane (DCM) and in other non-polar media. Via the ligand-exchange the water soluble Au_{55}-clusters were prepared also.

Magnetite and metallic or bimetallic nanoparticles coated by gold have a high potential for a number of research, technical and biomedical applications.

Using the different procedures we succeed in coating of magnetite nanoparticles and 6nm and 10nm Co particles by gold.

Acknowledgments

We thank a lot to Dr. D. Borin (Uni-Dresden) for magnetic measurements.

References

[1] N. Matoussevitch, V. Rakhuba, V. Samoilov, Authors Certificate USSR No 833545 (1981) „Method of preparation of magnetic fluids".

[2] V.Korotkov, A.Larin, N. Matoussevitch, Authors Certificate USSR No 968047 (1982) "Water-based magnetic fluid".

[3] G.Schmid, "Inorganic Synthesis" 1990, 27, p.214-218.

Thermomagnetic convection in a ferrofluid layer exposed to a time-periodic magnetic field

P. Matura and M. Lücke

Institut für Theoretische Physik
Universität des Saarlandes
D-66041 Saarbrücken, Germany

We have investigated the influence of a time-periodic and spatially homogeneous magnetic field on the linear stability properties and on the nonlinear response of a ferrofluid layer heated from below and from above (see Fig. 1). A competition between stabilizing thermal and viscous diffusion and destabilizing buoyancy and Kelvin forces occurs. Floquet theory is used to determine the stability boundaries of the motionless conductive state for a harmonic and subharmonic response. Full numerical simulations with a finite difference method were made to obtain nonlinear convective states (see Fig. 2). The effect of low and high frequency modulation on the stability boundaries as well as on the nonlinear oscillations that may occur is investigated [1].

Acknowledgments

This work was supported by the Deutsche Forschungsgemeinschaft.

References

[1] P. Matura and M. Lücke, *Thermomagnetic convection in a ferrofluid layer exposed to a time-periodic magnetic field*, accepted for publication in Phys. Rev. E.

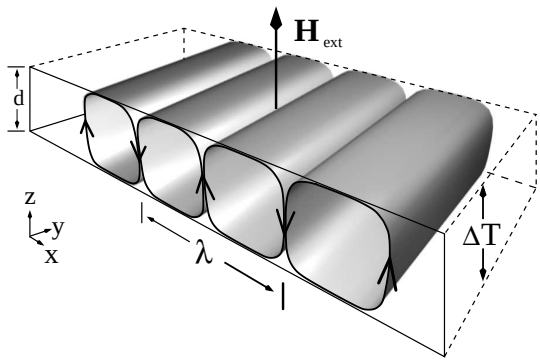

Figure 1: Schematic setup of the Rayleigh-Bénard system. A constant vertical temperature gradient $\Delta T/d$ and a spatially homogeneous external magnetic field $\mathbf{H}^{\rm ext}$ normal to the fluid layer is applied.

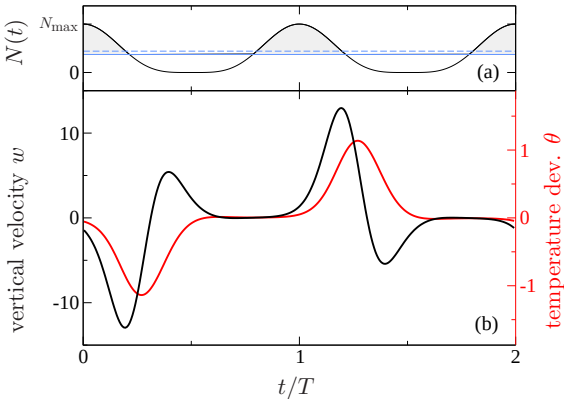

Figure 2: Subharmonic response displayed by temporal oscillations of (b) the vertical velocity w and the temperature deviation $\theta = \delta T - \delta T_{\rm cond}$ at midheight between two adjacent rolls for two periods of the modulation. The driving via the magnetic Rayleigh number $N(t)$ is shown in (a).

Magnetosensitive $CoFe_2O_4$ PAAm Hydrogels

R. Messing, N. Frickel, A. M. Schmidt[1]

[1]*Institut für Organische Chemie und Makromolekulare Chemie, Heinrich-Heine-Universität, Universitätsstr.1, D-40225 Düsseldorf, Germany, email: schmidt.annette@uni-duesseldorf.de*

The integration of magnetic nanoparticles into polymer networks offers the ability to influence the properties of the network and by applying an outer magnetic field (AC, DC). The magnetic nanoparticles serve as antennas for the response to the applied field. When magnetically blocked particles are applied, Brownian rotation is the predominant magnetic relaxation mechanism. The relaxation of the particles can be inhibited by integration into polymer gels by different pathways leading to hysteresis effects examined by magnetization measurements.

We present the first results on the quasistatic and dynamic magnetic properties of (PAAm) hydrogels filled with $CoFe_2O_4$ nanoparticles.

a)

b)

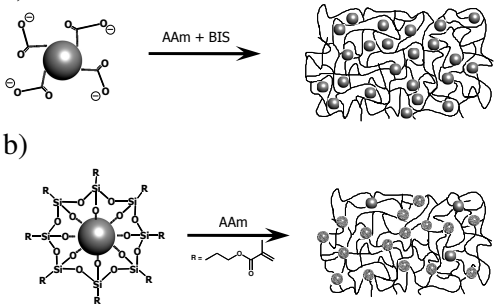

Fig. 1: Synthesis of PAAm hydrogels containing $CoFe_2O_4$ nanoparticles: a) $CoFe_2O_4$ incorporated without chemical bonding to the PAAm matrix b) $CoFe_2O_4$ bound covalently to the PAAm matrix; $CoFe_2O_4$ serve as crosslinker.

In the one case electrostatically particles are embedded in the hydrogel non-covalently. The hydrogel is crosslinked chemically by the use of the bifunctional crosslinker N,N'-methylenbisacrylamide (BIS). In the other case, the particles are surface functionalized with a monomer unit, resulting in a covalent attachment to the polymer network. The particles serve as multifunctional crosslinker in the hydrogel. In both types of materials, the particles surrounding ismanipulable by adjusting the swelling degree of the hydrogel.

The synthesized hydrogels are analyzed regarding to their crosslinking density their magnetic behavior by *Vibrating Sample Magnetometry* (VSM) and AC-susceptometry. The focus is on the dependence of the hysteresis effects on the properties of the surrounding matrix.

The results give first insight in the complex behavior of nanoparticle integrated polymer networks.

Acknowledgement

We gratefully acknowledge the DFG (SSP1259 and Emmy Noether Program) for financial support.

Investigations on Magnetic Particles Prepared by Cyclic Growth

R. Müller, S. Dutz, M. Zeisberger

Institut für Photonische Technologien e.V., Albert-Einstein-Str. 9, 07745 Jena

Introduction

Magnetic iron oxide nanoparticles (MNP) are promising tools for medical applications like hyperthermia or magnetic drug targeting. The relevant properties in these applications (specific heating power SHP of the particles in a magnetic AC field or the force on the particles in a gradient DC field) strongly depend on the particle size and size distribution.

In a previous work we have shown that bigger particles than the usual ones by simple precipitation can be produced by a "cyclic" precipitation method [1]: $NaHCO_3$ solution was added to a $FeCl_2$ /$FeCl_3$ solution (Fe^{2+}/Fe^{3+}-ratio = 1:1) up to pH = 7 which led to the formation of a brownish precipitate. Then a new Fe^{2+}/Fe^{3+} mixture was added and the precipitation was carried out again. This procedure was repeated up to four times. After that the solution was boiled for 10 min to form an almost black precipitate. The MNPs were then washed and dried. An advantage of the cyclic grown samples concerning the specific loss power for comparable crystallite size and coercivity, respectively, could be shown [1].
Information on the statistical properties of the samples containing a fraction of non-superparamagnetic particles that increases with the number of cycles can be provided by the switching field distribution *S(H)* (distribution of the amount of particles which switch their magnetization irreversibly at the field *H* [2]) with

$$S(H) = 1/M_{rs} \cdot \mathrm{d}M_r(H)/\mathrm{d}H.$$

S(H) can be calculated from initial remanence curves (gradual measurement of the remanent magnetization (H=0) vs previous magnetic field strength $M_r(H)$). S(H) was fitted by a log-normal distribution.

The influence of the statistical orientation of the particles and the distribution of the anisotropy constant on *S(H)* can be seen in [3].

The samples contain a certain fraction of superparamagnetic particles which is indicated by a reduced remanence ratio M_{rs}/M_s (saturation magnetization M_s and maximum remanent magnetization M_{rs}) and is determined from a usual magnetization loop.
In addition, magnetic hysteresis losses at different maximum field strength were calculated from minor loops. All measurements were carried out by VSM.

Results

Although the TEM image may suggest a remarkable growth (from usually ca. 10nm size) to several 10nm particle size after a four-cycle process, the mean crystallite size by X-ray diffraction is only 19 nm.

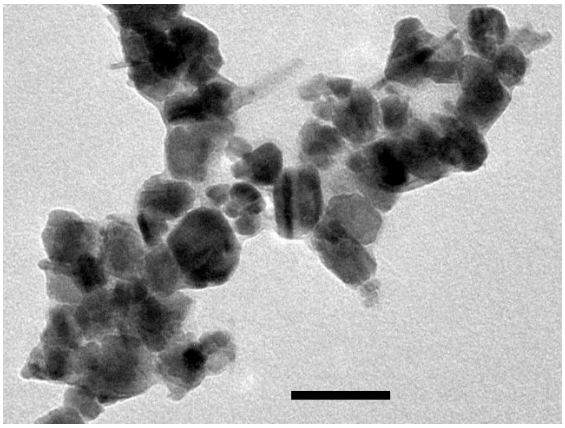

Fig. 1: TEM image of the 4cycle-sample, scale bar = 100nm

The remanence curves can be seen in Fig. 2. The fitted *S(H)* curves are shown in Fig. 3. The mean value of the *S(H)* increases as expected with increasing coercivity. The

ratio H_c/H_m increases with decreasing superparamagnetic particle fraction. The remanence ratio M_{rs}/M_s increases accordingly but even at four cycles it is far below one that can be expected in samples without superparamagnetic particles.

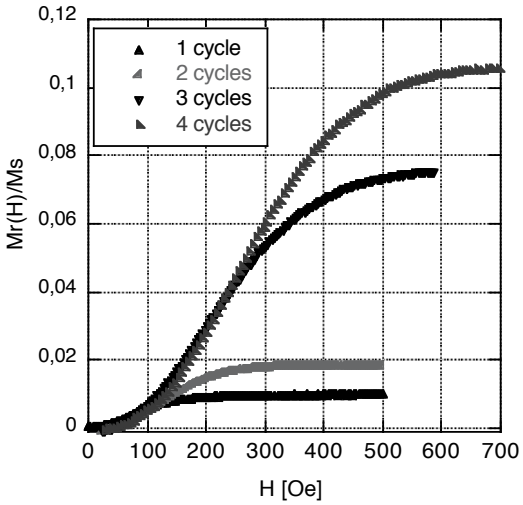

Fig. 2: Initial remanence curves of samples prepared by different cycles

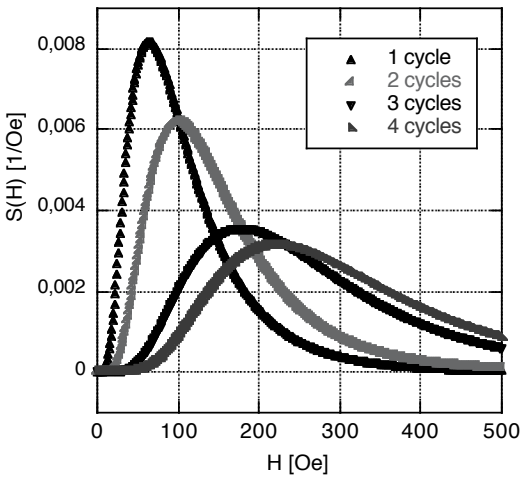

Fig. 3: Log-normal fits of the switching field distributions S(H)

Tab. 1. Magnetic parameters
(H_C: coercivity [Oe], m_{rs}: M_{rs}/M_s, H_m: mean value of the fitted switching field distribution *S(H)* [Oe], σ: width of the fitted *S(H)*)

Cycle	H_c	m_{rs}	H_m	σ	H_c/H_m
1	9	0,018	95	0,627	0.095
2	17	0,033	136	0,549	0.125
3	59	0,096	240	0,545	0.246
4	78	0,122	286	0,506	0.273

The development of the magnetic properties with increasing number of cycles can be seen in Table 1.

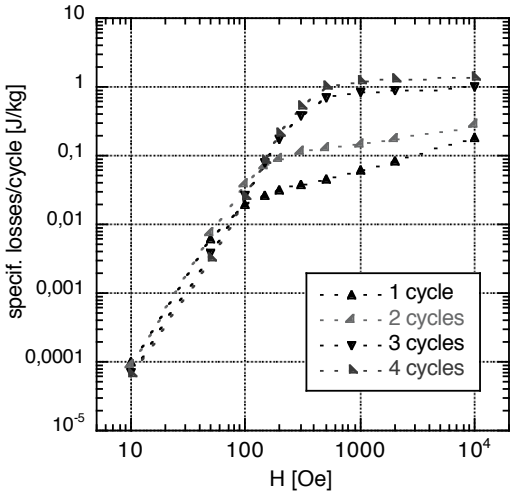

Fig. 4: Specific hysteresis losses per magnetization cycle vs maximum field strength

Fig. 4 shows the hysteresis losses for one magnetization cycle vs the maximum field strength. The field strength at which a saturation behaviour starts correspond roughly with the mean fields of *S(H)*.
The weak influence of the number of cycles on the losses at low fields (H_{max}<50 Oe) is remarkable.

Acknowledgement

We thank Ms K. Buder (FLI Jena) for help at the TEM investigations and Ms H. Steinmetz at the preparation.
This work was supported by DFG grant ZE825/1-1.

References

[1] R. Müller, H. Steinmetz, M. Zeisberger, Ch. Schmidt, S. Dutz, R. Hergt, W. Gawalek; Z. Phys. Chem. 220 (2006) 51-57

[2] H. Pfeiffer, Phys. Stat. Sol. A 118 (1990) 295

[3] M. Zeisberger, S. Dutz, J. Lehnert, R. Müller; Journal of Physics: Conference Series **149** (2009) 012115

Magnetic Nanoparticles for Gene Delivery: Some Determinants of Efficient Delivery Vectors

O. Mykhaylyk[1], Y. Sanchez-Antequera[1], N. Tresilwised[1], S. Thalhammer[2], D. Adigüzel[2], M. Döblinger[3], Th. Bein[3], P. Sonne Holm[1], Ch. Plank[1]

[1]Klinikum rechts der Isar, Institute of Experimental Oncology and Therapy Research, TUM, Munich, [2]Institute of Radiation Protection, AG NanoAnalytics, Neuherberg, [3]Department of Chemistry and Biochemistry, LMU, Munich, Germany

About thirty magnetic nanoparticles of the core-shell type comprising magnetite cores of about 10 nm stabilized and decorated by self-assembly of surfactant and polymers to be suitable as components of magnetic nucleic acids delivery vectors by magnetofection and their formulations with nucleic acids and adeno- as well as lentiviral particles were screened for their gene delivery efficiency in vitro. The group of the most efficient particles was defined and characterized with respect to their core composition, crystallite size, magnetization, coating composition using TEM, XRD, magnetization and XPS methods. Magnetic gene delivery formulations were optimized with account for the association of DNAs, siRNAs and adeno- and lentiviral particles with magnetic nanoparticles. A simple method for evaluation of the magnetophoretic mobility and, hence, of the magnetic moment was used to characterize the complexes and evaluate the number of magnetic nanoparticles associated with complexe(s) [1]. Together with TEM and AFM data, these approaches deliver information on the morphology, composition and magnetic properties of the complexes which are important for identifying the most efficient magnetic vectors. The developed transfection protocols [2,3] can be used for cells that are difficult to transfect, such as primary cells, and can also be applied to improve significantly viral nucleic acid delivery. With minor alterations, these protocols can also be useful for magnetic cell labelling for cell tracking studies. Specifically, we were interested in how physico-chemical and surface characteristics of iron oxide magnetic nanoparticles and their complexes with adeno- and lentiviruses correlate with the infectious potential in target cells. We have shown that magnetofection of oncolytic adenovirus does not alter the inherent oncolytic potential of the virus but that it rather enchances virus uptake into cells. Optimized assembling with selected magnetic nanoparticles lowers the IC50 of the adenovirus in 181RDB cells and lentivirus in umbical cord mesenchymal stem cells one order of magnitude. We suggest a “rule” to formulate virus magnetic complexes based on our fine-tuning of the nanoparticles-to-virus particles ratio in the range of 2.5-20 fg iron per physical virus particle depending on the nanomaterial used. We show also that an excess of magnetic nanoparticles can inhibit infection efficiency.

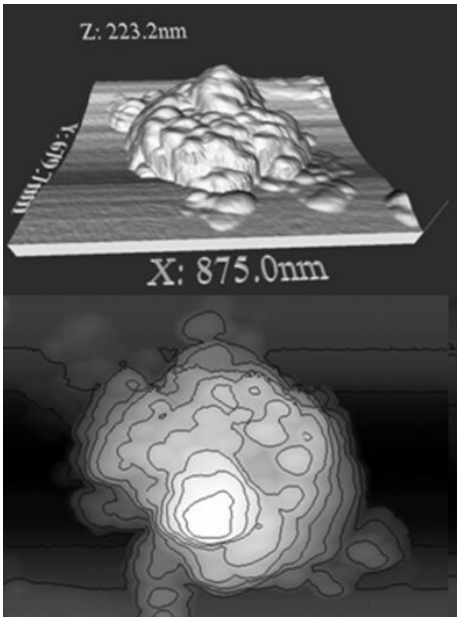

The figure shows an atomic force microscopy 3D image and a contour plot of adenovirus associated with magnetic nanopar-

ticles. The average size of the complexes is 171±17 nm. Taking into account that rather poor information is usually available on the structure and composition of the commercial magnetic nanomaterials, we hope that our published protocols on synthesis of magnetic nanoparticles, their thorough characterization, formulation of the plasmid, siRNA magnetic delivery vectors could enable further progress in the field.

Acknowledgments

This work was supported by the European Union through the Project FP6-LSHB-CT-2006-019038 “Magselectofection”, as well as by the German Ministry of Education and Research, Nanobiotechnology grants 13N8186 and 13N8538. Financial support from the Thailand Research Fund (TRF) through the Royal Golden Jubilee Ph.D. Program (Grant No.PHD/0002/2548), the German Research Foundation through the project PL 281/3-1 Nanoguide and German Excellence Initiative via the "Nanosystems Initiative Munich" are gratefully acknowledged.

References

[1] Mykhaylyk O, Zelphati O, Hammerschmid E, Anton M, Rosenecker J, Plank C. Recent advances in magnetofection and its potential to deliver siRNAs in vitro. Methods Mol Biol. 2009; 487:111-46.

[2] Mykhaylyk O, Sánchez Antequera Y, Vlaskou D and Plank Ch. Generation of magnetic nonviral gene transfer agents and magnetofection in vitro. Nature protocols. 2:2391-2411 (2007).

[3] Mykhaylyk O, Zelphati O, Rosenecker J, Plank C. siRNA delivery by magnetofection (review). Curr Opin Mol Ther. 2008 Oct; 10(5):493-505.

[4] Mykhaylyk O, Sánchez Antequera Y, Vlaskou D, Hammerschmid E, Zelphati O, Plank Ch, Liposomal magnetofection. Liposomes. Methods and Protocols, Volume 1: Pharmaceutical Nanocarriers Series: Methods in Molecular Biology, Chapter 34, Preliminary entry 2260, Weissig, Volkmar (Ed.) 2010, ISBN: 978-1-60327-359-6

Potential Use of Nanocapsules Containing Magnetic Nanoparticles Prepared by Inverse Miniemulsion for MRI

U. Paiphansiri[1], M. Dass[1], I. Brüstle[1], S. Sharma[2], V. Rasche[2], V. Mailänder[1]
K. Landfester[1]

[1] Max Planck Institute for Polymer Research, Ackermannweg 10, 55128 Mainz, Germany.
[2] Department of Internal Medicine II – Cardiology, University of Ulm, Albert-Einstein-Allee 23, 89081 Ulm, Germany.

Introduction

Superparamagnetic iron oxide nanoparticles are widely used as a negative contrast in Magnetic Resonance Imaging (MRI) and as cell labelling to monitor trafficking of transplanted cell owing to their strong effect in decrease of relaxivity based on transverse relaxation. Previous work has been demonstrated that intracellular uptake of iron nanoparticles coated with carboxydextran could be very well achieved. However, coagulation of such particles within the cells cannot be avoided [1]. This can be problematic for quantification of the intracellular iron content. Additionally, the sensitivity and relaxation behaviour of such aggregated nanoparticles is significantly deviated from the non-aggregated nanoparticles dispersion.

The present work is aimed to study the relaxivity behaviour of well-defined composite nanocapsules containing ultrasmall superparamagnetic particles (USPIO) or supravist™. Basically the nanocapsules were prepared via interfacial polyaddition in inverse (water-in-oil) miniemulsion system (see Figure 1). In principle, the miniemulsion process provides critically stabilised homogeneous small droplets dispersed in a continuous phase by ultrasonicating two-phase system. The narrowly distributed droplet size tunable from 70-500 nm is principally governed by the type and the amount of surfactant used as a stabiliser. One key characteristic of the miniemulsion is that no effective material exchange takes places between the droplets. In the case of an inverse miniemulsion, a salt or another hydrophilic material, presented in aqueous phase plays an important role of osmotic balancing Laplace pressure [2].

In the experiment, the obtained composite nanocapsules in organic continuous phase will be redispersed in aqueous dispersed phase before characterising their size, morphology, crosslinking reaction by FTIR, and relaxivity by clinical MRI scanner at 3 T.

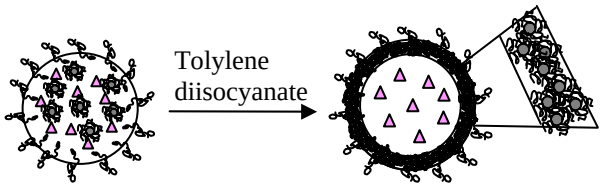

Aqueous miniemulsion droplet and nanocapsule dispersed in organic continuous phase.
- Magnetite nanoparticle coated with carboxydextran
- NaCl as osmotic controlling agent
- Oil soluble surfactant

Figure 1 Nanocapsule formation via interfacial polyaddition in inverse miniemulsion.

Result and discussion

Supravist™ or ultrasmall superparamagnetic iron oxide nanoparticles (USPIO) coated with carboxydextran having a diameter of about 13 nm (Figure 2a) is a clinical trial product for MRI. Since the carboxydextran as coating material of the

USPIO contains many reactive groups, they can react with diisocyanates (e.g. tolylene diisocyanate, TDI) at the water-oil droplet interface via a polyaddition reaction (Figure 1). Composite nanocapsules of 220 nm resulting from crosslinked dextran can be achieved (Figure 2b). The crosslinking of the dextran can be confirmed by FTIR spectra. The peaks at 3400, 1700 and 1600 cm^{-1} are contributing from amide bonds and CH stretch of the benzene ring from TDI. In order to investigate the distribution of the magnetite nanoparticles, nanocapsules fixed in EPON matrix and cross sectioned for TEM analysis. A defined core-shell structure was observed with USPIO embedded within the polymeric shell (Figure 2c).

The T_2 relaxivity of the nanocapsules dispersed in the aqueous phase was analysed by 3 T clinical whole body MR unit (TR /Echoes / Flip angle: 1500 ms /8 /90º). A significant increase in T_2 relaxivity of the nanocapsules compared to pristine Supravist™ was observed. The performance of the magnetite nanoparticles as contrast agent depends on many factors for instance size, clustering. The latter give rises to two-fold: first, those related to global structure of the cluster and to the magnetic field distribution around it, and secondly, those limited to the inner part of the aggregate. While the former ones highly affect T_2 and T_2*, the latter ones govern T_1. In this experiment, the nanocapsules of the Supravist™ can be considered as a large magnetised sphere, leading to a decrease of the observed relaxation time. The cellular uptake of these nanocapsules and the MRI study in *in-vitro* are currently in progress.

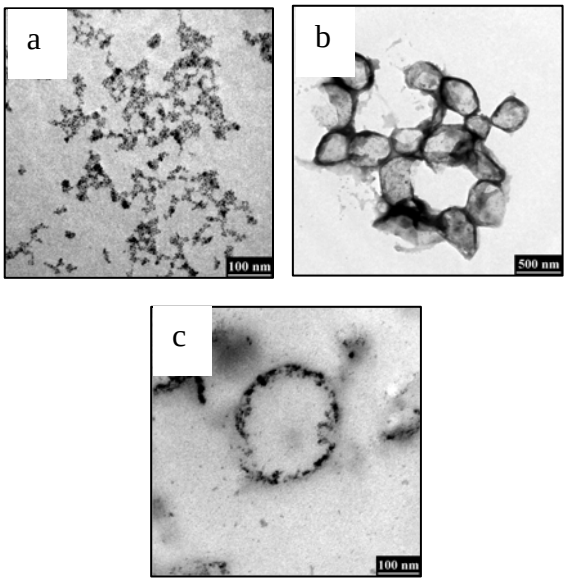

Figure 2 Morphology of a) USPIO of Supravist™, b) Nanocapsules containing the USPIO and c) Cross sectioned nanocapsule.

Conclusion

Well-defined nanocapsules containing Supravist™ within the polymeric shell can be prepared by inverse minimeulsion. The relaxivity of the nanocapsules is highly enhanced in comparison to Supravist™ dispersion. The nanocapsules can serve as a good candidate for potential use in MRI.

Acknowledgments

The research grant from Alexander von Humboldt foundation to U. P. is gratefully acknowledged.

References

[1] V. Mailänder, M. R Lorenz, V Holzapfel, A. Musyanovych, K. Fuchs, M. Wiesneth, P. Walther, K. Landfester, H. Schrezenmeier. Mol. Imaging Bio (2008) 10:138-146.

[2] K. Landfester. Ann Rev Mat Res (2006) 36:231-279.

Calibration of a polychromatic X-ray tomography equipment for biological tissue samples enriched with magnetic nanoparticles.

H. Rahn[1], D. Eberbeck[2], L. Trahms[2], and S. Odenbach[1]

[1] *TU Dresden, Institute of Fluid Mechanics, Chair of Magnetofluiddynamics,Dresden*
[2] *Department 8.2 Biosignals, Physikalisch-Technische Bundesanstalt, 10587 Berlin*

Magnetic Drug Targeting has been proposed as minimal invasive delivery of chemotherapeutic agent towards cancerous tissue. Magnetic Hyperthermia has been presented as local cancer treatment without the use of drugs, by generating a local temperature increase within a tumour using the strong influence of alternating magnetic field on magnetic nanoparticles. Among other things one of crucial factors of the efficiency of the therapeutic approaches is the homogeneous distribution of magnetic nanoparticles within the tumour. [1-3]

The common way of the determination is performed by histological cuts and microscopic analysis of the affected sections. This method provides very minute detail but only local, 2-dimensional information of the distribution of the magnetic material in a tumour sample and it is limited to ex-situ examinations.

X-ray microtomography offers the possibility of non-destructive, 3-dimensional investigations of the distribution of the magnetic nanoparticles within the tumour. In the present study, samples from tumours treated by MDT and tumour bearing mice after MHT have been analysed by this technique in two different laboratories: at TU Dresden, with a conventional CT setup and at DESY/HASYLAB, with synchrotron radiation CT.

The experiments carried out at TU Dresden have been successful in showing the distribution of the particles within the tumours, both in tumour sections as well as in whole animals (in-situ) [4].

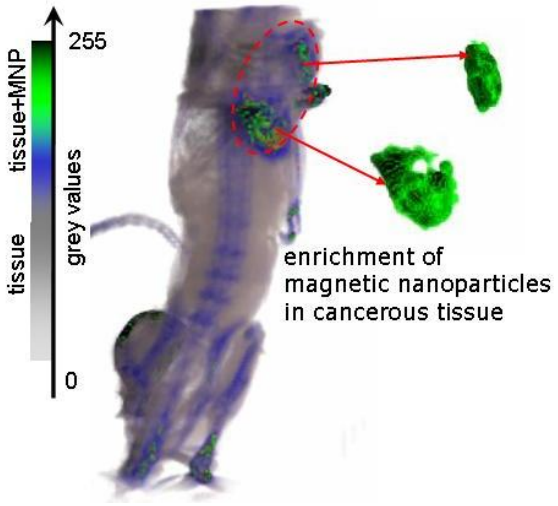

Fig.1: Tomographic representation of a mouse with tumour on its shoulder, which has been enriched with magnetic nanoparticles.

Using synchrotron radiation, the spatial resolution can be enhanced, and also quantitative analysis of the density distribution can be performed, which is not possible when a polychromatic source is used [5-6]. Furthermore, the polychromatic spectrum of the beam gives rise to the so called beam hardening artefact, which causes severe problems in quantitative analysis especially of soft-tissue samples with very similar densities, correspondingly similar attenuation coefficients. The analysis is only qualitative.

Fig. 2 shows the top view of a tomographic representation of a tumour in top view, which has been treated with magnetic nanoparticles. The different grey scales represent different densities within the sample. White marked zones stand for the highest density, the magnetic nanoparti-

cles; dark grey represents the biological tissue and the light grey areas show the paraffin where the sample is embedded.

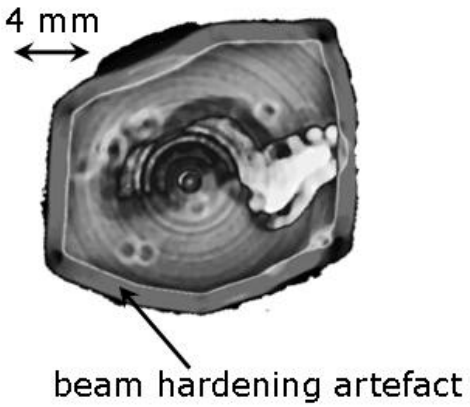

Fig.2: Example of beam hardening artefact can be seen as a middle grey boundary of the sample.

Here, the "beam hardening artefact" can be identified clearly as a separated boundary around the tumour. This area has an artificial density, which does not occur in the real object. Hence, it requires a quantification method for the data obtained with a polychromatic tomography equipment.
Calibration phantoms have been designed for a semi-quantitative evaluation tomographic data obtained from tissue samples enriched with magnetic nanoparticles, such as mice and extracted tumours. The phantoms consist of agarose-gel with a defined amount of magnetic nanoparticles. Agarose gel can be used as laboratory substitute matter for biological tissue. To adapt to the boundary conditions of MDT and MHT water based ferrofluid "MSG W11" from Ferrotec has been used.
For the measuring series the concentration of agarose-gel was constant at 20 mg/ml, while the concentration of ferrofluid varies from 1 mg/ml to 20 mg/ml.
The attenuation of the X-ray beam depends on the energy of the beam, on the atomic number as well as on the thickness of the traversed object. Preparing the phantoms in cone shape will give additional information concerning the thickness dependence of attenuation.

Additionally the phantoms are measured by Magnetorelaxometry (MRX – work group of Prof. Trahms at PTB Berlin) to achieve the absolute iron mass of the reference samples [7-9]. The correlation of grey values obtained with µCT and absolute iron mass ascertained by MRX leads to calibration curves for biological tissue samples enriched with magnetic nanoparticles to enable a semi-quantitative evaluation of polychromatic tomographic data.

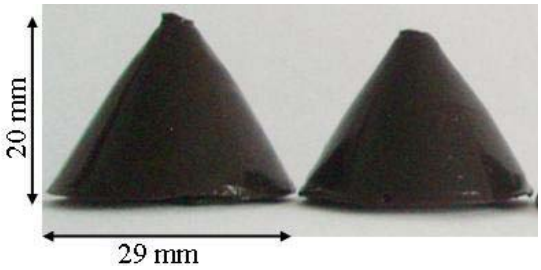

Fig.3: Agarose-gel cones with defined amount of diluted water based ferrofluid.

Acknowledgments

This project is funded by DFG with OD18/9 within SPP1104 and OD18/16-1.

References

[1] Marked in text with consecutive numbers in brackets [1]..., list with references showing the same numbers at the end of the text.

[1] Ch. Alexiou, et al., (2003) Magnetic Drug Targeting - Biodistribution of the Magnetic Carrier and the Chemotherapeutic agent Mitoxantrone after Locoregional Cancer Treatment. Journal of Drug Targeting, 11(3): p. 139-149.

[2] Ch. Alexiou, (2002) Trageted tumor theraphy with magnetic drug targeting. In Ferrofluids – Magnetically controllable Fluids and Their Applications. Ed. S. Odenbach, Springer LNP 594 Springer Verlag, Heidelberg, New York

[3] I. Hilger, et al., (2001) Electromagnetic Heating of Breast Tumors in Interventional Radiology: In Vitro and in Vivo Studies in Human Cadavers and Mice. Radiology, 218: p. 570-575.

[4] O. Brunke, S. Odenbach, R. Jurgons, C. Alexiou, I. Hilger, and F. Beckmann, (2006) Determination of magnetic particle distribution tumour tissue by means of X-ray tomography. J. Physics: Condensed Matter 18, S2903-S2971 .

[5] H. Rahn, I.Gomez-Morilla, R. Jurgons, Ch. Alexiou, S. Odenbach, J. of Physics: C. M., 20 204152 (4pp) (2008)

[6] Rahn H, Gomez-Morilla I, Jurgons R, Alexiou Ch, Eberbeck D, and Odenbach S, (2009) Tomographic examinations of magnetic nanoparticles used as drug carriers, Journal of Magnetism and Magnetic Materials, 2009.

[7] Wiekhorst F, Seliger C, Jurgons R, Steinhoff U, Eberbeck D, Trahms L, Alexiou C Quantification of magnetic nanoparticles by magnetorelaxometry and comparison to histology after magnetic drug targeting. J Nanosci Nanotechnol. 2006 Sep-Oct;6(9-10):3222-5.

[8] Eberbeck D, Bergemann Ch, Wiekhosrt F, Steinhoff U, and Trahms L, (2008) Quantification of specific bindings of biomolecules by magnetorelaxometry; J. Nanobiotechnology 6, 1477-3155-6-4

[9] Ludwig F, (2006), Technisches Messen 73 4

[9] Heim E, Harling S, Ludwig F, Menzel F, and Schilling M, (2008), J. Phys.: Condens. Matter 20 204106 (5 pp)

Flow control of ferrofluids exposed to magnetic fields

M. Reindl[1], A. Leschhorn[2], M. Lücke[2], S. Odenbach[1]

[1]*Institute of Fluid Mechanics, Chair of Magnetofluiddynamics, 01062 Dresden, Germany*
[2]*Institute of Theoretical Physics, Universität des Saarlandes, 66041 Saarbrücken, Germany*

Motivation

One reason for the change of viscous properties of ferrofluids under magnetic field influence is the hindrance of free particle rotation [1]: In a flowing ferrofluid, the vorticity of the flow and a non-parallel magnetic field exert counteracting torques on the (magnetically hard) particles, increasing the fluid's viscosity.

This behavior is reflected by an expression for the relaxation of magnetization as a member of the basic equations of ferrohydrodynamics. Since there are different approaches to describe the relaxation of magnetization existing, the question for the most appropriate one arises.

A comparison of theoretical and experimental data of a model system allows to study this question in detail. As a model system, a Taylor-Couette flow has been chosen to distinguish between the different influence of magnetic fields on the rheology of ferrofluids as well as on their flow behaviour.

Experimental

The fluid cell of the Taylor-Couette system is subjected to a homogeneous axial magnetic field and the flow profiles are measured by ultrasound Doppler velocimetry. With the ultrasound transducer being placed at the outer cylinder wall on top of the fluid cell, axial velocity profiles (Figure 1) get measurable and the different flow regimes thus distinguishable.

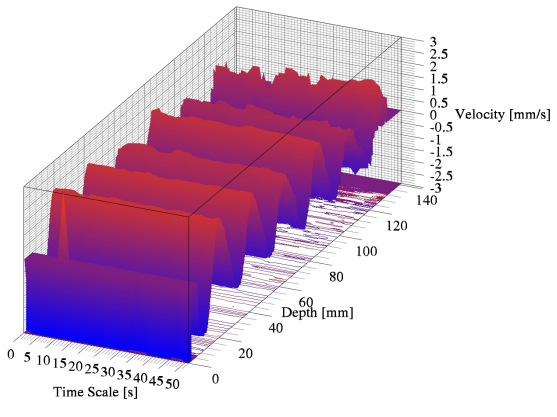

Figure 1: 3D Plot of a axial velocity profile of a Taylor vortex flow (ϵ=0.097).

The experiments were carried out with a magnetite based ferrofluid in a kerosene carrier. Since rheological investigations did not show any magnetoviscous effect, the effects observed must be solely ascribed to the hindrance of particle rotation, whereas interparticle interaction is negligible.

Results

The experiments show that under magnetic field influence lower wavenumbers are preferred over higher ones. This is in agreement to prior theoretical investigations [2]. An orientation over the stability of distinct wavenumbers at a given rotation rate of the outer cylinder and magnetic field strength is given in Figure 2.

Further investigations concern the transition from circular Couette flow to Tay-

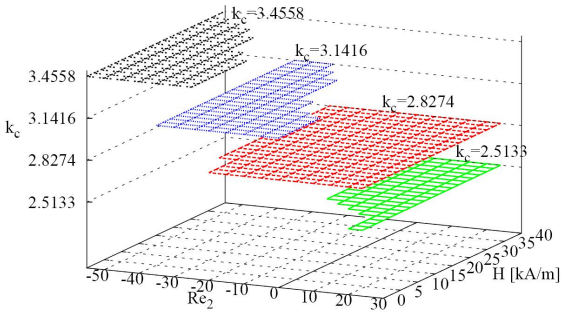

Figure 2: Surface plot of long-time stable wavenumbers k_c at different axial magnetic field strengths $\mathbf{H}_{ext}$ and rotation rates of the outer cylinder Re_2 .

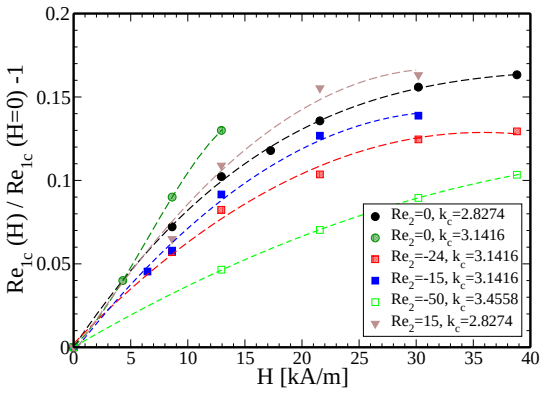

Figure 3: Shift of the onset of Taylor vortex flow depending on the axial magnetic field strength at different rotation rates of the outer cylinder.

lor vortex flow at different axial magnetic field strengths and rotation rates of the outer cylinder.

The experiments have shown that an axial magnetic field has a stabilizing effect on the circular Couette ground flow (CCF). This effect gets intensified by corotating and weakened by counterrotating cylinders (Figure 3). These results are in qualitative agreement to theoretical investigations of a linear stability analysis [3].

Summary and outlook

The effects observed in the experiments carried out so far may be solely ascribed to hindrance of free particle rotation. Hence, further investigations will comprise the influence of interparticle interaction of a Cobalt based ferrofluid.

Acknowledgments

The support by the DFG (OD 18/11) is greatly acknowledged.

References

[1] M. I. Shliomis: Effective viscosity of magnetic suspensions. Sov. Phys. JETP, 34:1291, 1972

[2] M. Niklas. Influence of magnetic fields on taylor vortex formation in magnetic fluids. Z. Phys. B, 68:493, 1987

[3] A. Leschhorn, M. Lücke, C. Hoffmann, S. Altmeyer: Stability of the Circular Couette Flow of a ferrofluid in an axial magnetic field: Influence of polydispersity, Phys. Rev. E. 036308 (2009)

Magnetic Capsules and Pickering Emulsions Stabilized by Core-Shell Particles

A. Kaiser,[2] A. M. Schmidt[1]

[1]*Institut für Organische Chemie und Makromolekulare Chemie, Heinrich-Heine-Universität, Universitätsstr.1, D-40225 Düsseldorf, Germany, email: schmidt.annette@uni-duesseldorf.de*
2 current address: Lehrstuhl für Präparative Polymerchemie, Universität Karlsruhe, Germany

Particle-stabilized emulsions, known as Pickering emulsions, have been firstly described by Ramsden and Pickering in the early 20th century,[1, 2] although men have taken advantage of this effect since ancient times. Today, the basic principles of emulsion stabilization by particles are still not fully understood, and they achieve growing interest in the context of nanoparticle organization at interfaces and for biomedical applications.

In our work we present results on magnetic Pickering emulsions, using superparamagnetic hybrid nanoparticles as susceptible stabilizers. By using the polymer shell of surface grafted iron oxide cores as adaptable solution promoter in a Θ-solvent,[3, 4] thermoreversible magnetic fluids are obtained that are mixed with water, leading to stable oil in water (o/w) emulsions (fig. 1).

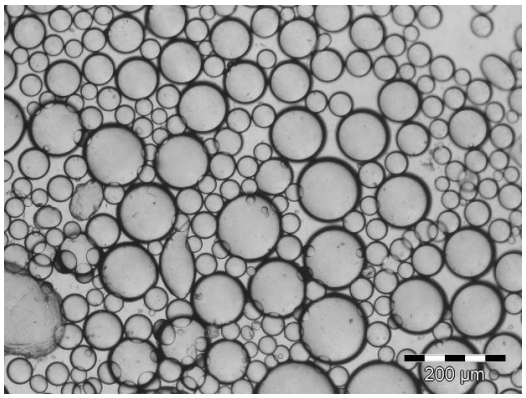

Fig. 1: O/w Pickering emulsion stabilized by magnetic hybrid nanoparticles.

Detailed investigations of the involved phase behaviour will be presented together with investigations on the long-term stability of the magnetic capsules towards temperature and in magnetic fields.

Magnetic Pickering emulsions are of interest for advanced drug delivery and release systems.

Acknowledgement
We gratefully acknowledge the DFG (SSP1104 and Emmy Noether Program) for financial support.

[1] W. Ramsden, *Proc. Roy. Soc. London* **1903**, *72*, 156. [2] S. U. Pickering, *J. Chem. Soc. Commun.* **1907**, *91*, 2001 [3] A. Kaiser, T. Gelbrich, A. M. Schmidt, *J. Phys. Cond. Matter*, **2006**,*18*, 2563. [4] A. Kaiser, A. M. Schmidt, *J. Phys. Chem. B*, **2008**, *112*, 1894.

Hydrodynamic Interaction

R. Schmitz[1]

[1] *Institut für Theoretische Physik C, RWTH Aachen*

Colloidal particles immersed in a fluid create long-ranged flows as they move, and they move in response to flow. Momentum transfer mediated by the host fluid causes a dynamic coupling of the particles, which is referred to as hydrodynamic interaction. Despite its long-recognized ubiquity, hydrodynamic interaction is still not completely understood and efficient algorithms for simulations are not easily available.

The theory of hydrodynamic interaction is based on the Stokes equations for low-Reynolds number, incompressible flow with Dirichlet boundary conditions on the particle surfaces. Given the particle velocities and, possibly, an external fluid flow, the solution to this boundary value problem describes the local fluid velocity in the presence of the particles. This local velocity determines, via the stress field, the surface forces exerted on the particles. It is convenient to introduce a resistance matrix, which relates the force moments exerted on the particles to their velocities and the gradients of the external flow.

Computation of the resistance matrix for a given particle configuration poses a number of challenges. In the first place, the boundary conditions have to be satisfied on all the particle surfaces simultaneously. Thus, hydrodynamic interaction is a true many-body interaction, superposition fails. Second, there are singularities when two of the particles are at close contact, which cannot be treated by multipole expansions. Finally, the long-range character of the interaction needs special attention.

To investigate the small-distance singularities we study the two-body problem using bi-spherical coordinates. Although these are perfectly adjusted to the geometry at hand, the hydrodynamic equations are not easily separable. Nevertheless it is possible to derive series expansions for the velocity fields and to determine the asymptotic behavior of the resistance functions at small and large separation.

A FERROGEL MICROACTOR - TOWARDS ARTIFICIAL CILIA

N. Schorr, J. Belardi, O. Prucker and J. Rühe[1]
V. Patel, S. Wells [2]

[1] *University of Freiburg, Department of Microsystems Engineering (IMTEK), D-79110 Freiburg, Germany*
[2] *Liquids Research Limited, Bangor, Gwynedd, United Kingdom, LL57 2UP*

Healthcare Lab-on-a-chip applications have triggered research activities dealing with microscaled manipulation of liquids. Many organisms utilize microscopic cilia in order to propel liquids. We fabricated *artificial cilia* from ferrogel microstructures.

Lab-on-a-chip systems can perform a large number of process steps in parallel using a fraction of sample liquid as their conventional equivalents. Flow in such microfluidic systems is laminar[1]. Many organisms utilize cilia, in order to propel liquids at low Reynolds numbers. These microsized hairlike cell projections[2] perform an asymmetric motion similar to the stroke of a swimmers arm. A cilia array builds up a net flow. Mimicking this propulsion mechanism, it is possible to manipulate fluids in microfluidic channels as recently shown for electrostatic actuated artificial cilia[3].

Ferrogels are hydrophilic polymer matrices filled with magnetic particles[4]. Low Young's modulus and magnetic features make them ideal candidates for actuators. Combined with a time dependent external magnetic field ferrogel actors provide a high degree of freedom in motion, which is essential to mimic the asymmetric motion of the natural archetype[5].

We realised *ferrogel cilia* based on a *N*,*N*-Dimethylacrylamide matrix[6] filled with surfactant stabilized super-paramagnetic nanoparticles. This composite was processed by photolithography. A sacrificial layer and immobilisation on a Si-substrate[7,8] lead to flexible magnetic microstructures. We show that the artificial cilia can be actuated by magnetic fields in liquid environment (Figure 1).

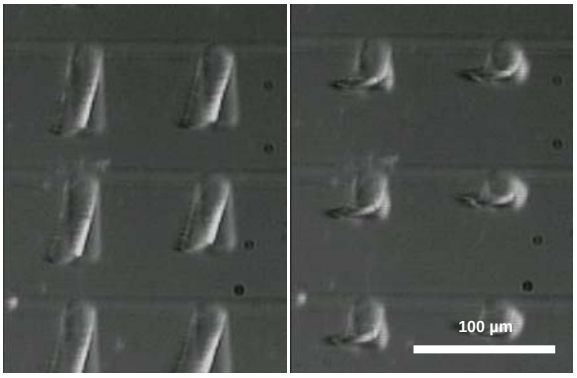

Figure 1: Artificial cilia in liquid exposed to differing magnetic field distributions.

Acknowledgments

We acknowledge financial support from the EU (NMP4-CT-2006-033274) within the Artic framework.

References

[1] T. M. Squires, S. R. Quake, *Reviews of Modern Physics* 77, 977-1026 (2005).
[2] P. Satir, S. T. Christensen, *Histochemistry and Cell Biology* 129, 687-693 (2008).
[3] J. den Toonder et al., *Lab on a Chip* 8, 533-541 (2008).
[4] M. Zrinyi, *Colloid and Polymer Science* 278, 98-103 (2000).
[5] S. N. Khaderi, M. G. H. M. Baltussen, P. D. Anderson, D. Ioan, J. M. J. den Toonder, P. R. Onck, *Physical Review E* 2009, 79.
[6] R. Toomey, D. Freidank, J. Ruhe, *Macromolecules* 37, 882-887 (2004).
[7] O. Prucker, C. A. Naumann, J. Ruhe, W. Knoll, C. W. Frank, *Journal of the American Chemical Society* 121, 8766-8770 (1999).
[8] K. Schuh, O. Prucker, J. Ruhe, *Macromolecules* 41, 9284-9289 (2008).

Magnetic labeling of the vaccine adjuvant $Al(OH)_3$ for magnetic resonance tracking

K. Thom[1], K. Aurich[1], J.-P. Kühn[2], W. Weitschies[1]

[1]*Institute of Pharmacy, University of Greifswald, 17487 Greifswald*
[2]*Institute of Diagnostic Radiology and Neuroradiologie, University of Greifswald, 17487 Greifswald*

Introduction

Already in 1926 Glenny et al. reported the use of aluminium as an adjuvant in vaccines. Since several decades it is commonly used e.g. in the form of aluminium hydroxide ($Al(OH)_3$) [1]. Nevertheless, the mode of action could not be ascertained in detail. For a long time a depot effect was accepted as an explanation, but in recent years it became clear that the effect is not only caused by this [2]. A novel method to investigate the fate of $Al(OH)_3$ in vivo could be magnetic resonance imaging (MRI). As $Al(OH)_3$ is not directly visible in MRI labeling with superparamagnetic iron oxide particles might be feasible. In this contribution we used ferucarbotran particles (Resovist®, Bayer Schering AG, Germany) for the generation of complexes with $Al(OH)_3$. Resovist® is a commercially available MRI contrast agent for imaging of liver lesions consisting of carboxydextran coated iron oxide nanoparticles as an injectable solution. Since it is a FDA-approved contrast agent, the potential for clinical trials is given.

Material and methods

Initially, complexes were characterized regarding their size and zeta potential by dynamic light scattering measurements (DLS). For this purpose, ferucarbotran particles and a colloidal suspension of $Al(OH)_3$ (Alhydrogel®, Sigma-Aldrich, Germany) were merged within the iron-aluminium-ratios 4:1 and 1:4 referring to the amount of substance. Water was the dispersant. The mixture was stored at room temperature for 1 h before determining size and zeta potential.
For analyzing whether ferucarbotran particles were adsorbed onto Alhydrogel® the mixture was centrifuged at 5.000 x g for 6 min followed by determination of the particle size in the supernatant.
Furthermore, ferucarbotran particles were linked with the fluorescence dye Texas Red-albumin (Invitrogen, Germany) by the periodate method [3] in order to demonstrate the composition of complexes by confocal laser scanning microscopy (CLSM) and fluorescence microscopy (FM).
The stability of the complexes was analyzed by determination of the iron concentration of supernatants from centrifugation experiments by atomic absorption spectroscopy (AAS).

Results and discussion

After incubation of ferucarbotran particles with Alhydrogel® a clearly visible agglomeration rapidly occurred. That was associated with sedimentation. The rate of sedimentation depended on the concentration of the suspension.
Enhancing the amount of Alhydrogel® in the mixture resulted in an augmentation of the mean particle size of the complexes up to 2800 nm (Fig. 1).
At a 1:4 Fe-Al-ratio the hydrodynamic diameter of particles is triplicated compared with Alhydrogel®. Hence, aggregates were generated.
After centrifugation in all supernatants particles with the typical size of the ferucarbotran particles were detected except in the 1:4-ratio. The use of a fourfold surplus of aluminiumhydroxid caused a complete binding of the iron oxide particles.

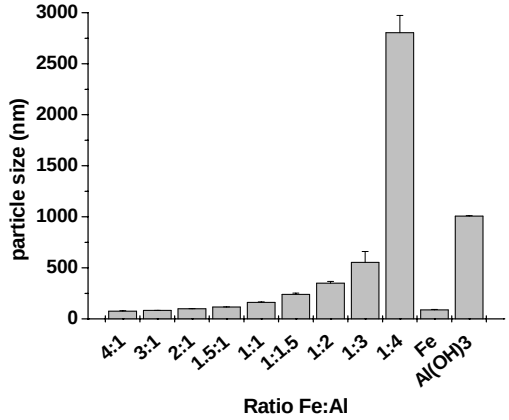

Figure 1. Mean hydrodynamic particle size (DLS) of aggregates formed after incubation of Resovist® particles with $Al(OH)_3$ in varying ratios, n=3 + SD.

Because of the gel character of Alhydrogel® complexes were difficult to see using CLSM and FM after fixation, even by utilization of liquid phases without any further preparation during microscopy. The edges of the complexes were not clearly visible and they showed a diffuse distribution of the ferocarbutran particles.

Conclusion and outlook

Alhydrogel® can be labeled with superparamagnetic nanoparticles for MR imaging. The increase in the particle size determined by DLS indicates binding of ferucarbotran particles due to aggregation.
In a next step characteristics and stability of the complexes in bovine serum albumin will be analyzed. Furthermore, detection of the aggregates by MRI will be performed.

References

[1] Baylor, N. W., Egan, W., Richman, P. Aluminium salts in vaccines-US perspectiv *Vaccine* 20 (2002), 18-23.

[2] Marrack, P., McKee, A. S., Munks, M. W. Towards an understanding of the adjuvant action of aluminium *Nat Rev Immunol* 9 (2009), 287-293.

[3] Romanus, E., Gross, C., Koetitz, R. et al. Monitoring of biological binding reactions by magneto-optical relaxation measurements *Magnetohydrodynamics* 37 (2001), 328-333

Adsorption of the Chemotherapeutic Agent Mitoxantron on Iron Oxide Nanoparticles

R. Tietze[1], R. Müller[2], S. Lyer[1], E. Schreiber[1], Ch. Alexiou[1], H. Steinmetz[2], M. Zeisberger[2]

[1] *Department of Oto-Rhino-Laryngology, Head and Neck Surgery, Section of experimental Oncology and Nanomedicine, University Erlangen-Nürnberg*
[2] *Institute of Photonic Technology Jena, Research group "Innovative Photonic Materials"*

Introduction

One disadvantage of conventional systemic application of chemotherapy in cancer treatment is the application-to-tumor-dose-ratio. This implies an often insufficient drug dose in the tumor, associated with severe side effects for the patient. Therefore the aim of local tumor therapy is to increase the dose of the administered therapeutic agent in the tumor and simultaneously reduce the overall dose.
Application of chemotherapeutic agents bound to magnetic nanoparticles is a promising approach of site specific drug deposition. Magnetic-Drug-Targeting (MDT) reduces negative side effects as the particles serve as a carrier system for mitoxantrone (MTO) when they are enriched by a focused external magnetic field to defined body compartments after application [1-3]. MTO is an anthracendion derivative which inhibits the DNA and RNA synthesis and causes DNA-strand breaks by intercalation [4]. It is used extensively in clinical trials to treat fatal diseases [5].
In this work the binding of MTO on iron oxide particles was investigated. We focused on the influence of initial particle preparation without any (biocompatible) particle coating.

Preparation of the particles

Particles for binding tests were prepared by different methods what may result in different particles, particles with different initial molecules adsorped at the surface (water, diethylene glycol (DEG), hydrogene carbonate) or in a different surface charge. The methods are not assessed concerning the resulting particle size or agglomeration tendency.
Method a) and b) are the known wet chemical precipitation methods from aqueous iron chloride solutions ($FeCl_2/FeCl_3$-ratio = 1:1.3) by means of alkaline media KOH (a)) and NH_4OH (b)), respectively, according to $Fe^{2+} + 2\ Fe^{3+} + 8OH \rightarrow Fe_3O_4 + 4H_2O$. Our typical particle sizes are in the range of 13 - 15 nm.
Method c) is a modified precipitation method [6]. A 1M $NaHCO_3$ solution was slowly added to a $FeCl_2/FeCl_3$ solution (Fe^{2+}/Fe^{3+}- ratio ≈ 1/1.3) up to pH ≈ 8, leading to the formation of a brownish precipitate. After that, the solution was boiled to form an almost black precipitate.
Aging on air leads to subsequent oxidation. Saturation magnetization and X-ray diffration measurements of particles of the methods a) to c) suggest a γ-Fe_2O_3-Fe_3O_4 solid solution or mixture close to γ-Fe_2O_3 but with pure spinell structure.
For comparison pure (non-magnetic) hematite α-Fe_2O_3 particles were prepared in method d) by hydrolysis of a 0.02M $FeCl_3$-solution (aging at 100°C for 48h [7]). The particle size is in the order of 100 nm.
Method e) is a precipitation in non-aqueous DEG solution following [8]. $FeCl_2 \cdot 4H_2O$ and $FeCl_3 \cdot 6H_2O$ were dissolved in DEG. Separately, KOH was dissolved in DEG and added to solution of metal chlorides at room temperature causing an immediate color change. The temperature of the resulting solution was raised during 0.5-1 h to 200 - 220 °C and then kept constant for

≈1h. The precipitate was cooled, and then centrifuged and washed with water. Beside spinell oxide the samples contain a small amount of hematite.

In all cases the particles were washed three times with water. In order to separate effects of the surface charge from effects of particle material or different possible adsorped molecules an „acidic“ aftertreatment of samples of methods a), b), c) and e) by adding diluted HCl to the particles up to pH≈3 and a subsequent washing with water (three times) was carried out.
In analogy, particles of method d) were treated with KOH up to pH≈9 and then washed again.
The subsequent pH-treatments had no significant influence on the magnetic properties of the particles.

Characterization methods

The HPLC analyses to detect the supernatant of the MTO doped ferrofluids were performed by a Waters Alliance® model consisting of a separation module and a dual absorbance detector. The eluate was monitored at 254 nm. Separation was carried out using a 3.0 x 100 mm X-Bridge™ Phenyl column (Waters®, Germany) with a particle diameter of 3.5 µm; the guard column consisted of the same material and was 3.0 x 20 mm of size. The mobile phase was made up of buffer (80 nM sodium formiate and formic acid, pH 3.0) and methanol (80:20 v/v). Flow was 1 ml/min, and column temperature 55°C.
The MTO amount analysed by HPLC was normalized by the particle concentrations of the fluids what was determined by measuring the particle mass after drying at 100°C.
The zeta-potential was measured on diluted samples (10 µl in 2 ml) by dynamic laser scattering (DLS, Nicomp 380 ZLS, Santa Barbara, USA).

Results

Although the particles by methods a), b) and c) are similar concerning the iron oxide phase, size and magnetic properties they differ in the amount of adsorped MTO. Particles precipitated with KOH or NH_4OH show much higher amounts than such prepared by method c). Especially in method a) and b) basic samples show a higher MTO amount than samples after “acidic treatment”.
Hematite particles reveal small MTO amounts not sufficient for medical purposes. As well the KOH-treated sample carries less MTO then the spinell oxide particles even taking into account the much smaller specific surface.
The samples precipitated in DEG what have zeta-potentials similar to samples mentioned above show also small MTO amounts not sufficient for medical purposes. Their attraction to a magnet is weaker than that of samples by methods a), b) and c) what can be explained by the lower specific magnetization of the particles.

Acknowledgments

This work was supported by the DFG contracts AL552/3-1 and ZE825/1-1.

References

[1] R. Jurgons, C. Seliger, A. Hilpert, L. Trahms, S. Odenbach, C. Alexiou. J. Phys.: Cond. Matter 18 (2006) S2893
[2] C. Alexiou, R. Jurgons, C. Seliger, O. Brunke, H. Iro, and S. Odenbach. Anticancer Res. 27 (2007) 2019
[3] C. Alexiou, R. Jurgons, G. Seliger, H. Iro. J. Nanosci. Nanotechnol. 6 (2006) 2762
[4] M.E. Fox, and P.J. Smith. Cancer Res 50 (1990) 5813
[5] D. Faulds, J.A. Balfour, P. Chrisp, and H.D. Langtry. Drugs 41 (1991) 400
[6] S. Dutz, W. Andrä, R. Hergt, R. Müller, C. Oestreich, Ch. Schmidt, J. Töpfer, M. Zeisberger, M. Bellemann, J. Magn. Magn. Mater. 311 (2007) 51-54
[7] M. Ozaki, S. Kratohvil, E. Matijevic, J. Coll. Interf. Sci. 102 (1984) 146-151
[8] D. Caruntu, G. Caruntu, C. O’Connor J. Phys. D: Appl. Phys. **40** (2007) 5801–5809

Experimental investigation of dipolar interaction in suspension of magnetic nanoparticles

D. Eberbeck, P. Zirpel, L. Trahms

Physikalisch-Technische Bundesanstalt, Berlin

Introduction

Magnetic nanoparticles (MNP) have found many applications in medicine, such as e.g. in magnetic drug targeting and hyperthermia. The efficiency of hyperthermia depends on the MNP's dynamic magnetic behaviour, which is influenced by their energy barriers ΔE. The energy barriers are determined by the internal anisotropy energies of the individual MNPs, but also by their magnetic dipolar interaction. At low temperatures, dense dipole configurations of MNP suspensions exhibit a slowing down of the moment dynamics due to this interaction (Eberbeck 1999), comparable to what is observed in spin glasses. Here, we investigate whether at physiological temperatures larger MNPs show a similar behaviour, that is displayed by a reduced relaxation velocity at higher concentrations.

Materials and methods

In present work we investigated two magnetite based MNP systems (i) the commonly used MRI contrast agent Resovist (mean core diameter about 12 nm), and SHP-20 (Ocean NanoTec, USA) with the larger mean core diameter of about 20 nm. We prepared a concentration series of fluid suspensions of MNP and of immobilised MNP by freeze drying. Additionally, SHP-20 MNP were immobilised in agarose gel. By magnetorelaxometry (MRX) we measured the relaxation of the sample's magnetisation after a polarising field was switched off. We analyzed the relaxation curves of fluid suspensions by fitting the data with the so called Cluster Moment Superposition Model (CMSM) [Eberbeck 2006], which describes the relaxation by a superposition of contributions of MNP clusters according to their diameter d_C. This yields the distribution $f(\mu_C,\sigma_C,d_C)$ of hydrodynamic sizes, or cluster sizes d_C, with the parameters median μ_C and dispersion parameter σ_C. The relaxation curves of samples with immobilized MNP were treated with the Moment Superposition Model (MSM) [Eberbeck 2006], which superimpose the Néel relaxation contributions of the different particle size fractions. This yields an effective anisotropy constant and an effective core size distribution with the median μ and the distribution parameter σ.

We also examined the quasistatic magnetization behaviour measuring the $M(H)$ curves by means of a commercial susceptometer (MPMS, Quantum Design).

Results and discussion

MRX-measurements

Over the investigated concentration range of $0.5\,\text{mmol/l} \le c_{Fe} \le 40\,\text{mmol/l}$ the relaxation curves of SHP-20 scale with the iron content, i.e. they exhibit the identical shape. In the case of Resovist the curves scale for iron concentrations below 100 mmol/l. Above this value the apparent time constant of the relaxations curves, $t_{1/e}$, increases. According to the CMSM, the cluster size distribution changes, as visualized by the concentration dependence of the distribution parameter σ_C in Fig. 1. Furthermore, we found that the salt content in the suspension medium also influences this size distribution.

The analysis of the Néel relaxation of freeze dried Resovist samples also reveals a concentration independent distribution function of the effective core size distribution, as expressed by the parameter σ in Figure 1, at $c_{Fe} \le 20\,\text{mmol/l}$. In this range

the effective anisotropy constant K_{eff} is also independent on c_{Fe}. At $c_{Fe} > 20$ mmol/l for

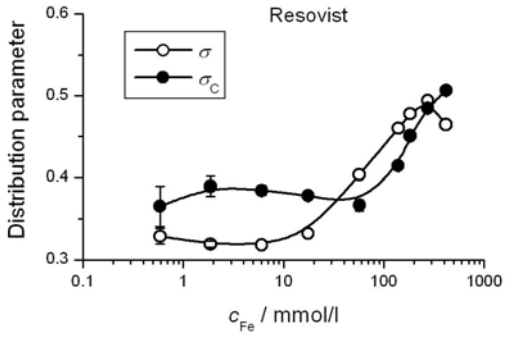

Figure 1: Distribution parameters of the hydrodynamic or cluster size distribution, σ_C, and effective magnetic core size distribution, σ, respectively, represented as a function of the iron content of different Resovist samples. The lines serve as guides to eyes.

Resovist, and at about 5 mmol/l for SHP-20, the relaxation curves do no longer scale with the iron concentration. While for Resovist we observed a strong change in the corresponding distribution parameter σ, analysis of the SHP-20 data reveals a change of the median of only 4 %, and a change of the reduced relaxation amplitude of 40 %. For both MNP types the relaxation time constant increases with c_{Fe}.

We attribute the deviation from scaling in the concentration dependent relaxation curves to the presence of magnetic interaction between the MNP moments: With the assumed increase of the spatial pair correlation of MNPs towards higher concentrations (Eberbeck 1999b), also the dipole-dipole interaction ($\propto r^{-3}$) should increase, leading to a stiffening of the moment system, similar to earlier observations on smaller MNPs at lower temperatures (Morup 1995, Eberbeck 1999).

Additionally, we found a difference between the relaxation curves of immobilised SHP-20 and their suspension in agarose gel. The magnetisation dynamics in agarose gel is slowed, indicated by the decrease of the apparent relaxation time by 38% and 5% at $c(\mathrm{Fe}) = 11$ mmol/l and 1.5 mmol/l, respectively. Furthermore, we found examples that the salt concentration in the suspension also alters the magnetisation dynamics of immobilised MNPs.

Note that for Resovist, respectively SHP-20, the change of the magnetic relaxation is only partially (Fig. 1) or not accompanied by changes in observed hydrodynamic size distribution. This may be related to our upper resolution limit of actually $d_C = 50$ nm.

M(H)-measurements

We also compared the magnetisation of concentrated samples with that of a more diluted one, calculating the relative difference (Fig. 3). The negative differences at median field strength indicate the stiffening of the magnetic system.

In conclusion, we attribute the stiffening and slowing of the magnetisation dynamics to the onset of glass like behaviour caused by competing dipolar interaction. This interaction is apparently modulated by changes in the spatial correlation of the MNP.

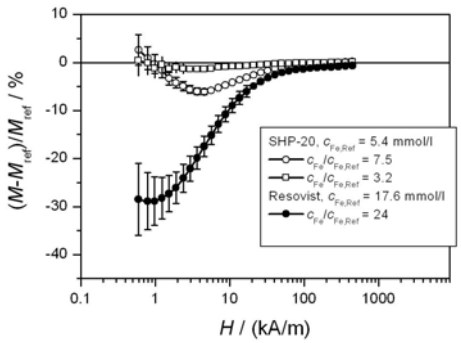

Figure 2: Differences of the magnetisation curves $M(H)$ of concentrated and diluted (reference) MNP-suspensions. The error bars are mainly determined by the uncertainty of a small offset magnetisation.

Acknowledgments

The research was supported by BMBF project Nanomagnetomedizin FKZ-13N9150.

References

[Eberbeck 2006] D. Eberbeck, F. Wiekhorst, U. Steinhoff, L. Trahms, J. Phys.: Condens. matter 18 (2006), S2829-S2846

[Eberbeck 1999] D. Eberbeck, *EPJ* B, 10 (1999), 237-245

[Eberbeck 1999b] D. Eberbeck and J. Bläsing, J. Appl. Cryst. 32 (1999), 273-280

[Morup 1995] S. Mørup, F. Bødker, P. V. Hendriksen and S. Linderoth, Phys. Rev. B 52, 1 (1995), 287-294.

Fluorescent Superparamagnetic Biodegradable Poly(L-lactide) Nanoparticles by Combination of Miniemulsion and Emulsion/Solvent Evaporation Techniques

M. Urban[1], A. Musyanovych[1], G. Schmidtke-Schrezenmeier[2], H. Schrezenmeier[2], V. Mailänder[1], K. Landfester[1]

[1] *Max Planck Institute for Polymer Research, Ackermannweg 10, 55128 Mainz, Germany*
[2] *Institute for Transfusion Medicine and Immunogenetics,University of Ulm, Helmholtzstr. 10, 89081 Ulm, Germany*

E-Mail: musyanov@mpip-mainz.mpg.de

Fluorescent, superparamagnetic and biodegradable nanoparticles exhibit properties that make them to be interesting in biomedical fields of application. These particles can be used for immobilization of nucleic acids, proteins and enzymes, immunoassays, purification and isolation of RNA or DNA, magnetic cell and protein separation, magnetically controlled delivery of anti-cancer drugs, magnetic resonance imaging (MRI), hypothermia, etc.

The miniemulsion technique allows the formation of stable and monodisperse droplets between 50 and 500 nm by shearing a heterophase system. The surfactant inhibits the coalescence of the droplets and the osmotic pressure agent prevents Ostwald ripening.

Biodegradable and fluorescent polylactide nanospheres loaded with iron oxide particles (25 nm) were prepared by a combination of miniemulsion and emulsion/solvent evaporation techniques. Dynamic light scattering (DLS) and transmission electron microscopy (TEM) studies indicate that the obtained particles have uniform and spherical shape with an average size between 100-120 nm (Figure 1). The encapsulation homogeneity was determined by preparative ultracentrifugation, which shows that the density and density distribution of the composite particles increases with increasing amount of encapsulated iron oxide. Thermogravimetric analysis shows that particles with the content of iron oxide up to 39 wt.-% could be achieved. The influence of the ultrasonication duration on the molecular weight of the polymer was studied using gel permeation chromatography (GPC). It was found that longer ultrasonication time reduces the molecular weight of the polymer, resulting in the formation of smaller droplets and subsequently smaller composite particles. The initial polymer has a molecular weight of 145 000 $g \cdot mol^{-1}$ (M_W) which reduces to 89 100 $g \cdot mol^{-1}$ after 10 min of ultrasonication.

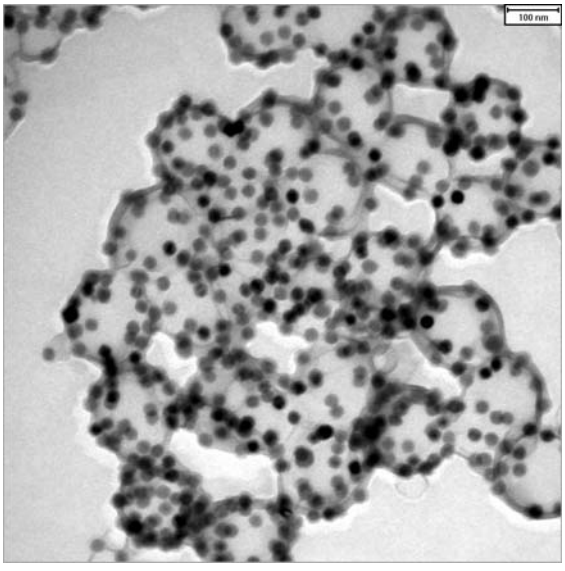

Figure 1: TEM image of poly(L-lacitde) nanoparticles with encapsulated iron oxide.

The magnetic properties of the iron oxide nanoparticles and the magnetic composite particles, prepared using different ultra-

sonication time were characterized using vibrating sample magnetometry (VSM). All samples show superparamagnetic behaviour. The saturation magnetization of the encapsulated iron oxide particles is comparable to the values of the non encapsulated iron oxide.
Cellular uptake studies with mesenchymal stem cells were carried out showing excellent cell uptake and very good viability. The cells were analyzed using confocal laser scanning microscopy (CLSM), fluorescence activated cell sorting (FACS) and transmission electron microscopy (TEM) (Figure 2).

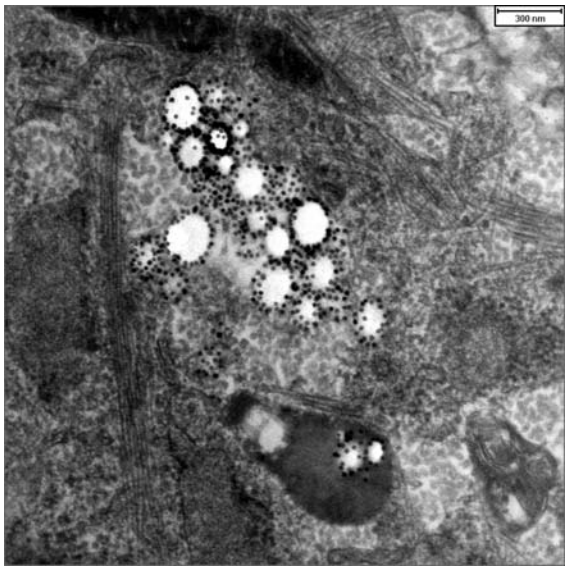

Figure 2: TEM image of magnetic poly(L-lactide) nanoparticles taken up by the mesenchymal stem cells.

Acknowledgments

Thanks to the Verband der Chemischen Industrie (VCI) for financial support of this project.

References

[1] M. Urban, A. Musyanovych, K. Landfester, *Macromol. Chem. Phys.* **2009**, *210*, 961-970.

Novel Catechol Containing Shell Materials for Magnetic Nanoparticles

K. Wagner[1], T. Seemann[2], R. Wyrwa[1], R. Müller[3], J. H. Clement[4], M. Schnabelrauch[1]

[1] *INNOVENT e.V., Prüssingstraße 27 B, D-07745 Jena; e-mail: kw@innovent-jena.de*
[2] *Fachhochschule Jena, University of Applied Science Jena, Carl-Zeiss-Promenade 2, D-07745 Jena*
[3] *IPHT, Albert-Einstein-Straße 10, D-07745* Jena
[4] *Klinik für Innere Medizin II, Universitätsklinikum Jena, Erlanger Allee 101, D-07740 Jena*

Magnetic nanoparticles are of growing importance in medicine and biotechnology, e.g. in the magnet resonance tomography, cell separation or magnetic drug targeting. The nanoparticles used in biomedical applications are covered with different coatings. The most popular are derivatives of polysaccharides such as carboxymethyl dextran. These carboxymethyl dextran-coated particles exhibit a high degree of biocompatibility and the carboxylic group of the shell material offers the possibility for the covalent immobilization of various biomolecules. But the stability of the magnetic fluids strongly depends on the concentration and the surrounding medium. Therefore we present a new approach of nanoparticle synthesis based on magnetite and maghemite using catecholic hydroxyl groups containing molecules as shell material. Catechols are known as ligands for iron(III)-ions forming stable complexes. Therefore these ligands seem to be able to stabilize magnetic nanoparticles. In particular levodopa, dopamine and hydrocaffeic acid (fig. 1) were chosen due to their pertinence in biological systems.

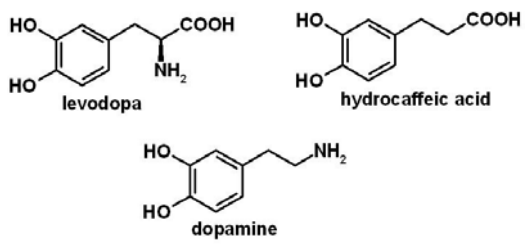

Figure 1: Used catecholic shell materials

An additional advantage is glucuronidation of catechols by human hepatic, gastric and intestinal microsomal glucuronosyltransferases that could lead to fast clearance of the nanoparticals after fulfillment their function. To emphasize possible clinical application the general cytotoxicity and cell uptake should be investigated by different cell lines.

The magnetic cores were synthesized by usual coprecipitation of iron(II)- and iron(III)-ions under basic conditions obtaining magnetic nanoparticles with mean core diameters around 10 nm. Afterwards the prepared particles were coated by the catecholic ligands. Because of the chemical structures especially of the amino group containing catechols, defined conditions of synthesis, notably temperature and pH, had to be elaborated that allows the attachment to the iron(III)-ions. The prepared magnetic fluids were chemically characterized, particularly the amount of iron and the Fe(II)/Fe(III) ratio were determined. In case of levodopa and dopamine the quantity of shell material was determined by a modified ninhydrin method for amino group determination. Also the physical properties like hydrodynamic diameter, zeta potential and magnetic behavior were measured.

The cytocompatibility of the novel core-shell particles was investigated in the live/dead assay using the 3T3 cell line and the fluorescent dyes fluorescein diacetate/ ethidium bromide. No toxic results were found after 24 hours. In first studies we investigated the interaction of the magnetic nanoparticles with tumor cells from breast cancer cell line MCF-7 and leukocytes. Cells were incubated time-dependent with

nanoparticles. The magnetically labeled cells were separated by MACS using a SuperMACS and MS columns. We found, that the MCF-7 cells showed intense interaction with these particles whereas the leukocytes showed a lower tendency of interaction.

In conclusion, we could prepare stable iron oxide based magnetic nanoparticles coated by catecholic hydroxyl group containing molecules. The coating strategy opens new possibilities in synthesis and biological functionalization of this type of nanomaterial. This approach basically allows the preparation of nanoparticles with more complex catecholic molecules for achievement of a selective uptake of magnetic nanoparticles into relevant cells or tissue.

This work was supported by the Bundesministerium für Wirtschaft und Technologie under contract number VF080018.

Peculiarities of shifted magnetic dipoles.

R. Weeber[1], J. Cerda[1],
S. Kantorovich[1,2], C. Holm[1].

[1] *ICP, Stuttgart, Germany*
[2] *USU, Ekaterinburg, Russia*

Homogeneously magnetized spherical particles can be safely associated with magnetic dipoles placed in the particle centres. The interaction between these particles is known and favours the "head-to-tail" position. In the present study we shift magnetic moments from the particle centres and investigate the influence of this shift on the particle-particle magnetic dipole-dipole (MDD) interaction. We study the deformation of the pair energy landscape theoretically and make simulations to elucidate the influence of the shift on the collective behaviour in the system.

Pair MDD and Energy Landscapes.

Let us assume we have two identical dipolar particles (1 and 2). The particle radius is denoted by R, the moments (m_1 and m_2 respectively) are shifted from the centres of particles, so that the distance from the particle centre to the dipole is d. The moment always points radially out of the particle. We introduce the angle ψ, which stands for the angle between z axis and the first magnetic moment m_1, and φ denotes the angle between z axis and the first magnetic moment m_1, for details, see Fig. 1. We will use the notation $d/R = \alpha$ to charactarise the relative shift of the dipole. It is easy to calculate the energy of magnetic dipole-dipole (MDD) interaction in this case.
In Fig. 2 the energy landscapes of MDD are presented for different values of the shift α. Angles φ and ψ correspond to Fig. 1. Both angles are in the range $[0, 2\pi]$. In Fig. 7a we have no shift ($\alpha =$

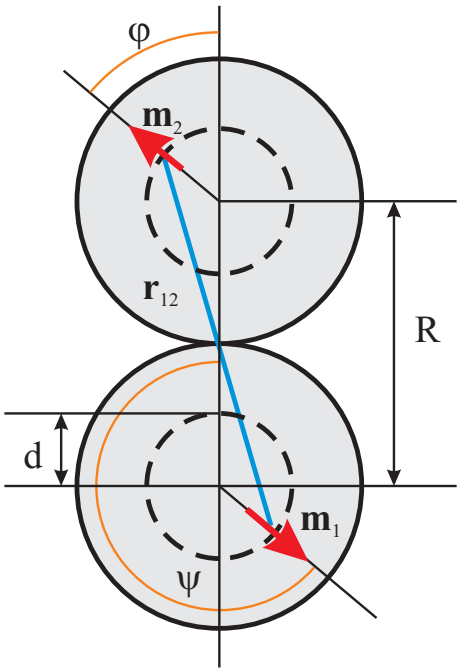

Figure 1: The geometry we use: both moments are placed inside the particle with the radius R at a distance d from particle centre, both moments can rotate pointing radially, the distance used for calculating the MDD interaction is r_{12}. φ is the angle between z axis and the second magnetic moment m_2, ψ is the angle between z axis and the first magnetic moment m_1.

0). Here we see the traditional landscape with 5 minima at parallel "head-to-tail" orientation and 4 maxima which correspond to antiparallel orientation. Then, with the increase of α (Fig. 7b - $\alpha = 0.3$, Fig. 7c - $\alpha = 0.6$, Fig. 7d - $\alpha = 0.9$) we see that two maxima, which correspond to ($\varphi = 0$, $\psi = \pi$) and ($\varphi = 2\pi$, $\psi = \pi$), slowly vanish, and new "wells" appear in the landscape.
First of all, along $\varphi = 0$ axes the maxima degenerates into a local minimum. Also, a new "well" appears along $\psi = 0$ axes. Analytical analysis shows that for shifts below $1 - \frac{\sqrt{3}}{3} \sim 0.423$ there are only 2 extrema $\varphi = 0$ and $\varphi = \pi$, but at the value of $\alpha = 1 - \frac{\sqrt{3}}{3}$ a sudden jump occurs, and the new extremum appears. For shifts smaller than $\alpha = 1 - \sqrt{3}/3$, $\varphi = 0$

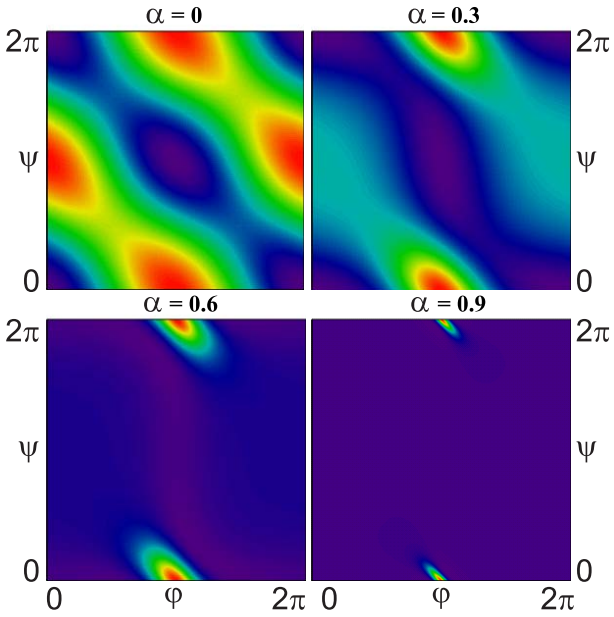

Figure 2: Energy landscapes for different values of the shift α: from the left to the right, from the top to the bottom $\alpha = 0$; $\alpha = 0.3$; $\alpha = 0.6$; $\alpha = 0.9$. Angles φ and ψ correspond to Fig. 1.

is the minimum, for larger shifts it turns to be the maximum. $\varphi = \pi$ is the maximum for all α, but $\alpha = 1$, where the energy diverges. The last extremum is $\varphi = \arccos\left\{-4\frac{g(\alpha)}{h(\alpha)} + \sqrt{24\left(\frac{g(\alpha)}{h(\alpha)}\right)^2 - 15}\right\}$, where functions $g(\alpha) = (2-\alpha)^2 - \alpha^2$ and $h(\alpha) = 2(2-\alpha)\alpha$ are introduced to simplify the functional form, and for all α from the interval [0,1) it provides the minimum of the energy. It is worth saying that the position of the latter minimum monotonously goes to π when α goes to unity, which corresponds to the antiparallel (!) orientation of magnetic moments.

Monte Carlo Simulations

We also study small clusters and solutions of particles with shifted dipoles using simple Metropolis Monte Carlo simulations. The energies were calculated using direct summation over all dipolar interactions. The particles, usually 2-50, are confined within a finite area, thus forming a quasi 2-dimensional system, as has been studied before for unshifted dipoles [1]. We examine first the ground state structures using a simulated annealing protocol. While for small shifts we expect to find only slightly changed ground states, at high displacements, two- or three-particle structures with antiparallel moments may emerge.

Conclusion

We investigate the peculiarities brought by the shift of the magnetic dipole from the centre of the particle. We discover that the shift exerts a huge influence on the pair potential and leads to the appearance of new energy minima and maxima. Our computer simulations as well show that the microstructure of the system with shifted dipoles differs considerably from the one of classical magnetic single-domain particles. This study, besides being interesting by itself, can be treated as the first step to understand experiments with capped colloidal particles performed by Erbe et. al [2].

Acknowledgments

This research was carried out with the financial support of DFG - RFBR Grant No. HO 1108/12-1. One of the authors (SK) was supported by the Grant of President RF MK-412.2008.2. The research was partially supported by RFBR Grant 08-02-00647 and CRDF Grant PG07-005-02.

References

[1] Prokopieva T. et al., Phys. Rev. E, accepted (2009);

[2] Erbe A. et al., Phys. Rev. E 77, 031407 (2008);

List of Participants

Robert Abraham
Institut für Organische und Makromolekulare Chemie II
Heinrich-Heine-Universität Düsseldorf
Gebäude 26.33 Raum 00.30
Universitätsstr. 1
D-40225 Düsseldorf
Tel.: 0211-811 3630
Fax: 0211-811 5840
E-mail: robert.abraham@uni-duesseldorf.de

Christoph Alexiou
Klinik und Poliklinik für Hals-, Nasen- und Ohrenkranke
Waldstr. 1
91054 Erlangen
Tel.: 09131-853 4769
Fax: 09131-853 4828
E-mail: C.Alexiou@web.de

Romy Baumann
Ernst-Moritz-Arndt-Universität Greifswald
Institut für Pharmazie
Biopharmazie und Pharmazeutische Technologie
Friedrich-Ludwig-Jahn-Straße 17
17487 Greifswald
Tel.: 03834-864 4814
Fax: 03834-864 886
E-mail: romy.baumann@uni-greifswald.de

Silke Behrens
Division of Chemical-Physical Processing
Institut for Thechnical Chemistry (ITC-CPV)
Forschungszentrum Karlsruhe GmbH
Herman-von-Helmholtz-Platz 1
76344 Eggenstein-Leopoldshafen, Germany
Tel.: 7247-82 6512
Fax: 7247-82 2244
E-mail: silke.behrens@itc-cpv.fzk.de

Jacob Belardi
Universität Freiburg
Department of Microsystems Engineering (IMTEK)
79110 Freiburg
Tel.: 0761-203 7167
Fax: 0761-203 7162
E-mail: belardi@imtek.de

Philipp Bender
Universität des Saarlandes
FR 7.3 Technische Physik / Prof. Dr. Rainer Birringer
Campus D2 2, Postfach 151150
Tel.: 0681-302 5189
Fax: 0681-302 5222
E-mail: philipp-bender@web.de

Alex Bian
Institut für Organische und Makromolekulare Chemie II
Heinrich-Heine-Universität Düsseldorf
Gebäude 26.33 Raum 00.30
Universitätsstr. 1
D-40225 Düsseldorf
Tel.: 0211-811 4134
Fax: 0211-811 5840
E-mail: aybian@ucalgary.ca

Valter Boehm
Technische Universität Ilmenau
Technische Mechanik
PF 100565
98684 Ilmenau
Tel.: 03677-69 1845
Fax: 03677-69 1823
E-mail: valter.boehm@tu-ilmenau.de

Dmitry Borin
Technische Universität Dresden
Fakultät Maschinenwesen
Lehrstuhl für Magnetofluiddynamik
01062 Dresden
Tel.: 0351-463 32307
Fax: 0351-463 33384
E-mail: dmitry.borin@tu-dresden.de

Paul Brown
Institut für Organische und Makromolekulare Chemie II
Heinrich-Heine-Universität Düsseldorf
Gebäude 26.33 Raum 00.30
Universitätsstr. 1
D-40225 Düsseldorf
Tel.: 0211-811 3630
Fax: 0211-811 5840
E-mail: pb1409@gmail.com

Norbert Buske
MagneticFluids
Köpenicker Landstr. 203
12437 Berlin
Tel.: 030- 53007805
E-mail: n.buske@magneticfluids.de

Juan J. Cerda
Institute for Computational Physics
Universität Stuttgart
Pfaffenwaldring 27
70569 Stuttgart
Tel.: 0711-685 67609
Fax: 0711-685 63658
E-mail: jcerda@icp.uni-stuttgart.de

Joachim Clement
Klinik für Innere Medizin II
Friedrich-Schiller-Universität Jena
Erlanger Allee 101
07740 Jena
Tel.: 36419 325820
Fax: 36419 325822
E-mail: Joachim.Clement@med.uni-jena.de

Dietmar Eberbeck
Physikalisch-Technische Bundesanstalt Berlin
Abbestr. 2-12
10587 Berlin
Tel.: 030-3481 7208
Fax: 030-3481 7361
E-mail: dietmar.eberbeck@ptb.de

Harald Engler
Technische Universität Dresden
Fakultät Maschinenwesen
Lehrstuhl für Magnetofluiddynamik
01062 Dresden
Tel.: 0351-463 32034
Fax: 0351-463 33384
E-mail: harald.engler@tu-dresden.de

Natalie Frickel
Institut für Organische und Makromolekulare Chemie II
Heinrich-Heine-Universität Düsseldorf
Gebäude 26.33 Raum 00.30
Universitätsstr. 1
D-40225 Düsseldorf
Tel.: 0211-811 3630
Fax: 0211-811 5840
E-mail: natalia.frickel@uni-duesseldorf.de

Thomas Friedrich
Experimentalphysik 5
Universität Bayreuth
95440 Bayreuth
Tel.: 0921-55 3339
Fax: 0921-55 3647
E-mail: thomas.friedrich@uni-bayreuth.de

Thorsten Gelbrich
QIAGEN GmbH
Corporate Research
QIAGEN Strasse 1
40724 Hilden
Tel.: 02103 29 16369
Fax: 02103 29 26369
E-mail:
Thorsten.Gelbrich@qiagen.com

Kurt Gitter
Technische Universität Dresden
Fakultät Maschinenwesen
Lehrstuhl für Magnetofluiddynamik
01062 Dresden
Tel.: 0351-463 35158
Fax: 0351-463 33384
E-mail: kurt.gitter@tu-dresden.de

Gunnar Glöckl
Ernst-Moritz-Arndt-Universität Greifswald
Institut für Pharmazie
Biopharmazie und Pharmazeutische Technologie
Friedrich-Ludwig-Jahn-Straße 17
17487 Greifswald
Tel.: 03834-864 809
Fax: 03834-864 886
E-mail: gunnar.gloeckl@uni-greifswald.de

Christian Gollwitzer
Experimentalphysik 5
Universität Bayreuth
95440 Bayreuth
Tel.: 0921-55 3337
Fax: 0921-55 3647
E-mail: Christian.Gollwitzer@uni-bayreuth.de

Angelika Gorschinski
Division of Chemical-Physical Processing
Institut for Thechnical Chemistry (ITC-CPV)
Forschungszentrum Karlsruhe GmbH
Herman-von-Helmholtz-Platz 1
76344 Eggenstein-Leopoldshafen, Germany
Tel.: 7247-82 4229
Fax: 7247-82 2244
E-mail: angelika.gorschinski@itc-cpv.fzk.de

Annegret Günther
Universität des Saarlandes
FR 7.3 Technische Physik / Prof. Dr. Rainer Birringer
Campus D2 2, Postfach 151150
Tel.: 0681-302 5203
Fax: 0681-302 5222
E-mail: annegret.guenther@web.de

Celin Gürler
Institut für Organische und Makromolekulare Chemie II
Heinrich-Heine-Universität Düsseldorf
Gebäude 26.33 Raum 00.30
Universitätsstr. 1
D-40225 Düsseldorf
Tel.: 0211-811 4134
Fax: 0211-811 5840
E-mail: celin.guerler@uni-duesseldorf.de

Erik Heim
Technische Universität Braunschweig, Fakultät 5
Institut für Elektrische Messtechnik und Grundlagen der Elektrotechnik
Hans-Sommer-Straße 66, D-38106 Braunschweig
Tel.: 0531-391 3876
Fax: 0531-391 5768
E-mail: e.heim@tu-bs.de

Dirk Heinrich
Institut für Festkörperphysik
Technische Universität Berlin
Hardenbergstraße 36
10623Berlin
Tel.: 030-3142 2476
Fax: 030-3142 7705
E-mail: dhein@physik.tu-berlin.de

Rolf Hempelmann
Universität des Saarlandes
Physikalische Chemie
Gebäude 9.2
D-66123 Saarbrücken
Tel.: 0681-302 4750
Fax: 0681-302 4759
E-mail: hempelmann@rz.uni-sb.de

Siegfried Hess
Institut f. Theoretische Physik
Techn. Univ. Berlin, EW 7-1
Hardenbergstr. 36
10623 Berlin
Tel.: 030-3142 3763
Fax: 030-3142 1130
E-mail: S.Hess@physik.tu-berlin.de

Christian Hoffmann
Universität des Saarlandes
Theoretische Physik, Geb. 38
66041 Saarbrücken
Tel.: 0681-302 5585
Fax: 0681-302 4316
E-mail: hoffmann@cs.uni-sb.de

Christian Holm
Institute for Computational Physics
Universität Stuttgart
Pfaffenwaldring 27
70569 Stuttgart
Germany
Tel.: 0711-6856 3593
Fax: 0711-6856 3685
E-mail: holm@icp.uni-stuttgart.de

Patrick Ilg
Institut f. Polymere
Wolfgang-Pauli-Str. 10
ETH Zürich, HCI H 541
CH-8093 Zürich
Tel.: (41) 44-632 839
Fax: (41) 44-632 1076
E-mail: patrick.ilg@mat.ethz.ch

Thomas John
Otto-von-Guericke Universität
FNW/IEP/ANP
Room: 032 in G16
Universitätsplatz 2
39106 Magdeburg
Tel.: 0391-671 1026
Fax: 0391-671 8108
E-mail: thomas.john@physik.uni-magdeburg.de

Sofia Kantorovich
FIAS
JW Goethe - Universität
Max-von-Laue Strasse 1
D-60438 Frankfurt/Main
Tel.: 069-7984 7532
Fax: 069-7984 7611
E-mail: kantorovich@fias.uni-frankfurt.de

Sabine Klapp
Institut für Theoretische Physik
Sekretariat PN 7-1
Technische Universität Berlin
Hardenbergstraße 36
D-10623 Berlin

Tel.: 030-314 23763
Fax: 030-314 21130
E-mail: klapp@physik.tu-berlin.de

Hans-Joachim Krause
Institut für Bio- und Nanosysteme (IBN-2)
Forschungszentrum Jülich
52425 Jülich
Tel.: 02461-61 2955
Fax: 02461-61 2630
E-mail: h.-j.krause@fz-juelich.de

Marina Krekhova
Macromolecular Chemistry II
University of Bayreuth
Building NW II, Universitätsstr. 30
95440 Bayreuth
Tel.: 0921-55 3306
Fax: 0921-55 3393
E-mail: marina.krekhova@uni-bayreuth.de

Martin Krichler
Technische Universität Dresden
Fakultät Maschinenwesen
Lehrstuhl für Magnetofluiddynamik
01062 Dresden
Tel.: 0351-463 34672
Fax: 0351-463 33384
E-mail: martin.krichler@tu-dresden.de

Carl Krill
Institut für Mikro- und Nanomaterialien
Fakultät für Ingenieurwissenschaften und Informatik
Universität Ulm
Albert-Einstein-Allee 47
D-89081 Ulm
Tel.: 0731-50254 76
Fax: 0731-50254 88
E-mail: carl.krill@uni-ulm.de

Tobias Lang
Experimentalphysik 5
Universität Bayreuth
95440 Bayreuth
Tel.: 0921-55 3318
Fax: 0921-55 3647
E-mail: tobias.lang@uni-bayreuth.de

Adrian Lange
Technische Universität Dresden
Fakultät Maschinenwesen
Lehrstuhl für Magnetofluiddynamik
01062 Dresden
Tel.: 0351-463 39867
Fax: 0351-463 33384
E-mail: adrian.lange@tu-dresden.de

Dietmar Lerche
L.U.M. GmbH
Rudower Chaussee 29
12489 Berlin
Tel.: 030-6780 6030
Fax: 030-6780 6058
E-mail: D.Lerche@lum-gmbh.de

Andreas Leschhorn
Universität des Saarlandes
Theoretische Physik, Geb. 38
66041 Saarbrücken
Tel.: 0681-302 4217
Fax: 0681-302 4316
E-mail: andy@lusi.uni-sb.de

Manfred Lücke
Universität des Saarlandes
Theoretische Physik, Geb. 38
66041 Saarbrücken
Tel.: 0681-302 3402
Fax: 0681-302 4316
E-mail: luecke@lusi.uni-sb.de

Frank Ludwig
Technische Universität Braunschweig, Fakultät 5
Institut für Elektrische Messtechnik und Grundlagen der Elektrotechnik
Hans-Sommer-Straße 66, D-38106 Braunschweig
Tel.: 0531-391 3863
Fax: 0531-391 5768
E-mail: f.ludwig@tu-bs.de

Stefan Lyer
Klinik und Poliklinik für Hals-, Nasen- und Ohrenkranke
Waldstr. 1
91054 Erlangen
Tel.: 09131-853 4769
Fax: 09131-853 4828
E-mail: stefan.lyer@uk-erlangen.de

Gernot Marten
Institut für Organische und Makromolekulare Chemie II
Heinrich-Heine-Universität Düsseldorf
Gebäude 26.33 Raum 00.30
Universitätsstr. 1
D-40225 Düsseldorf
Tel.: 0211-811 4134
Fax: 0211-811 5840
E-mail: gernot.marten@uni-duesseldorf.de

Nina Mattoussevitch
STREM Chemicals GmbH
Berliner Str. 56
77 694 Kehl
Tel.: (0033) 390-245 222
E-mail: nina-stremgmbh@web.de

Pascal Matura
Universität des Saarlandes
Theoretische Physik, Geb. 38
66041 Saarbrücken
Tel.: 0681-302 3442
Fax: 0681-302 4316
E-mail: andy@lusi.uni-sb.de

Robert Müller
IPHT
Albert-Einstein-Str. 9
07745 Jena
Tel.: 03641-2060 0
E-mail: robert.mueller@ipht-jena.de

Olga Mykhaylyk
Institut für Experimentelle Onkologie und Therapieforschung der TU München
Ismaninger Str. 22
81675 München
Tel.: 089-4140 4475
Fax: 089-4140 6182
E-mail: Olga.mykhaylyk@lrz.tu-muenchen.de

Stefan Odenbach
Technische Universität Dresden
Fakultät Maschinenwesen
Lehrstuhl für Magnetofluiddynamik
01062 Dresden
Tel.: 0351-463 32062
Fax: 0351-463 33384
E-mail: stefan.odenbach@tu-dresden.de

Umaporn Paiphansiri
Max-Planck-Institut für Polymerforschung
Postfach 3148
D-55021 Mainz
Tel.: 06131-379 300
Fax: 06131-379 330
E-mail: paiphan@mpip-mainz.mpg.de

Christian Plank
Institut für Experimentelle Onkologie und Therapieforschung der TU München
Ismaninger Str. 22
81675 München
Tel.: 089-4140 4453
Fax: 089-4140 4476
E-mail: plank@lrz.tu-muenchen.de

Jana Popp
Technische Universität Ilmenau
Technische Mechanik
PF 100565
98684 Ilmenau
Tel.: 03677-69 1845
Fax: 03677-69 1823
E-mail: jana.popp@tu-ilmenau.de

Helene Rahn
Technische Universität Dresden
Fakultät Maschinenwesen
Lehrstuhl für Magnetofluiddynamik
01062 Dresden
Tel.: 0351-463 34353
Fax: 0351-463 33384
E-mail: helene.rahn@tu-dresden.de

Matthias Reindl
Technische Universität Dresden
Fakultät Maschinenwesen
Lehrstuhl für Magnetofluiddynamik
01062 Dresden
Tel.: 0351-463 39868
Fax: 0351-463 33384
E-mail: matthias.reindl@tu-dresden.de

Reinhard Richter
Experimentalphysik 5
Universität Bayreuth
95440 Bayreuth
Tel.: 0921-55 3351
Fax: 0921-55 3647
E-mail: reinhard.richter@uni-bayreuth.de

Holger Schmalz
Macromolecular Chemistry II
University of Bayreuth
Building NW II, Universitätsstr. 30
95440 Bayreuth
Tel.: 0921-55 3395
Fax: 0921-55 3393
E-mail: Holger.Schmalz@uni-bayreuth.de

Annette Schmidt
Institut für Organische und Makromolekulare Chemie II
Heinrich-Heine-Universität Düsseldorf
Gebäude 26.33 Raum 00.30
Universitätsstr. 1
D-40225 Düsseldorf
Tel.: 0211-811 4820
Fax: 0211-811 5840
E-mail: Schmidt.Annette@uni-duesseldorf.de

Rudi Schmitz
RWTH Aachen, Institut für Theoretische Physik C,
Templergraben 55, 52056 Aachen
Tel.: 0241-80 27023
Fax: 0241-80 22188
E-mail: mail@rudischmitz.de

Nicolas Schorr
Universität Freiburg
Department of Microsystems Engineering (IMTEK)
79110 Freiburg
Tel.: 0761-203 7453
Fax: 0761-203 7162
E-mail: Nicolas.Schorr@imtek.uni-freiburg.de

Verena Sterr
Universität Oldenburg, Fakultät V,
Statistische Physik, C.-v.-Ossietzky-Str. 114 - 118, 26111 Oldenburg
Tel.: 0441-798 3673
Fax: 0441-798 3080
E-mail: sterr@theorie.physik.uni-oldenburg.de

Klaus Stierstadt
Ludwig-Maximilians Universität München
Sektion Physik
Schellingstr. 4
80799 München
Tel.: 089- 3689327
Fax: 089- 21803391
E-mail: klaus.stierstadt@physik.uni-muenchen.de

Kathleen Thom
Ernst-Moritz-Arndt-Universität Greifswald
Institut für Pharmazie
Biopharmazie und Pharmazeutische Technologie
Friedrich-Ludwig-Jahn-Straße 17
17487 Greifswald
Tel.: 03834-864 808
Fax: 03834-864 886
E-mail: kathleen.thom@uni-greifswald.de

Rainer Tietze
Klinik und Poliklinik für Hals-, Nasen- und Ohrenkranke
Waldstr. 1
91054 Erlangen
Tel.: 09131-853 4769
Fax: 09131-853 4828
E-mail: rainer.tietze@uk-erlangen.de

Lutz Trahms
Physikalisch-Technische
Bundesanstalt Berlin
Abbestr. 2-12
10587 Berlin
Tel.: 030-3481 7208
Fax: 030-3481 7361
E-mail: lutz.trahms@ptb.de

Sylvia Türk
Technische Universität Dresden
Fakultät Maschinenwesen
Lehrstuhl für Magnetofluiddynamik
01062 Dresden
Tel.: 0351-463 34819
Fax: 0351-463 33384
E-mail: sylvia.tuerk@tu-dresden.de

Markus Urban
Max-Planck-Institut für
Polymerforschung
Postfach 3148
D-55021 Mainz
Tel.: 6131-379 501
Fax: 6131-379 330
E-mail: urban@mpip-
mainz.mpg.de

Kerstin Wagner
INNOVENT e. V.
Bereich Biomaterialien
Prüssingstraße 27B
07745 Jena
Tel.: 03641-282 555
Fax: 03641-282 530
E-mail: kw@innovent-jena.de

Rudolf Weeber
Institute for Computational Physics
Universität Stuttgart
Pfaffenwaldring 27
70569 Stuttgart
Germany
Tel.: 0711-685 67609
Fax: 0711-685 63658
E-mail: weeber@ica1.uni-
stuttgart.de

Albrecht Wiedenmann
Institut Max von Laue - Paul
Langevin
Large Scale Structure Group
Tel.: (0033) 4-7620 7744
E-mail: wiedenmann@ill.fr

Ralf Wyrwa
INNOVENT e. V.
Bereich Biomaterialien
Prüssingstraße 27B
07745 Jena
Tel.: 03641-282 555
Fax: 03641-282 530
E-mail: rw@innovent-jena.de

Igor Zeidis
Technische Universität Ilmenau
Technische Mechanik
PF 100565
98684 Ilmenau
Tel.: 03677-69 2474
Fax: 03677-69 1823
E-mail: igor.zeidis@tu-ilmenau.de

Matthias Zeisberger
IPHT
Albert-Einstein-Str. 9
07745 Jena
Tel.: 03641-206 107
Fax: 03641-206 199
E-mail: matthias.zeisberger@ipht-
jena.de

Klaus Zimmermann
Technische Universität Ilmenau
Technische Mechanik
PF 100565
98684 Ilmenau
Tel.: 03677-69 2474
Fax: 03677-69 1823
E-mail: klaus.zimmermann@tu-
ilmenau.de

Andrey Zubarev
Ural State University
Department of Mathematical
Physics
620083, Lenin Av. 51
Ekaterinburg, Russia
Tel.: 007-343 3507541
Fax: 007-343 3507401
E-mail: Andrey.Zubarev@usu.ru